UNIVERSITY OF MALTA
L-Università ta' Malta

Advanced intervention methods for pear fruit fungi and characterization of their growth dynamics

Ph.D. thesis

Supervisor: Prof. Vasilis P. Valdramidis

Co-supervisors: Dr. Ruben Gatt, Mr. Stephen Decelis

Candidate: Davide Sardella

To my wife Diana

Acknowledgements

Firstly, I would like to express all my gratefulness to Prof. Vasilis Valdramidis for giving me the opportunity of doing this Ph.D. under his supervision, for trusting me, for his motivation during the difficulties and for the freedom that allowed me to perform my research experiments in the way I preferred.

I would also like to thank my co-supervisors, Dr. Ruben Gatt and Mr. Stephen Decelis for all their support and their precious suggestions.

I thank my labmates and colleagues Dr. David Millan Sango, Dr. Luke Mizzi and Ms. Christina Chatzitzika for all the fun and the nice time spent together during these unforgettable years.

Last, but not least, I would like to thank my family: my parents who always believed in me and my wife Diana who fills everyday my life with joy and love.

Grazie!

Abstract

As many of the most popular fungicides are expected to be banned, due to their high toxicity and potential carcinogenicity to humans, there is the need to better characterize the pear postharvest fungal pathogens in order to design new specific intervention solutions against them. The postharvest fungi *Penicillium expansum*, *Alternaria alternata*, *Botrytis cinerea* and *Rhizopus stolonifer* have been selected for this study. A primary cardinal model with inflection (CMI) prediction approach showed that *R. stolonifer* was the most aggressive fungus since it had the highest μ_{opt}= 1.22±0.02 [h^{-1}], while *P. expansum* could be the most psychrophilic fungus since it showed the lowest estimated T_{min} = -7.2°C. Hereafter, the efficacy of zinc oxide nanoparticles (ZnO NPs) has been investigated against the fungal isolates through a preliminarily implemented turbidimetric assay on semi-solid PDA medium. Results showed that ZnO NPs were successfully inhibiting the growth of the four isolates and that turbidimetry is a reliable technique for assessing their antifungal activity. The updated version of the Lambert Pearson model was used to estimate the MIC and the NIC values for the fungus *Penicillium expansum*, which were found to be 9.8 and 1.8 mM respectively. The physiological effects and the mode of action of ZnO NPs were also investigated by scanning electron microscopy (SEM) and by a chemical assay with EDTA, showing that ZnO NPs cause irreversible morphological aberrations on the fungal structures of all the isolates and that ions release is crucial for their antifungal activity. Finally, the efficacy of compressed polyurethane foams (PU), as an effective antifungal filtration system, is assessed. Controlling the air particulate could be achieved giving potential for future applications in postharvest storage   facilities.

Table of contents

List of figures

List of tables

List of abbreviations

ABS = Acrylonitrile Butadiene Styrene

AgNPs = Silver Nanoparticles

BAM = Bacteriological Analytical Manual

CA = Controlled Atmosphere

CCA = Coconut Cream Agar

CFUs = Colony Forming Units

CYA = Czapek Yeast-extract Agar

CMI = Cardinal Model with Inflection

DRBC = Dichloran Rose Bengal agar with Chloramphenicol

EDTA = Ethylenediaminetetraacetic acid

EHT = Extra High Tension

EPA = Environmental Protection Agency

FAO = Food and Agriculture Organization

FDA = Food and Drug Administration

GRAS = Generally Recognised As Safe

GRG = Generalised Reduced Gradient

HEPA = High Efficiency Particulate Air Filter

HPLC = High Performance Liquid Chromatography

LPM = Lambert-Pearson Model

MEA = Malt Extract Agar

MA = Modified Atmosphere

MIC = Minimum Inhibitory Concentration

MSE = Mean Squared Error

NIC = Non-Inhibitory Concentration

O.D. = Optical Density

OTA = Ochratoxin A

PDA = Potato Dextrose Agar

PPA = Pear Pulp Agar

PPB = Pear Pulp Broth

PPI = Pores Per Inch

PU = Polyurethane

ROS = Reactive Oxygen Species

SDA = Sabouraud Dextrose Agar

SEM = Scanning Electron Microscopy

TSB = Tryptone Soy Broth

YED = Yeast Extract Dextrose

ZnO NPs = Zinc Oxide Nanoparticles

Chapter 1. Introduction

Pears rank third among the most important tree fruits grown in the world. Global pear production accounted for 22,619,716 tons in 2013 according to FAO statistics. Being a highly perishable product, pears need to undergo proper postharvest treatment in order to be commercialised in optimal conditions. Postharvest management is a set of post-production practices, which include: washing, selection, controlled-atmosphere storage and fungicides application on fruits. Such practices aim at eliminating undesirable elements to prevent fruit spoilage and to ensure that the product complies with established quality standards. The pears growers' sector is currently facing a period of turmoil as many of the most popular chemical treatments, such as the fungicide thiabendazole, are expected to be banned according to a new EU legislation (Directive 2009/128/EC). There is therefore the need to identify important fungal diseases and investigate new intervention solutions in postharvest disease management that comply with the new EU legislation and give a positive answer to public concerns about food safety and human health. Apart from fungicide treatment, another aspect of the postharvest process that deserves more attention and needs implementation, is the air decontamination in fruit warehouses. Circulating particulate matter is indeed a carrier of fungal spores responsible for additional microbial contamination to the fruit and the currently available solutions are limited and with high costs when applied on industrial scale. Postharvest storage practices are thus currently focusing on novel antifungal compounds, which are effective against fungal pathogens and less toxic to humans, together with improved and more affordable air decontamination systems which may also help reduce fungicides application.

1.1 Aims and objectives

The aim of this PhD thesis was to investigate the efficacy of alternative antifungal compounds for postharvest disease control. Specifically, this was achieved by assessing the efficacy of zinc oxide nanoparticles (ZnO NPs) against some of the most important pear postharvest fungal pathogens, namely *Penicillium expansum*, *Botrytis cinerea*, *Rhizopus stolonifer* and *Alternaria alternata.* After characterizing the aggressiveness of each fungal isolate involved in this study, an improved turbidimetric protocol was developed in order to study the fungal growth in presence of ZnO NPs and quantitative data about the antifungal activity of ZnO NPs obtained with the support of mathematical prediction models. Hereafter, the mechanism of action of ZnO NPs was also elucidated by microscopic analysis (i.e., Scanning Electron Microscopy (SEM) imaging) of the fungal structures from the samples treated with ZnO NPs and through a chemical assay aimed at verifying the importance of ions release for the antifungal effect of ZnO NPs. Finally, the spore trapping efficacy of compressed polyurethane (PU) foams was assessed with an experiment of environmental air sampling.

A detailed description of the objectives of each chapter of this thesis is given below.

Literature review

☐ Providing an exhaustive overview of the most important postharvest fungal diseases of pear fruit.

☐ Highlighting the importance of identifying novel antifungal compounds and the recent interest towards metal nanoparticles in the scientific community.

☐ Emphasizing the key role of air decontamination in food-processing environments.

Modelling the growth of pear postharvest fungal isolates at different temperatures

☐ Quantitatively assessing the growth dynamics of the fungal isolates under several constant temperatures.

☐ Estimating the optimal growth temperature of the fungi by predictive mycology tools.

☐ Validating the models developed.

Optimized turbidimetric protocol for the assessment of the growth of pear postharvest fungi

☐ Identifying the most suitable combination of nutrient media and inoculum size to provide uniform and reproducible results by the use of a turbidimetric assay.

☐ Revising and complementing the experimental design also by predictive mycology tools.

Assessing the efficacy of ZnO nanoparticles against postharvest fungal isolates by automated turbidimetric analysis

☐ Assessing the antifungal activity of ZnO NPs against the fungal isolates through an automated turdidimetric assay.

☐ Estimating the Minimum Inhibitory Concentration (MIC) and Non Inhibitory Concentration (NIC) for *P. expansum* by predictive mycology tools.

Physiological effects and mode of action of ZnO nanoparticles against postharvest fungal contaminants

- Assessing the antifungal activity of ZnO nanoparticles against the fungal isolates by the "poisoned food" technique.

- Elucidating the morphological aberrations induced on the fungi by ZnO NPs treatment.

- Understanding the mechanisms responsible for ZnO NPs antifungal activity.

Assessing the air filtration efficacy of compressed and uncompressed polyurethane foams

- Investigating the change in fungal spore filtration efficacy when a conventional polyurethane foam is compressed to different ratios.

1.2 Structure of the thesis

Chapter 2 Literature review

A detailed review of the pear postharvest fungal diseases is provided with a complete description of the fungi responsible for the disease and the symptoms they produce on pears. Novel postharvest disease control strategies, such as the use of metal nanoparticles as an antifungal agent and the use of compressed polyurethane foams to decontaminate the air from storage facilities, are presented in relation to the most recent scientific literature.

Part of this work was published in peer-reviewed journals:

D. Sardella, A. Muscat, J.P. Brincat, R. Gatt, S. Decelis, V. Valdramidis (2016). A comprehensive review of the pear fungal diseases. *International Journal of Fruit Science. 16*(4). 351-377.

J.P. Brincat, **D. Sardella**, A. Muscat, S. Decelis, J. Grima, V. Valdramidis, R. Gatt (2016). A review of the state-of-the art in air filtration technologies as may be applied to cold storage warehouses. *Trends in Food Science and Technology. 50.* 175- 185

Chapter 3 Modelling the growth of pear postharvest fungal isolates at different temperatures

The effect of temperature on the mycelium growth kinetics of four postharvest fungal isolates (i.e., *Penicillium expansum*, *Alternaria alternata*, *Botrytis cinerea* and *Rhizopus stolonifer*) was assessed. A cardinal model with inflection (CMI) was used to describe the effect of the temperature on the growth rate (μ) and the lag time (λ) of each isolate. Cardinal temperature

values such as T_{min}, T_{max} and T_{opt} were estimated and isolates were sorted according to their aggressiveness. Additionally, model validation was performed on a medium prepared from squeezed pear pulp and on artificially wound-inoculated pear fruits. Results from the CMI prediction showed that *R. stolonifer* was the most aggressive fungus since it had the highest $\mu_{opt}=$ 1.22±0.02 [h^{-1}], while *P. expansum* could be the most psychrophilic fungus. Model validation on pear pulp agar showed growth rate over-prediction in the case of *R. stolonifer* and *B. cinerea* but a good correlation in the case of *P. expansum* and *A. alternata*. *In vivo* experiments on pear fruits showed discrepancies from the synthetic and the simulated counterparts for all the fungi with the only exception of *P. expansum*.

Part of this work was submitted to a peer-reviewed journal for publication.

D. Sardella, R. Gatt, S. Decelis, V. Valdramidis (2017). Modelling the growth of pear postharvest isolates at different temperatures (submitted).

Chapter 4 Optimized turbidimetric protocol for the assessment of the growth of pear postharvest fungi

The growth of the selected fungal isolates was investigated at different inoculum concentrations and in three nutrient media (Sabouraud Dextrose Agar (SDA), Potato Dextrose Agar (PDA) and Yeast Extract Dextrose agar (YED)) with a turbidimetric assay on 96-well microplates. Sequential optical density measurements were performed to generate O.D. *vs* time plots while the growth responses were expressed quantitatively as trapezoidal area. YED medium showed the lowest variation among replicated experiments, followed by PDA without having a

significant difference. The inoculum size had a minimal effect on the variation of the fungal dynamics. Microscopic assessment of the fungal growth in the microwells confirmed that YED medium allowed the most homogeneous development of the studied fungi.

Part of this work was submitted to a peer-reviewed journal for publication.

D. Sardella, R. Gatt, V. Valdramidis (2017). Turbidimetric assessment of the growth of filamentous fungi and the antifungal activity of ZnO nanoparticles (submitted).

Chapter 5 Assessing the efficacy of ZnO nanoparticles against postharvest fungal isolates by automated turbidimetric analysis

The antifungal effect of ZnO NPs against the postharvest pathogenic fungal isolates was investigated in this study. An automated turbidimetric assay was performed in order to collect sequential optical density measurements, representative of the fungal growth in the wells of the microtitration plates. Quantitative data were obtained, indicating that ZnO NPs were successfully inhibiting the growth of the four isolates. Additional data were collected and processed by the updated version of the Lambert Pearson model to estimate the MIC and the NIC values for the fungus *Penicillium expansum*. Results confirmed that turbidimetry is a reliable technique for assessing the antifungal activity of ZnO NPs and that zinc oxide is an effective fungicide.

Part of this work was published in a peer-reviewed journal:

D. Sardella, R. Gatt, V. Valdramidis (2017). Assessing the efficacy of zinc oxide nanoparticles against *Penicillium expansum* by automated turbidimetric analysis. *Mycology.* 0, 1–6.

Chapter 6 Physiological effects and mode of action of ZnO nanoparticles against postharvest fungal contaminants

A preliminary quantitative assessment of the activity of the ZnO NPs against the fungal isolates was performed by measuring mycelium diameter growth onto Potato Dextrose Agar (PDA) plates loaded with different ZnO NPs concentrations ranging from 0 mM to 15 mM (poisoned food technique). Hereafter, the rate of the fungal diameter increase was quantified by linear regression modelling. Microscopic analysis was performed by scanning electron microscopy (SEM) images of agar plugs excised from plates with 0 mM and 12mM ZnO. All the fungi were inhibited by ZnO NPs at concentrations higher than 6 mM. SEM images showed clear morphological aberrations in the fungal structures of all the isolates grown in presence of ZnO. Additionally, knowing that the chelating agent EDTA sequesters metal ions, it was added to fungal inoculated PDA plates with ZnO to study the NPs' mode of action. Cultures where ZnO was mixed with EDTA showed a decrease in the antifungal effect of the nanoparticles.

Part of this work was published in a peer-reviewed journal:

D. Sardella, R. Gatt, V. Valdramidis (2017). Physiological effects and mode of action of ZnO nanoparticles against postharvest fungal contaminants. *Food Research International* 101, 274–279.

Chapter 7 Assessing the air filtration efficacy of compressed and uncompressed polyurethane foams

After performing a comparative assessment, we showed that uncompressed polyurethane foams may be used as a "primary" protection against gross air contamination, although they suffered a saturation effect when increasing their thickness above a certain extent. On the contrary, foam compression reduced the pore size resulting in a more sinuous path for the air particles and in a significant increase in air filtration efficiency, proportional to the compression rate. Compressed polyurethane foam filters thus could be a more efficient way to control the particle content in the air, if compared to the uncompressed ones, and a good option for controlling the air particulate in postharvest storage facilities; considering also their lower cost compared to more popular foam filters available on the market.

Part of this work was submitted to a peer-reviewed journal for publication.

D. Sardella, V. Valdramidis , R. Gatt, (2017). Assessing the air filtration efficacy of compressed and uncompressed polyurethane foams (submitted).

Chapter 8. General conclusions and future perspectives

Conclusions from the major findings in relation to advanced intervention methods for pear fruit fungi and characterization of their growth dynamics are presented. Future research activities are also showcased.

Chapter 2: Literature review

2.1 *Pear postharvest fungal diseases and new intervention solutions for their control*

2.1.1. Postharvest pear fungal diseases

Pears, *Pyrus communis* L., are the most important temperate-zone fruits and rank third among the most important tree fruits grown in the world (Snowdon, 1990). Amongst the top pear-producing countries there are China, Italy, the United States, Spain, Argentina, South Korea, Turkey, Japan, South Africa and Belgium according to the FAO (Food and Agriculture Organization of the United Nations (FAO), 2014). Forty percent of Europe's total production corresponds to Conference pears, which are mainly cultivated in Belgium and the Netherlands, with a small crop production also in Spain. Other popular varieties are the Abate Fetel, William Bon Crétien/Bartlett, Rocha, Blanquilla (Spadova estiva), Beurre'/Bosc (Kaiser Alexander) (Sutton et al., 2014). In China, there are two divisions of cultivated species: the North China local pear (*Pyrus ussuriensis* Maxim.) and hybrids of *P. ussuriensis*: *P. pyrifolia* (Burm. f.) Nakai, and *P. bretschneideri* Rehder (Sutton et al., 2014). Currently, the primary European pear cultivars in North America are Bartlett (Williams Bon Crétien), d'Anjou, Beurré Bosc and Doyenné du Comice (Sutton et al., 2014).

The market price of fruits depends on their attractiveness and eating quality, which need to be retained for as long as possible after harvest in order to match supply to demand (Jackson, 2003). Pear fruits are highly perishable and susceptible to postharvest decay, thus they must be harvested at proper maturity, handled carefully and stored promptly. Postharvest practices consist of the management and control of variables such as temperature and relative humidity,

the selection and use of packaging and the application of fungicides (FAO, 2009). However, despite these precaution, pears are still subject to attacks by numerous postharvest pathogens, especially fungi belonging to the genera *Penicillium*, *Botrytis*, *Alternaria* (Jackson, 2003; Sutton et al., 2014) but also *Gloeosporium*, *Rhizopus*, *Phialophora* and *Mucor* (Sardella et al., 2016). Such infections usually occur in the field but they are either quiescent or escape notice at harvest and they represent a serious issue during postharvest storage.

Blue mould, known also as soft rot or wet rot, has been reported as the most important postharvest disease in apples and pears which causes destructive rot in most of all the producer countries, namely the USA, the UK, Poland, Italy, Israel, India and Australia (Snowdon, 1990). Blue mould originates primarily from infection of wounds such as punctures, bruises and limb rubs on the fruit. The first symptoms are soft watery brown spots which undergo rapid enlargement at temperatures between 20°C and 25°C (Snowdon, 1990). The lesions have a very sharp margin between diseased and healthy tissues and decayed tissue can be readily separated from the healthy one, leaving it like a "bowl" (see also Figure 2.1) (Pierson et al., 1971; Shim et al., 2002). Blue or blue-green spore masses may appear on the decayed area, starting at the infection site. Decayed fruit has an earthy musty odour. The presence of blue-green spore masses at the decayed area and the associated musty odour are the positive diagnostic indications of blue mould (Jones and Aldwinckle,1990; Shim et al., 2002). Blue mould occurs on all the varieties of pears around the world. Three forms of the disease can occur: check rot, stem and neck rot, and pinhole rot (Monroe, 2009; Pierson et al., 1971). Check rot develops on the check of the fruit and it occurs on all varieties of pears. It's the form of the disease most frequently found in the market. Stem and neck rot is a form of the disease that develops from stem infections in fleshy-stemmed varieties such as d'Anjou and Comice. The fungus grows down through the stem which

remains firm, but darkens. It spreads through vascular tissues into the neck of the fruit where the flesh becomes soft and watery (Pierson et al., 1971). Pinhole rot is a form of the disease that occurs mainly on Winter Nelis, a variety with large prominent lenticels. It first appears as numerous minute spots of decay scattered over the surface of the fruit, with infection apparently taking place at the lenticels. As the disease progresses the spots increase in size, finally coalescing to decompose the entire fruit (Pierson et al.,1971). *Penicillium expansum* is one of the oldest described *Penicillium* species and it has been established as the main cause of blue mold (Pitt & Hocking, 2009; Sutton et al., 2014). At least 17 *Penicillium* spp. have been isolated from naturally infected pome fruits with blue mold but *P. expansum* is by far the most common species (Sutton et al., 2014). Nevertheless, *P. expansum* has been isolated from a wide range of other fruits including tomatoes, strawberries, avocados, mangoes, grapes (Pitt & Hocking, 2009; Snowdon, 1990) indicating that it is a broad spectrum pathogen on fruits. Before the advent of controlled-atmosphere facilities and postharvest fungicides, it accounted for 90% of the total postharvest losses of apples and pears. Nowadays, incidence of blue mold is less than 1% but it still remains the most common postharvest decay in pome fruits (Sardella et al., 2016; Sutton et al., 2014).

Figure 2.1: Pear fruit showing symptoms of infection by blue mold

Gray mould is another important storage disease of pears, especially varieties that are stored for long periods (Pierson et al., 1971). Gray mould is considered as the second most important infection in pears after blue mould rot (Jones and Aldwinckle, 1990; Ogawa and English, 1991). Losses as high as 20-60% due to gray mould are not uncommon after an extended period of storage, particularly in fruit that was not treated with fungicides prior to storage. This is because gray mould has the ability to spread from decayed to healthy fruit by fruit-to-fruit contact during storage and this process is enhanced by high relative humidity (WSU, 2015). The disease develops more rapidly in cold storage temperatures unlike other postharvest decay, with the exception of mucor rot (Jones and Aldwinckle, 1990). Gray mould originates primarily from infection of wounds such as punctures and bruises that are created at harvest and during postharvest handling. Stem-end gray mould is common on d'Anjou pears (Xiao, 2006). This rot is often difficult to identify because its symptoms vary with fruit age and variety (Pierson et al., 1971). The rot tends to start as a small brown spot with diffuse margins. As the rot progresses, older portions of the decay darken, whereas the edges remain lighter (Monroe, 2009). The decayed area is spongy and diseased tissue is not separable from the healthy tissue, which is different from blue mould (WSU, 2015). Under high relative humidity conditions, fluffy white to gray mycelium and grayish spore masses may appear on the decayed area (Xiao, 2006). The internal decayed flesh appears light brown to brown at the margin and on advanced decayed fruit, sclerotia may form on the lesion surface (Xiao, 2006). Generally gray mould does not have a distinct odour, but in advanced stages it may have a pleasant fermented odour that distinguishes it from other storage rots (Pierson et al., 1971; WSU, 2015). The causal agent of gray mould is *Botrytis cinerea* Pers. – teleomorph *Botryotinia fuckeliana* (de Bary) Whetzel - and is widely

distributed in nature and thrives on decaying plant matter (Pierson et al., 1971) (an example on pear contamination is given in Figure 2.2). Conidia of the fungus are dispersed mainly by air currents and water splash. At harvest, pear fruit is detached from the trees and fresh wounds at the stem are exposed to potential contamination by *B.cinerea* (WSU, 2015). Outdoors, *Botrytis* overwinters in the soil in the form of a mycelium on plant debris, and as black, hard, flat or irregular sclerotia in the soil and plant debris, or mixed with seed. The fungus requires free moisture for germination and cool (15°C to 25°C) weather with little wind for optimal infection, growth, sporulation and spore release. *Botrytis* is also active at lower temperatures (0°C to 10°C). Infection rarely occurs at temperatures above 25°C and once it occurs, the fungus grows over a range of 0° to 35°C (University of Illinois, 2000). *B. cinerea* is able to move through the stem of the fruit to reach the flesh after a period of time in cold storage and then cause decay. It has been shown that the incidence of gray mould is correlated with spore levels on the fruit surface. *B. cinerea* has been reported to invade floral parts of pear fruit during bloom, causing calyx-end rot during storage (WSU, 2015).

Figure 2.2: Pear fruit showing symptoms of infection by gray mold

Alternaria rot is a problem in apple and pear in most areas of the world where these fruits are grown. An increase in the incidence of this disease has been associated with postharvest use of benzimidazole fungicides for the control of blue and gray mold (Jones and Aldwinckle, 1990). Alternaria rot is characterized by round, brown to black, dry, firm, shallow lesions around skin breaks or at the calyx or stem depression. Advanced rots become spongy and the affected flesh is streaked with black. On pear, the stem decay appears as slow-moving, black lesions extending from the abscission zone toward the flesh. Dark-colored mycelium may be seen on the surface of lesions under moist conditions. At cold storage temperatures, the rot develops slowly, and lesions are usually less than 25 mm in diameter after 5 months. The lesions are often indistinguishable from those caused by *Ulocladium* spp (Jones and Aldwinckle, 1990). For an example of *Alternaria* rot, refer to Figure 2.3. The causal organism is *Alternaria alternata* (Fr.) Keissler. *Alternaria alternata* is a weak pathogen and saprophyte which can live on dead or debilitated tissue of many plants. It can infect fruit before or after harvest. However, fruit inoculated up to 7 weeks before harvest do not rot on the tree but develop symptoms within 2 months at 0°C. The fungus infects fruit through weak or injured tissue associated with mechanical or chemical injury, scald, soft scald, physiological senescence, sunburn and chilling injury (Jones and Aldwinckle, 1990). *A. alternata* (Fr.) Keissler has been recorded on pears in Israel, Chile, Canada and the USA. *A. kikuchiana* S. Tanaka is reported to cause serious damage to pears in Japan and Korea (Snowdon, 1990). It has also been reported (Li et al., 2007) that *Alternaria alternata* can cause rot on "Pingguoli pear" (*Pyrus bretschneri* Rehd. Cv. Pingguoli), one of the most important cultivated crops in China. Alternaria rot on Pingguoli pear occurs after latent infection: fruit surface can be asymptomatic within 60 days of storage under cold condition (0°C,

RH 85-90%), but black-grey hyphae could be seen in the lenticels or calyx tube of pears after 90 days of storage (Li et al., 2007).

Figure 2.3: Pear fruit showing symptoms of infection by Alternaria rot

Bull's eye rot, previously known as "Gloeosporium rot" (Snowdon, 1990), is caused by *Neofabraea* spp. and is a another postharvest disease which is common in the Pacific Northwest of the United States as well as in Europe and in other growing areas (Henriquez et al., 2004, 2008). Fruits can be infected in the orchard at any time during the growing season, and spores or incipient infections remain latent until development of symptoms after several months of postharvest storage (Henriquez et al., 2004; Jones and Aldwinckle, 1990). *Neofabraea perennans* Kienholz, also known as *Pezicula perennans* Kienholz, and *N. alba* E.J. Guthrie Verkley, also known as *Pezicula alba* E.J. Guthrie, are the principal species associated with bull's eye rot of pear in the Pacific Northwest (WSU, 2015). These pathogens cause cankers on branches or develop saprophitically on trees. Conidia of *N. perennans* and *N. alba* are produced throughout the year on pear trees, but the highest sporulation occurs at the end of summer and during fall

(Henriquez et al., 2008). These conidia are splash-dispersed to fruit. Infection can occur any time after petal-fall; however, fruit susceptibility increases as the growing season progresses (Henriquez et al., 2008). Bull's-eye rot-spots have light brown centers and a dark brown border (Pscheidt, 2014). Decayed tissue is firm, cream-colored spore masses in the aged decayed area may appear. Rot does not spread from one fruit to another and it does not show up in the orchard but after months of storage (Pscheidt, 2014).

Rhizopus rot occurs occasionally on pears that have been injured or are over-ripe (Pierson et al., 1971). This disease mainly occurs during sale, transports, marketshelf and storage (Pitt and Hocking, 2009; Snowdon, 1990). Rot starts in a single fruit, which then becomes surrounded by a coarse, loose "nest" of mycelium. Growth spreads rapidly, involving several fruits adjacent to the originally infected one, and sometimes all the fruit in a box, in only 2-3 days (Pitt and Hocking, 2009). After harvest, *Rhizopus* is omnipresent as a saprophyte and sometimes as a weak parasite on stored organs of plants. When the epidermal cells are collapsed, the fungus emerges through the wounds and produces aerial sporangiophores, sporangia, stolons, and rhizoids, the latter capable of piercing the softened epidermis. The rot spots are brown and the affected flesh is soft and watery with a sour smell. A dense growth of the coarse gray fungus often covers the rotted areas (Pierson et al., 1971). Infections develop from spores or by contact, the latter method causing most of the losses in fruit boxes. *Rhizopus* is a mould that grows at temperatures between 5°C and 30°C with an optimum at around 25°C (El-Arbi et al., 2014; Schipper, 1984). In a humid environment, this plant pathogen grows rapidly and produces a black and loose mycelium with white aerial fruiting later becoming black. *R. stolonifer* is characterized by coarse and rampant growth and the establishment of the infection takes 2 to 6 hours. *R. stolonifer* is a

cosmopolitan fungus located mainly in warehouses on the conditioning material and on stored fruits (Sardella et al., 2016).

Mucor rot is a fungal disease of pears in the United States, Canada, Australia, South Africa and Europe where it occurs less constantly than blue mould and gray mould. Mucor rot is generally not a major problem, particularly when good harvest management and water-sanitation practices at packing are implemented (WSU, 2015). Mucor rot develops at the stem or calyx end of the fruit or at puncture wounds in the skin. Stem-end mucor rot is seen on d'Anjou pears (WSU,2015). The decayed area is light brown to brown with a sharp margin. The decayed tissue is very soft and juicy and can be readily separated from the healthy one. Gray mycelium with dark sporangia may appear on the decayed area. Mucor rot has also a sweet odour. Sporangiophores with sporangia may protrude through cracks in the skin. After about 2 months in cold storage at 0°C, infected fruit completely decay, releasing large quantities of juice containing sporangiospores, which cause additional infections (Jones and Aldwinckle, 1990). Mucor rot is caused primarily by *Mucor piriformis* E. Fischer. Other species of *Mucor* that have been reported to cause decay include *M. mucedo* P. Mich. Ex Saint-Amans, *M. racemosus* Fres., and *M. strictus* Hagem (Jones and Aldwinckle, 1990). *Mucor piriformis* is a soilborne pathogen and survives in the orchard soil. The pathogen enters packing facilities through infested soils or organic debris adhering to field bins. Drench solutions and dump-tank water are the primary source of inoculum for fruit infection at drenching and packing (WSU, 2015).

Side rot of pear, caused by *Phialophora malorum* McColloch, known also as *Sporotrichum malorum* Kidd & Beaumont and *S. carpogenum* Ruehle (Jones and Aldwinckle, 1990) , is an important disease of long-term stored pears, rarely observed before three months of storage and appearing more frequently after pears have been stored for 4-5 months at -1°C (Sugar and Spotts,

1992). This disease, known earlier as "*Sporotrichum* rot", produces roughly circular, slightly sunken, brown spots with distinct margins. The fungus appears to enter fruit most commonly through punctures and lenticels (Ogawa and English, 1991). The rotted tissues are wet and slimy under the intact skin, but are dry and spongy if the skin has been broken. The decayed tissues separate readily from the healthy tissues, leaving a saucer-shaped cavity usually less than ¼ inch deep. If there is no visible mycelium, side rot is indistinguishable from the decay caused by *Cladosporium herbarum* (Pers.) Link, without isolating the pathogen from a lesion. Bosc pear is very susceptible (Pierson et al., 1971).

2.1.2. Postharvest disease control and use of nanoparticles as novel antifungal agent

Postharvest disease losses cause important reductions in fruit quantity and quality thus rendering products unsaleable or decreasing their value. Besides the economic considerations, consumption of diseased fruit also implies potential risks for human health. Controlled atmosphere (CA) storage has been reported as a technology that can contribute, under certain circumstances, to greatly extend the marketable life of fruits. As a matter of fact, an enormous amount of interest and research has been reported on CA storage and modified atmosphere (MA) packaging of fruits in order to prolong their availability and retain their quality (Thompson, 2010). CA storage of pear fruit implies specific requirements in terms of $\%O_2$ (0.5 – 4%) and $\%CO_2$ (0 – 3%) (Gorny, 2001). Nevertheless, CA or MA should be used as a supplent to, and not as a subsitute for, proper temperature and humidity management and pesticides application. Traditional strategies for postharvest disease control and prevention include mainly the use of fungicides. In the postharvest phase, fungicides are often applied to control infections already established on

the surface tissues or to protect against infections which may occur during storage and handling (Coates et al., 1997). Increasing concerns about the use of fungicides continue to be expressed regarding their health hazards, their impact on environmental pollution and the proliferation of resistant biotypes of fungal pathogens (Palou et al., 2015). Several chemical agents, used in storage facilities, have been developed to control postharvest diseases, such as: deoxyglucose, clorine dioxide and calcium chloride (Pitt & Hocking, 2009). Furthermore, other compounds, for instance benzimidazole, which effectively controlled diseases such as blue mold for more than 20 years, are no longer effective due to the development of resistant fungal populations (Sutton et al., 2014), while applications of fludioxonil, pyrimethanil and pyraclostrobin-boscalid can still provide good control (Sutton et al., 2014). However, it has been shown that pyraclostrabin and fludioxonil are highly to very highly toxic to invertebrates, vertebrates and algae in freshwater and marine systems (Elskus, 2012) while pyrimethanil is classified by the U.S. Environmental Protection Agency (EPA) as a possible human carcinogen since it produces thyroid tumors in rats (Elskus, 2012; Hurley, Hill, & Whiting, 1998). Postharvest disease management is thus currently suffering on one hand, as many control strategies are not anymore effective and, on the other hand, as most of the current effective compounds have shown to be toxic and harmful to humans or to aquatic communities. It is therefore important to explore novel approaches which may replace current synthetic fungicides (He et al., 2011).

The advent of nanotechnology, which involves the manufacture and use of materials with size up to 100 nm, has brought great opportunities for the development of new materials with antimicrobial properties(Espitia et al., 2012). Recently, metal nanoparticles have received increasing attention due to strong antimicrobial properties and low toxicity towards mammalian cells and have been already applied in food preservation, burn dressings, safe cosmetics, medical

devices, water treatment and other range of products (Moritz & Geszke-Moritz, 2013). Additional benefits coming from the use of inorganic nanoparticles aretheir improved stability in comparison with the traditional antimicrobial agents (Dutta et al., 2012) and some of them even contain mineral elements essential to humans(Espitia et al., 2012; Roselli, et al., 2003). The main metal and metal oxide nanoparticles are based on: silver, copper, copper oxide and zinc oxide (Moritz & Geszke-Moritz, 2013). Silver has been in use since time immemorial in the form of metallic silver, silver nitrate, silver sulfadiazine for the treatment of burns, wounds and several bacterial infections (Rai, Yadav, & Gade, 2009). Metallic silver in the form of silver nanoparticles has made a remarkable comeback as a potential antimicrobial agent (Rai et al., 2009) emerging up with diverse medical applications such as: silver based dressings, silver coated medicinal devices, nanogels and nanolotions. One of the main advantages of using silver is that the microorganisms are unlikely to develop resistance against it. Copper and its compounds have also been used for centuries as effective antibacterial, antifungal and antiviral agents (Ingle, Duran, & Rai, 2014). An added advantage of copper nanoparticles is that they oxidize and form copper oxide nanoparticles, which can easily mix with polymers and macromolecules and are relatively stable in terms of both chemical and physical properties (Cioffi et al., 2005; Usman et al., 2012). Zinc oxide (ZnO) is an inorganic compound widely used in everyday applications. Research on ZnO as an antimicrobial agent started in the early 1950s (Espitia et al., 2012) but the real move towards the use of ZnO as an antimicrobial was in 1995 when Sawai and his colleagues demonstrated its antimicrobial activity against several bacterial strains (Sawai, 2003; Sawai et al., 1997; Sawai et al., 1998). Zn NPs are non-toxic in appropriate quantities and show strong antimicrobial activity even at low concentration, ranging from 12 mM up to 100 mM (Savi et al., 2013). Some forms of zinc, including zinc oxide, are

listed in the generally recognised as safe substances (GRAS) and authorised for the fortification of foods (Savi et al., 2013; FDA, 2016). Knowledge about the biological effects of ZnO nanoparticles has generated a great deal of interest for their use as alternative antimicrobial compounds. Furthermore, the potential use of ZnO nanoparticles for controlling phytopathogenic fungi has also recently arisen in the scientific community (Arciniegas-Grijalba et al., 2017) thanks to several study which have shown their efficacy in controlling plant fungal pathogens. For instance, ZnO nanoparticles have shown significant antifungal activity against the coffee fungus *Erythricium salmonicolor* (Arciniegas-Grijalba et al., 2017) as well as against the crop pathogen *Fusarium graminareum* (Dimkpa et al., 2013) and the postharvest fungus *Penicillium expansum* (He et al., 2011). The toxigenic fungi *Aspergillus flavus* and *Penicillium citrinum* are also efficiently inhibited by ZnO NPs and Zn-compounds, such as zinc sulphate and zinc perchlorate (Savi et al., 2013), thus indicating that ZnO NPs can be also useful for the prevention of toxins accumulation in food. ZnO nanoparticles have also been tested as a potential coating agent on strawberries (Aponiene et al., 2015) while photoactived ZnO nanoparticles in suspension have revealed significant inhibition of *Botrytis cinerea* (Kairyte et al., 2013). Additionally, ZnO nanoparticles have been incorporated in different materials including glass, low density polyethylene (LDPE), polypropylene (PP), polyurethane (PU), paper and chitosan (Espitia et al., 2012). For example, paper coated with ZnO NPs has shown antimicrobial activity (Ghule et al., 2006) while ZnO nanorods deposited onto glass surface showed antifungal activity against *Candida albicans* (Eskandari et al., 2011). ZnO nanoparticles can therefore provide alternative solutions to food industry challenges related to product safety (Silvestre, Duraccio, & Cimmino, 2011) as well as to plant fungal diseases control.

2.1.3. Air-filtration systems

Although a lot of emphasis is laid on controlled atmosphere storage and fungicides application onto the fruits in postharvest warehouses (Suslow, 2005), poor attention is paid, so far, to the quality of the air in terms of circulating particulate matter, even though it has been shown that the presence of spores in the air inside these facilities affects the quality of the product negatively (Brincat et al., 2016; Ocón et al., 2011). Highly resistant fungal spores can cause spoilage of fruit and foodstuffs in storage facilities, therefore their presence must be controlled. The most common way to eliminate bioaerosols from the internal environment of facilities is by air filtration (Brincat et al., 2016). Special care needs be taken to assess the suitability of the filters to the particular circumstances which they would be operating in. In particular, the pressure drop across the filter should be low, in order to minimize operational cost. An eventual filter would primarily need to remove spores from the air. This implies that the particles which need to be removed from the air have a relatively constant size of a few μm (Brincat et al., 2016). The setup cost of the filter, as well as any running costs, need to be taken into consideration. The most used air filtration systems to reduce the abundance of fungal spores in such environments are High Efficiency Particulate Air (HEPA) filters as they are known to be amongst the most efficient filters available for particles trapping (Brincat et al., 2016). In these devices, the material which is trapped by the filter forms a "cake". As soon as the thickness of the cake increases, the path that particles are forced to travel through becomes longer and more contorted (Brincat et al., 2016). This increases the filter's efficiency but also the pressure drop so that, at some point, the filter needs to be replaced (Brincat et al., 2016; Novick et al., 1992). Specifically, HEPA filters need to be replaced on a yearly basis and their pressure drop increases with continual use (Novick et al., 1992). An alternative to HEPA filters is represented by polyurethane (PU) foams.

PU foams, like HEPA filters, trap particles on the surface of their fibres. As particles travel through the foam, which has a very elevated internal surface area, they are likely to adhere to it (Brincat et al., 2016). Foams are porous, cellular solids with a very high surface area. Each foam has a nominal number of Pores Per Inch (PPI), which determines how dense the foam is. Increasing the PPI of the foam will make it denser. Polyurethane (PU) foams are often applied as filters in water-purification systems, and air-flow purification systems. The term 'polyurethane foam' is an umbrella definition for cellular solids made of polymeric material. The most common types of polyurethane foams are the polyester and polyether foams. PU foams, like HEPA filters, are physical filters, which means that they trap particles on the surface of their fibres. As particles travel through the foam, which has a very elevated internal surface area, they are likely to adhere to it. The random arrangement of the ribs and nodes in open-cell foams makes the flow of air or water inside it necessarily non-laminar, which increases the probability that particles in the flow come into contact with it. Although, polymeric foams are not as efficient as HEPA filters, they present the important advantage of being tunable to specific needs (Brincat et al., 2016) . The PPI and the thickness of the polyurethane foam filter can be fine-tuned to find the optimal compromise between efficiency and pressure drop. Increasing the PPI makes the foam more efficient as a filter. Similarly, increasing the thickness of the foam filter will also increase the efficiency. However, at the same time, increasing the PPI or the thickness will also increase the pressure drop. Owing to this, the efficiency and pressure drop of foam filters should be adjusted to some optimal value (Roesler, 1966). Although relative humidity is known to alter the mechanical properties of polyurethane foam, an extensive literature research has revealed that the number of studies investigating the effects of relative humidity on the effectiveness of polyurethane foam filters is extremely limited. Polyurethane is hydrophobic,

implying that its mechanical structure should not be modified by the presence of water. Polyurethane foams are indeed often employed as water filters (Brincat et al., 2016). The air filtration efficiency and the pressure drop across the filter could change with increasing relative humidity though, as it does for the HEPA filters. The effects of relative humidity should therefore be investigated before using these filters in the cold storage warehouses. The fungal growth problem is also important since polyurethane foams present a very high surface area and a substantial volume (compared to HEPA filters) which is suitable for fungal growth. This causes a number of problems, including the loss of filtering efficiency over time, and the fact that the filter itself becomes a source of spores which is undesirable because of potential cross contamination in food storage environments. Fungal growth could be countered either by replacing the foam frequently, or by actively disinfecting the foam filter.

Chapter 3: Modelling the growth of pear postharvest fungal isolates at different temperatures

3.1 Introduction

3.1.1. Postharvest fruit storage and cold-resistant fungi

Maintaining fruit quality begins with cooling it soon after harvest to reduce respiration and ripening process. Almost all pears are currently placed in cold storage facilities within hours of harvest and cooled to 0-4°C (Sutton et al., 2014). Controlled-atmosphere storage involves also the rapid reduction of oxygen levels to ≈2% and it usually lasts for 6-10 months after harvest (Sutton et al., 2014). However, as stated before (Chapter 2), during this time pears are subject to attacks by numerous postharvest pathogens, especially fungi belonging to the genera *Penicillium*, *Botrytis*, *Alternaria* (Jackson, 2003; Sutton et al., 2014)but also *Gloeosporium*, *Rhizopus*, *Phialophora* and *Mucor* (Sardella et al., 2016). Such infections usually occur in the field but they are either quiescent or escape notice at harvest.

Postharvest rot fungi generally grow best at about 20-25°C, with a maximum between 27-32°C depending on the species (Sommer, 1982; Sutton et al., 2014). Controlled-atmosphere storage has thus drastically reduced the incidence of most of these diseases. However, concern is sometimes expressed that postharvest disease fungi might adapt, by mutation and selection, to grow at abnormally low temperatures, as in the case of *Rhizopus stolonifer*. (Sommer, 1982, 1989). For instance, cold-resistant *Rhizopus stolonifer* strains with low temperature limits for growth and infection have been found, and subsequently artificially grown, on strawberry fruit in New Zealand (Siefkes-Boer et al., 2009). Furthermore, it has been reported that *P. expansum* and

B. cinerea are also able to grow at temperatures as low as -2°C and their conidia can germinate at 0°C (Sutton et al., 2014).

3.1.2. Fungal aggressiveness comparison by predictive mycology studies

Experiments aimed at investigating the growth behaviour of fungi and comparing their aggressiveness are conducted at various constant temperatures, on different substrates and with different types of inoculation. For example, fungi can be inoculated on Petri dishes with a suitable medium for growth, which can be either synthetic or obtained from raw ingredients, on which spores swell and after a few hours germ tubes protrude and growth starts (Gougouli et al., 2011; Sommer, 1989). Different intervals of time, depending on the species and on the inoculum size, are chosen to study the germination and development of a colony. Studies performed onto Petri dishes, usually consist of the measurement of colony diameter, also reported as "radial growth rate" (Pitt & Hocking, 2009). A growth rate function can then be derived by performing a regression analysis on the linear part of the data correlating colony diameter increase with time (Marín et al., 2005). Another way to perform this kind of studies is by artificially wound-inoculated fruits. Such studies are based on the same principle as those on Petri dishes, but with the difference that they are carried out *in vivo*. Fruits are usually punctured with a sterile needle and conidial suspensions are inoculated into the wounds with a syringe or a sterile tip. Several studies have been performed on different fruits, such as: apples, pears, strawberries, peaches, oranges and apricots (Brooks and Cooley, 1928; El-Kazzaz, 1983; Feng and Zheng, 2007; Fieira et al., 2013; Harper et al., 1972; Sommer, 1982). For instance, the effect of temperature on the growth rate and the lag phase of *P. expansum* has been assessed on apples (Baert et al., 2007), *P.*

expansum's growth has also been compared with the one of *B. cinerea* on grape berries and synthetic grape juice medium (Judet-Correia et al, 2010), while *A. alternata* has been investigated on a medium prepared from fresh tomato pulp (Pose et al., 2009). These studies are generally useful for the validation of a predictive model (Judet-Correia et al., 2010; Tassou et al., 2009)) as well as for performing challenge tests via artificially contaminated commercial products (Gougouli et al., 2011). Further comparative quantitative studies (always developed basing on predictive models) of the growth of *Botrytis cinerea* and *Penicillium expansum* performed on PDA and validated on grape berries, identified the former as the most aggressive one but the latter as the most cold-resistant (Judet-Correia et al., 2010). Therefore, there is a need to further compare the aggressiveness of some of these fungal contaminants at a range of temperatures, not only to assess their growth dynamics (i.e., growth rate or lag time) but also in order to identify the temperature cardinal values especially at low temperatures close to conditions representing postharvest cold-storage. It is also very important that such studies are performed for a series of fungi (more than two) and under the same substrates, so they can be more conclusive. Specifically, these studies are needed in order to assess the dynamics of fungal contaminants present in pear fruits which are currently lacking in the literature.

3.2 Objective

The aim of this study was to quantitatively assess the growth dynamics of *Penicillium expansum*, *Botrytis cinerea*, *Rhizopus stolonifer* and *Alternaria alternata* under several constant temperatures. Based on the optimal growth temperature of the above mentioned fungi, estimated by predictive mycology tools, additional *in vitro* and *in vivo* studies on a nutrient agar prepared

from pear pulp and on fresh pear fruits, respectively, are performed to compare the aggressiveness of the fungi and validate the models developed with data coming from a synthetic medium.

3.3 Materials and methods

3.3.1. Fungal isolates and preparation of inocula

The postharvest disease fungi *Penicillium expansum*, *Botrytis cinerea*, *Rhizopus stolonifer* and *Alternaria alternata* used in this study were obtained from the fungal collection of the Postharvest Pathology group of IRTA (Spain). Fungal spores were harvested from 5-day old Malt Extract Agar (MEA) (Biolife,Milano,Italy) cultures by flooding the plates with a 0.05% Tween-80 solution and by scraping off the plates' surface with a sterile bent rod. The resulting suspension was aseptically filtered through a 4-layer sterile gauze to remove any mycelial contamination. Final spores' concentration was adjusted to 10^5 spores/mL with a haemocytometer for all the isolates.

3.3.2. Inoculation and growth measurements on SDA and Pear Pulp Agar plates

This study was performed on two different media: Sabouraud Dextrose Agar (SDA) (Biolife, Milano, Italy) and Pear Pulp Agar (PPA) obtained from fresh pear fruit. PPA was prepared by modifying the procedure illustrated by Pitt and Hocking (2009) for Potato Dextrose Agar by replacing potatoes with "Abate Fetel" pears and without adding dextrose. 250 grams of pears were peeled, diced and boiled into 500 mL of distilled water for 30 min. After boiling, the pear extract was decanted into a graduated cylinder and its volume was brought back to 500 mL by squeezing the remaining pear pulp and adding distilled water. The refraction index and the Brix

% of this pear extract were measured at 20°C with a refractometer (Atago, Japan) and were found to be n_D=1.34026 and 5%, respectively. Finally, 15g of agar were added and mixed thoroughly in a final volume of 1L. After autoclaving at 121°C for 15 min, media were poured into sterile Petri dishes and left to solidify. The water activity (a_w) of each medium, i.e., SDA and PPA, was measured with a Rotronic™ water activity meter (Bassersdorf, Switzerland) and was found to be a_w= 0.963 at 24°C for both of them. Four perpendicular diameters were drawn onto the plates' reverse sides to allow growth diameter measurement. SDA plates were inoculated in the centre with 10 μL of the previously prepared fungal spores' suspensions and incubated at several temperatures in a range comprised between 5 and 30°C. Experiments were perfomed in triplicate. The growth responses of each fungal isolate on SDA were plotted against time and then linear regression analyses were performed for the estimation of the growth rate (μ) and the lag time (λ) using Ms Excel®. The estimated μ and λ were further expressed as a function of temperature using the Cardinal Model with Inflection (CMI) developed by Rosso et al. (1995) as shown by Gougouli et al. (2011):

$$\mu = \frac{\mu_{opt}\,(T - T_{\max})(T - T_{min})^2}{(T_{opt} - T_{min})\left[(T_{opt} - T_{min})(T - T_{opt}) - (T_{opt} - T_{max})(T_{opt} + T_{min} - 2T)\right]}$$

$$1/\lambda = \frac{(1/\lambda_{opt})(T - T_{max})(T - T_{min})^2}{(T_{opt} - T_{min})\left[(T_{opt} - T_{min})(T - T_{opt}) - (T_{opt} - T_{max})(T_{opt} + T_{min} - 2T)\right]}$$

where T_{opt}, T_{min} and T_{max} are the theoretical optimum, minimum and maximum temperature for growth (°C), respectively and μ_{opt} and λ_{opt} are the growth rate and the lag time at the optimum temperature, respectively. The standard errors of the parameters were calculated using the following equation

$$SE = \sqrt{[(J^T \times J)^{-1}]}$$

where SE is the standard error and J is the Jacobian matrix containing the partial derivatives of the model output with respect to the model parameters evaluated at each measurement point. While the performance of the regression analysis is reported through the Mean Squared Error (MSE).

Data from PPA cultures were used as a validation study to assess the performance of the above mentioned model. For this purpose, PPA plates were inoculated in the same way as the SDA ones but they were incubated at 15°C, 30°C and at the T_{opt} estimated by the CMI for each fungal isolate. After performing linear regression analyses, the obtained growth rates were compared with the corresponding μ values estimated by the CMI on the SDA cultures. Comparison between the predicted growth rate, $\mu_{predicted}$ and the observed growth rate $\mu_{observed}$ was assessed by using the accuracy, A_f and the bias, B_f factors (Ross, 1996).

$$A_f = 10^{\left(\Sigma \left| \log\left(\frac{\mu_{predicted}}{\mu_{observed}}\right) \right| / n\right)}$$

$$B_f = 10^{\left(\Sigma \log\left(\frac{\mu_{predicted}}{\mu_{observed}}\right) / n\right)}$$

3.3.3. Comparative assessment with an *in vivo* assay on artificially wounded and inoculated pear fruit

In vivo experimental results were also collected in order to compare the growth kinetics at the optimal temperature (T_{opt}) with those obtained from the PPA and SDA experimental approaches. For the inoculum preparation, spores' suspensions of all the previously mentioned fungi were obtained as described before (section 3.3.1). For the *in vivo* assay, "Abate fetel" pears were

selected according to homogeneous size, weight, maturity, colour and absence of injuries. Pears were superficially disinfected by dipping them in a 2% sodium hypochlorite solution for 15 min in agitation. Hereafter, fruits were rinsed three times in distilled water and dried under a flow cabinet at room temperature. One wound (3 mm wide and 3 mm deep) was made onto each fruit and 20 µl of spores' suspension were injected. Each fungal isolate was inoculated onto three fruits and the whole experiment was performed at least in duplicate. Fruits were finally packed into sterile polypropylene bags and incubated at the predicted optimal temperature (T_{opt}) per each fungus calculated from the results of the CMI with the SDA plates (section 2.3.2). After the rots' symptoms started appearing, diameter maximum (Ø max) and diameter minimum (Ø min) of the lesions onto the inoculated fruits were measured at different time intervals. The obtained data were plotted as ellipsoids in Ms Excel®, representing the actual surface area of the lesions.

3.4 Results
3.4.1. Modelling the effect of the temperature on SDA plates

Figure 3.1 shows the effect of the temperature on the diameter growth rate of the fungi involved in this study by representative fitted curves of the CMI. CMI had a good fitting capacity as reported by the low MSE values (Table 3.1). From the graphs it can be clearly deduced that, among the four isolates, *R. stolonifer* appears to be the most aggressive one since it shows the highest μ_{opt} value. The aggressiveness of the four isolates can be sorted as follows: *R. stolonifer>B. cinerea>A. alternata>P.expansum*. The estimated values for T_{min}, T_{max} and T_{opt} obtained from the CMI (Table 3.1), revealed that *P. expansum* had the lowest estimated T_{min}= - 7.2°C,followed by *A. alternata* (T_{min}= -5.2°C). Although these values are nominal and are estimated outside the experimental region, they suggest that these fungi may resist to very low temperature storage conditions.
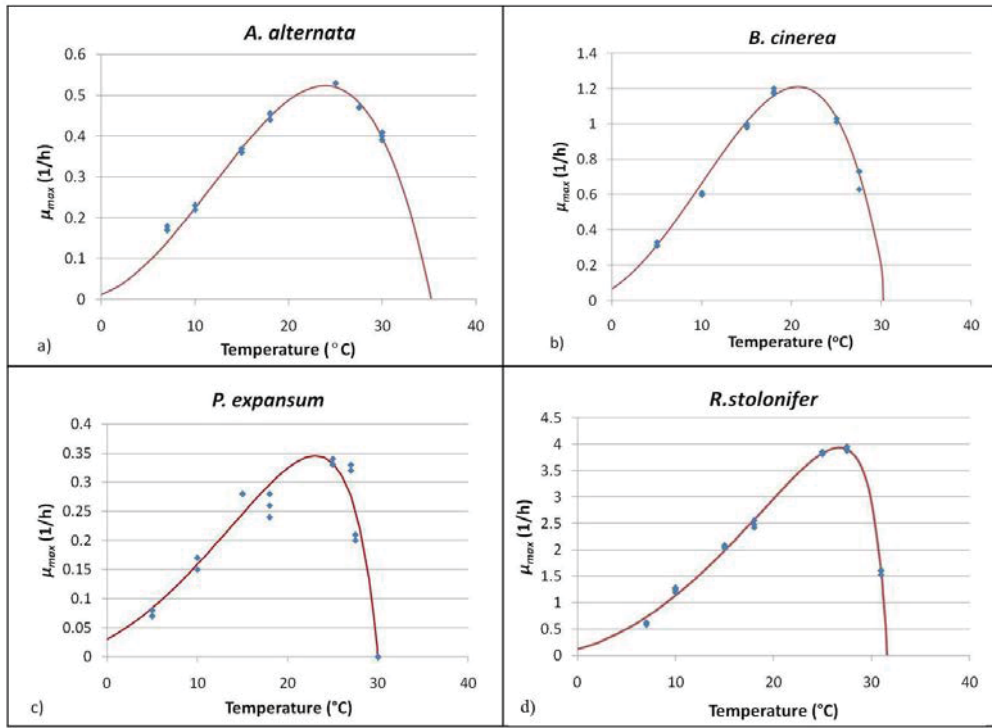
Figure 3.1. *Effect of the storage temperature on the growth rate (µ) of the four fungal isolates on SDA fitted with the CMI (continuous line). Scattered points represent the observed values. Inoculum size was 10^5 spores/mL for all the isolates. Scale is different due to differences in growth rates among the isolates. For a comparison with the same scale refer to Figure 3.3.*

Table 3.1. *Estimated values of T_{opt}, T_{min} and T_{max} and corresponding SE from the CMI for all the fungal isolates.*

	μ_{opt}(1/h)	T_{opt}(°C)	T_{min} (°C)	T_{max} (°C)	MSE
P. expansum	0.35□0.01	23.10□0.42	-7.24□2.74	29.99□0.11	0.0011
B. cinerea	1.22□0.02	20.93□0.22	-3.76□0.79	30.18□0.31	0.0008
R. stolonifer	3.94□0.04	26.71□0.23	-4.69□0.76	31.60□0.08	0.0084
A. alternata	0.52□0.01	24.15□0.01	-5.22□0.99	34.66□0.53	0.0001

Graphs from Figure 3.2, where the reciprocal lag time is plotted against the temperature, show also significant differences among the selected isolates. Noticeably, also in this case, *R. stolonifer*'s appears to be the most aggressive isolate in terms of growth speed, since it has the shortest λ_{opt} amongst all the isolates. The four isolates can be sorted according to their lag time duration as follows: *R. stolonifer<A. alternata<P. expansum<B. cinerea*.
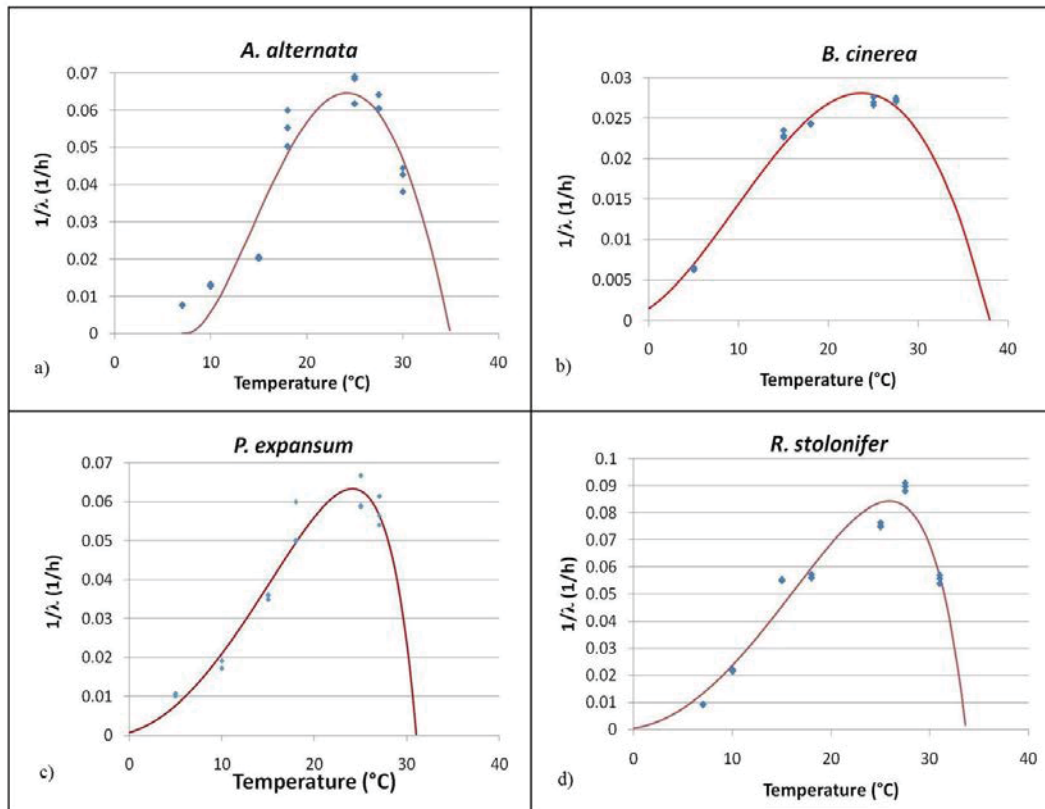
Figure 3.2. *Effect of the storage temperature on the reciprocal lag time (1/λ) of the four fungal isolates grown on SDA fitted with the CMI (continuous line). Scattered points represent observed values of the reciprocal lag time (1/λ).*

3.4.2. Model validation

As stated before, it is imperative to validate any model that will be used to perform predictions under conditions that have not been used to develop the models. Therefore, the model was

validated by collecting data in a different substrate, i.e., PPA. The accuracy (A_f) and bias (B_f) factors were considered in order to evaluate the performance capability of the model. On the one hand, the accuracy factor indicates how close, on average, predictions are to observations (values close to 1 are indicative of small deviations). On the other hand, the bias factore valuated whether the observed values lie above or below the prediction line (i.e., $B_f<1$, under-prediction and $B_f>1$ over-prediction) (Ross, 1996; Valdramidis et al., 2007).

As shown in Table 3.2, in the case of *R. stolonifer* and *B. cinerea* there is an over-prediction of the model if compared to the PPA counterpart. Furthermore, such over-prediction is more significant in the case of *R. stolonifer*. In the case of *P. expansum* and *A. alternata* there is a good correlation between observed and predicted values as also shown in Figure 3.3.

Table 3.2. *Accuracy factors (A_f) and bias factors (B_f) for each of the fungal predictive models.*

	A_f	B_f
R. stolonifer	2.37	2.37
B. cinerea	1.65	1.65
P. expansum	1.45	0.68
A. alternata	1.58	0.63
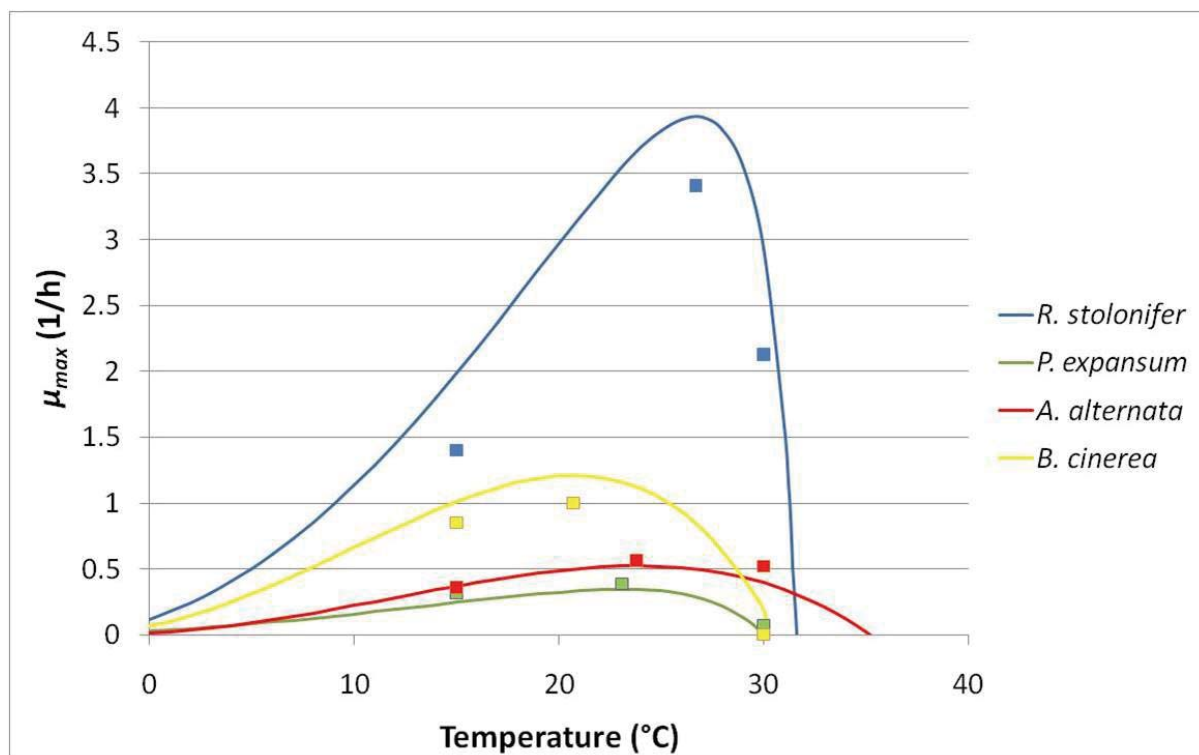
Figure 3.3. *Validation studies of the model with fungal study collected on PPA. Continuous lines correspond to predicted growth rate values by the model, while scattered points are the observed growth rates from the PPA experiments.*

3.4.3. In vivo studies

Studies on fungal growth on pear fruits were performed to further compare the kinetic parameters between the synthetic and the simulated pear medium. Graphs from Figure 3.4 show the results from the *in vivo* studies on the wound-inoculated pears. Diameter maximum and minimum of the lesions produced by the fungi are plotted as ellipsoids expanding in function of the time. Additionally, lesions' diameter maximum was plotted against time in order to calculate the growth rate by linear regression.
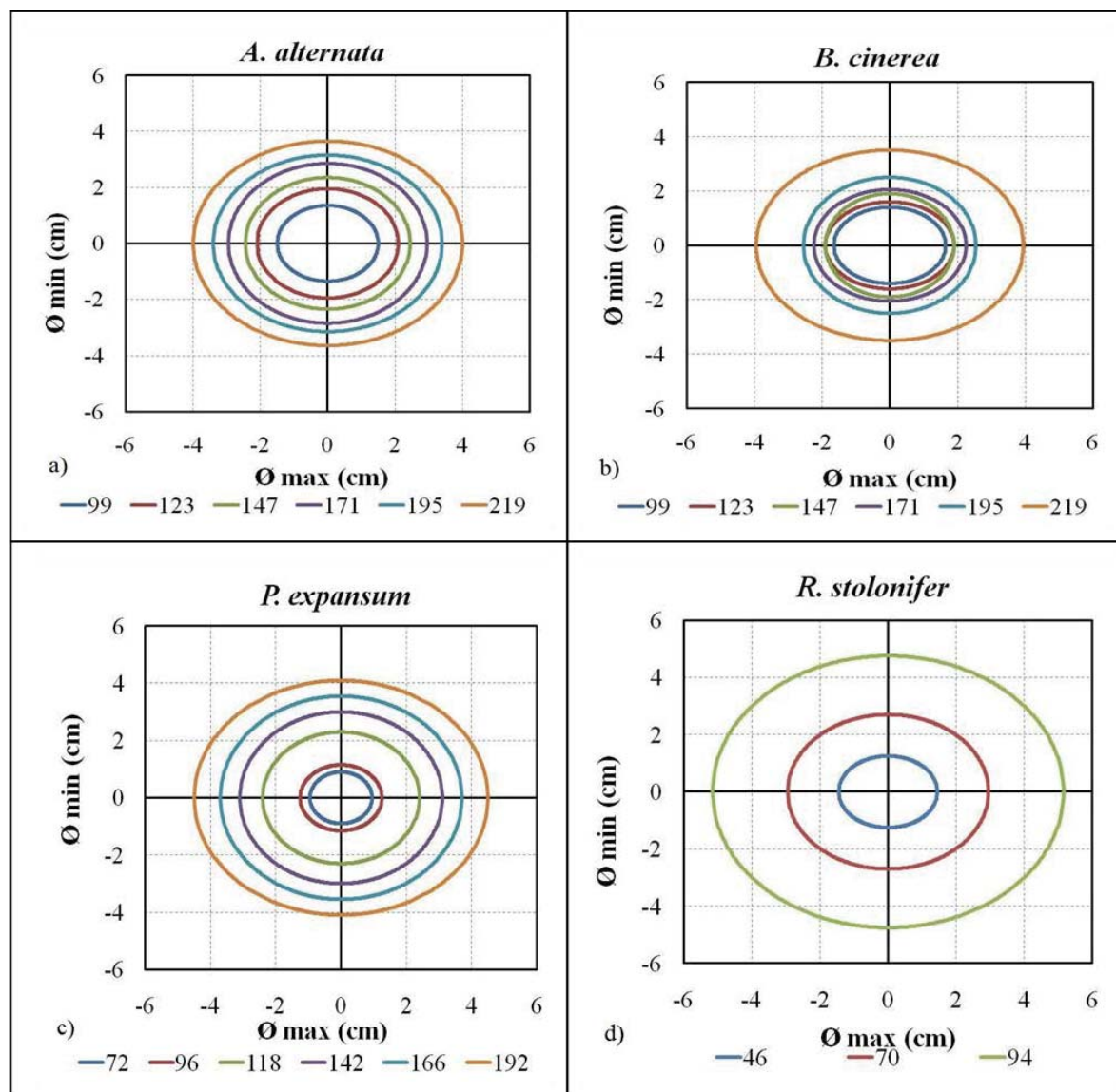
Figure 3.4. *Growth results on artificially inoculated pear fruit. Diameter maximum is plotted against diameter minimum. Diametric increase with time is plotted with different colours of concentric ellipses representing the surface area of the lesions.*

From the results we can clearly deduct that, also in this case, *R. stolonifer* is the most aggressive fungus since it has a significant higher growth rate (Table 3.3), compared to the other isolates. However, in this case, *R. stolonifer* is followed by *P. expansum*, *A. alternata* and finally by *B. cinerea* (Figure 3.5) in terms of aggressiveness, a different situation than what described previously.

Table 3.3. *Comparison between growth rates obtained on PPA and artificially inoculated pear fruit at the estimated optimal temperatures from the CMI. Small and capital letters show the statistical analysis (t-test) performed between fungi. A similar analysis was performed between media.*

	T (°C)	PPA	Pear
B. cinerea	20.7	1.00 ± 0.00 [a]	$0.16 \pm 1.41 \times 10^{-3}$ [A]
R. stolonifer	26.7	$3.41 \pm 2.28 \times 10^{-3}$ [b]	0.77 ± 0.00 [B]
P. expansum	23.1	$0.38 \pm 2.08 \times 10^{-3}$ [c]	$0.30 \pm 0.70 \times 10^{-3}$ [C]
A. alternata	23.8	$0.57 \pm 0.57 \times 10^{-3}$ [d]	0.20 ± 0.00 [D]
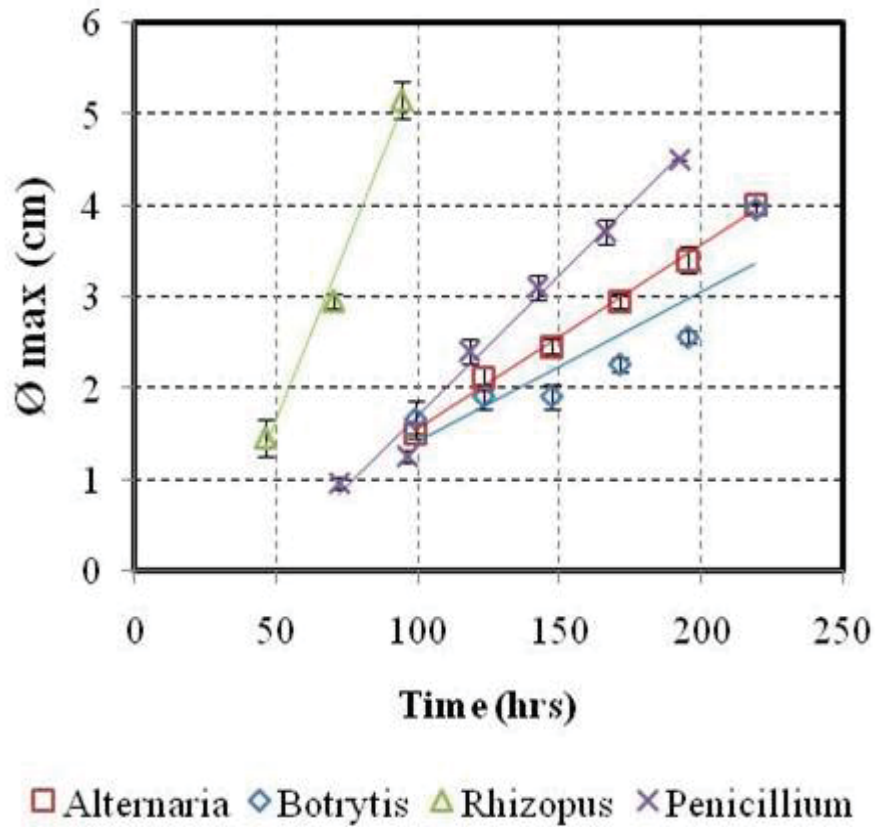
Figure 3.5. *Comparison of diameter maximum increase against time for all the four fungal isolates on artificially inoculated pear fruit.*

Furthermore, with the only exception of *P. expansum*, a significant difference in the growth rate values can be observed if compared to the values obtained from the PPA plates (Table 3.3).

3.5 Discussion

3.5.1. Modelling the effect of the temperature on SDA plates

The very low estimated value of T_{min} for *P. expansum* complies with the assumption that *P. expansum* is a psychrophile (Pitt and Hocking, 2009): minimum temperatures for its growth have been reported to be as low as -6°C (Brooks and Hansford, 1923), -3°C (Panasenko, 1967; Sommer, 1989) and -2°C (Mislivec and Tuite, 1970) with also a quite strong growth at 0°C (Kuehn and Gunderson, 1963). Regarding the aggressiveness of *R. stolonifer,* this is also supported by previous comparative studies showing that isolates from the genus *Rhizopus* had high growth rates if compared to other genera. In a study about the development of a predictive model for quality control in yogurt production (Gougouli et al., 2011), the authors found that among a selection of 14 fungal isolates, *Rhizopus oryzae* was the most aggressive. The genus *Rhizopus,* and in particular *R. stolonifer*, is characterised by coarse, rampant growth and rapidly maturing spores which make it a source of endless contamination (Pitt and Hocking, 2009). *R. stolonifer* and *R. oryzae* belong to the class of the Zygomycetes which are characterised by coenocytic hyphae with no or very few septa (Pitt and Hocking, 2009) usually found at the bases of the reproductive organs and only occasionally elsewhere (Alexopoulos and Mims, 1979). Absence of septa enhances rapid translocation and absorption of nutrients, hence conferring rapidity of growth to the fungus (Pitt and Hocking, 2009). Under favourable conditions, *R. stolonifer*'s spores germinate by germ tube that quickly develops into a fluffy, many-branched, white, aerial mycelium (Alexopoulos and Mims, 1979). *R. stolonifer* has been reported to grow from 4.5 or 5°C up to 30°C or 35-37°C (Pierson, 1966; Pitt and Hocking, 2009; Schipper, 1984), with an optimum near 25°C (Pitt and Hocking, 2009). Concern is also sometimes expressed that postharvest disease organisms might adapt, by mutation or selection, to grow at lower temperatures. As a matter of fact, a low temperature strain of *R. stolonifer* was observed

when the fungus was repeatedly grown at barely permitting growth temperatures (Sommer, 1989). Furthermore, in a study about the effects of cold-storage temperatures on 39 selected *Rhizopus* spp. isolates (Siefkes-Boer et al.,2009), it was found that, at the temperatures of 1.1 and -0.5°C only four and ten isolates, respectively, out of the 39 did not manage to grow, while all the isolates were able to grow at temperature > 3°C. Such "cold-tolerant" isolates were able to produce leak symptoms on artificially wounded strawberries (Siefkes-Boer et al., 2009). *B. cinerea* is also known to be a very aggressive fungus (Abu Qamar et al., 2016; Dean et al., 2012)which is able to complete an infection cycle within 3-4 days under optimal growth conditions (Lahlali et al., 2007). In the current study it had the second highest growth rate, after *Rhizopus*. Estimations of the cardinal temperatures from previous studies on PDA at a_w=0.99 (Daniela Judet-Correia et al., 2010) found an optimal temperature of 21.4°C with a minimum at -1.39°C and a maximum at 29.1°C. On the other hand, growth rates of *P. expansum* were also compared with those of *B. cinerea* by Judet-Correia et al. (2010) by means of the CMI, finding that *P. expansum* was the most psychrophilic fungus with an estimated T_{min}= -4.4°C, while *B. cinerea* showed a T_{min}= -1.39°C. Additionally, the optimal growth rate of *B. cinerea* was significantly higher than the one of *P. expansum* (Judet-Correia et al., 2010). This comparative analysis between *B. cinerea* and *P. expansum* is in agreement with our study regarding the most psychrophilic fungus in relation to the growth rate.

A. alternata is second to *R. stolonifer* in terms of lag time duration and it places itself between *B. cinerea* and *P. expansum* in terms of growth rate. Some reports have shown that *A. alternata* is not a particularly cold-resistant fungus as minimum growth temperature has been reported between 5 and 6.5°C (Pitt and Hocking, 2009; Pose et al., 2009). However, it has also been reported that *A. alternata* can cause significant rots on stone fruit at 0°C and has a T_{min}= -2.77°C

for growth in peaches, plums and nectarines (Sommer, 1989) which is closer with the theoretical T_{min} estimated from the CMI model in the current study. Furthermore, according to this study, *A. alternata* is the isolate with the highest T_{max}= 35.2°C. Interestingly, it has been observed (Pose et al., 2009) that *A. alternata*'s most favourable temperatures for growth are both 21°C and 35°C as they show the shortest germination time with very slight differences among different a_w values. *A. alternata*'s growth was also observed at 37°C (Palou et al., 2012).

3.5.2. Model validation

In a previously mentioned study (Judet-Correia et al., 2010), model validation was performed from results obtained with PDA on a simulated grape juice medium and a grape juice agar. In that study, the bias factors (B_f) were close to 1 for both *P. expansum* and *B. cinerea*. Accuracy factors (A_f) were much more dependent on the species and on the medium and were higher than 1 for both the isolates. *B. cinerea* showed slightly bigger deviation than *P. expansum*, especially on simulated grape juice medium (Judet-Correia et al., 2010). *B. cinerea* showed higher values of A_f and B_f than *P. expansum* also in the case of our study. Nevertheless, the highest deviation, amongst all our isolates, was observed for *R. stolonifer* (Table 3.2). The failure of the model to describe accurately the growth responses of *B. cinerea* and *R. stolonifer* indicates that SDA should be considered with caution when assessing the cardinal values of these two fungi. Models for these two fungi should be developed in the future either by directly using PPA plates or developing model structures that are extended in order to capture the discrepancy between the tested media. In a similar study (Baert et al., 2007) the growth of selected *P. expansum* strains was studied on an apple puree medium at different temperatures by several developed models and an external validation was performed on inoculated apples. Obtained A_f and B_f values from apples indicated conservative prediction of growth rates but a clear deviation and

43

underestimation for the lag phase between predictions and observed values on apples (Baert et al., 2007). As also stated by Baert et al. (2007), these results highlight that the approximation given by the use of synthetic or simulated media for the development of predictive models can lead to unrealistic predictions and a validation on a real food matrix is therefore always necessary. In our studies, it is evident that the *in vitro models* developed to describe the dynamics of *P. expansum* results in accurate predictions at *in vivo* environments. The other fungal models should be used with caution or should be extended by developing correction factors or collecting data directly in more realistic or *in vivo* environments.

3.6 Conclusions

The prediction model and the synthetic medium used in this study were suitable to describe the *in vitro* mycelium growth as a function of the temperature for different postharvest fungal isolates. Validation on a simulated pear medium showed that predictions were realistic for almost all the isolates with some deviation in the case of *R. stolonifer* and *B. cinerea*. However, when the same isolates were grown on a real food matrix at the predicted optimal temperatures, with the only exception of *P. expansum*, significant different growth rates were obtained between pears and pear pulp agar medium. These results indicate that the nutrient substrate has a big influence on the fungal growth rate and that a simulated medium may provide results which are distant from what happens on food. Such limitation must always be considered in predictive mycology studies and implemented by accuracy and/or correction factors in order to develop the most accurate and precise predictive models.

Chapter 4: Optimized turbidimetric protocol for the assessment of the growth of pear postharvest fungi.

4.1 Introduction

4.1.1. Assessment approaches of fungal growth

The estimation of fungal growth is a challenging procedure since no primary standard exists as for yeasts and bacteria (Pitt & Hocking, 2009). This is because fungi do not grow as single cells, but as hyphal filaments that cannot be quantified by the usual enumeration techniques used in bacteriology. In addition, fungi differentiate to produce spores, resulting in large increases in viable counts often with little relationship to biomass (Pitt, 1984; Taniwaki et al., 2006). Different techniques have been developed to assess the fungal growth, although they all show some limitations. Measurement of colony diameter, also reported as *radial growth rate* studies, is the most direct *in vitro* measure. It consists of measuring the diameter of macroscopic colonies onto solid media at different time intervals. A growth rate function can then be derived by performing a regression analysis on the linear part of the data correlating colony diameter increasewith time (Sonia Marín et al., 2005).However, this method shows poor correlation with fungal biomass since it is not related to colony density (Taniwaki et al., 2006; Wells and Uota,1970) and does not take in account the three-dimensional growth of filamentous fungi (Medina, Lambert, & Magan, 2012). Additionally, filamentous fungi are morphologically complex microorganisms, exhibiting different structural forms which vary considerably within fungi depending on genes, nature of the inoculum, medium constituents, temperature, pH, culturing conditions (Papagianni, 2004) as well as on the presence of chemical compounds (Zafra *et al.*2015).

Counting of viable propagules, i.e., colony forming units (CFUs), is another simple technique

derived from bacteriology that suffers from serious drawbacks since viable counts usually reflect spore numbers rather than the fungal biomass (Pitt, 1984). Alternatively, germination studies can be used to assess the fungal growth since spore germination is an essential developmental stage in the life cycle of all filamentous fungi (d'Enfert, 1997). Germination consists of the conversion of a *dormant* spore into an active one due to breaking of internal metabolic blocks, followed by an increase in both spore diameter and biomass (Gougouli et al., 2011). After a certain time, a germ tube protrudes from the enlarged spore which is considered to have germinated when the length of the tube is greater or equal to the greatest dimension of the spore (Dantigny, Guilmart, & Bensoussan, 2005; Gougouli et al., 2011). Furthermore, the relation between spores germination and mycelium growth has been studied combining microscopic and macroscopic techniques with mathematical prediction models (Gougouli & Koutsoumanis, 2012). The distributions of the mycelium lag time were found to be similar to those of the germination time, but shifted with a significant delay compared to germination studies. Like in the previous cases, this technique will also need to be correlated to fungal biomass. For example, a kinetic model has been developed and validated (Bizukojc & Ledakowicz, 2006) to predict indirectly the biomass concentration of *Aspergillus niger*.

Evidently, fungal biomass is considered as a fundamental measure of fungal growth and different assays, usually destructive, have been implemented for its quantification. The most direct one consists of the estimation of the mycelium dry weight, but it lacks sensitivity since soluble fungal components may be extracted, resulting in a loss of dry weight (Taniwaki et al., 2006). Chemical assays are more sensitive and rely mostly on some unique components of the fungus that are not found in other microorganisms or in solid substrates (Pitt and Hocking, 2009). On one hand, chitin assay was one of the most common indirect method for estimating fungal biomass used in

the past but it has been now largely replaced by the ergosterol assay (Pitt and Hocking, 2009).Chitin is the major glucosamine polymer in both conidial and mycelial cell walls, hence it can be used to estimate fungal growth. The major methods used to analyze its concentrations consisted of an initial enzymatic hydrolysis followed by quantification of the degradation products using different techniques, such as colorimetry, chromatography and fluorescence microscopy (Cousin, 1996; Pitt & Hocking, 2009). The principal sources of error of the chitin assay were the necessity of a conversion factor to equate glucosamine concentration to mycelial dry weight and the effect of the substrate composition, since sugars could lead to an over-estimation of the chitin content (Cousin, 1996; Pitt and Hocking, 2009). On the other hand, ergosterol is a fungal-specific membrane lipid so it is inherently likely to be correlated with hyphal growth and biomass. The most common and widely used method for ergosterol quantification is High Performance Liquid Chromatography HPLC (Marin et al., 2005). Numerous studies have assessed the relationship between fungal growth and ergosterol production, using both liquid and solid substrates (Marín et al., 2008; Noll et al., 2016; Taniwaki et al., 2001). However, ergosterol levels can vary with medium composition, culture conditions and the measurement of ergosterol alone does not give the absolute amount of fungus present (Taniwaki et al., 2006). Furthermore, it should be carefully used as an indicator of the living fungal biomass since it is significantly sensitive to photochemical degradation (Mille-Lindblom & Tranvik, 2004). Finally, it should be highlighted that the method is laborious and in most cases destructive.

Measuring the optical density (O.D.) of growing cultures is a common method to quantify various important parameters like cell concentration, biomass production or changes in the cell morphology. Turbidimetry is a non-destructive, simple and reliable method in which fungi or

bacteria are grown in wells of microtitration plates and their growth is monitored by measuring the increase of the O.D. of the microcultures with a microtitre reader. The use of the microtitre reader became increasingly popular for measuring the turbidity of bacterial cultures because of the ability of this instrument to analyse up to 96 samples in few seconds (Broekaert et al., 1990). Furthermore, turbidimetry needs minimal amounts of sample and it can benefit from a computerized processing of the data which gives the possibility of performing kinetic growth studies (Skytta et al., 1991). However, in order to adapt this technique to unevenly growing filamentous fungi, parameters like inoculum size, medium composition and agar content need to be optimized (Broekaert et al., 1990; Medina et al., 2012) since they are closely related to the optical properties of the sample and they may significantly influence the outcomes of the experiments. There are few fungal turbidimetric studies which mostly aimed at assessing the antifungal properties of some compounds (Gkana et al., 2016; Medina et al., 2012; Meletiadis et al., 2003; Meletiadis et al., 2001; Rossi-Rodrigues et al., 2009). In these studies several parameters have been already optimized, such as agar concentration and inoculum size (Medina et al., 2012), but there is a lack of information regarding the choice of these two parameters also in relation to the nutrient medium. Due to the great variability in the growth rate, sporulation time and nutrient requirements among filamentous fungi in relation to different culture media, the suitability of every medium for the turbidimetric assay should not be implicitly assumed (Meletiadis et al., 2001).

4.2 Objective

The objective of this work was to quantitatively assess the growth and morphology of four postharvest filamentous fungi (i.e.: *Penicillium expansum*, *Alternaria alternata*, *Botrytis cinerea*,

Rhizopus stolonifer) in order to identify the most suitable combination of nutrient media and inoculum size that permits the development of an experimental protocol able to provide uniform and reproducible results by the use of a turbidimetric assay. Furthermore, the experimental design of this technique is revised and complemented also by predictive mycology tools.

4.3 Materials and methods

4.3.1. Preparation of inocula

Fungal spores were harvested from 5-day old MEA Petri dish cultures by adding 10 mL of a 0.05% Tween-80 solution and by scraping off the plates' surfaces with a sterile bent rod. The resulting suspensions were aseptically filtered through a 4-layer sterile gauze to remove any mycelial contamination. The turbidity of each suspension was adjusted to an optical density (O.D.) value of 0.25 at 600 nm with a colorimeter (Jensen, Northern Carolina, U.S.A.) for all the fungi. Spores' concentrations were determined with a haemocytometer and were found to be $3x10^6$ spores/mL for *A. alternata*, $2x10^5$ spores/mL for *B. cinerea*, $4x10^5$ spores/mL for *R. stolonifer* and $2x10^6$ spores/mL for *P. expansum*. Two 10-fold sequential dilutions were also prepared from each neat suspension for all the fungi.

4.3.2. Preparation of media

Three different nutrient media were prepared for these experiments: Sabouraud Dextrose Agar (SDA) with 4g of dextrose and 1g of peptone in 100mL of distilled water. Yeast-Extract Dextrose Agar (YED) with 15g of dextrose, 2g of yeast-extract and 0.05g of magnesium sulphate in 100mL of distilled water. Potato Dextrose Agar (PDA) was prepared from raw potatoes in

order to get a more satisfactory potato infusion than commercially dehydrated forms (J. Pitt & Hocking, 2009; Rinaldi, 1982).To prepare the potato infusion, 20g of sliced, peeled potatoes (Category: Agata, Origin: Italy) were boiled in 100 mL of distilled water for 30 min. After boiling, the potato infusion was cooled down to room temperature and potato slices were filtered through a cheesecloth decanting the effluent into the rest of the infusion. The refraction index of the potato infusion was measured for each replicate experiment with a refractometer (ATAGO, Japan) and was found to be n_D= 1.3340±0.0001 at 25ºC. Finally, 2g of dextrose were added to the infusion, mixed thoroughly with agar and final volume was brought back to 100mL with distilled water. All media were sterilized by autoclaving at 121°C for 15 min.

4.3.3. Assessment of growth

A turbidimetric assay was used to assess the filamentous fungal growth. Semi-solid preparations of SDA, YED and PDA were used. Agar content for all the media was 0.125% w/v since it has been shown (Medina et al. 2012) to give reproducible and consistent results.150 μl of each medium and 20 μl of each inoculum suspension were decanted and mixed into each well of standard 96-well flat-bottom plates for microtitration (Thermo Scientific, Denmark). Plates were incubated at 25ºC into a Tecan Sunrise™ microtitre reader. O.D. was read at 600 nm automatically every 20 min without shaking. Sequential O.D. measurements were used to generate growth curves for each fungus, medium and inoculum size. Quantification of the fungal growth kinetics was performed by applying the trapezoidal method in Microsoft Excel®.

4.3.4. Microscopic examination

The structure of the fungi was also examined microscopically during the growth studies. Therefore, an additional microtitration plate was prepared for each fungus in the same way of

those for the turbidimetric assay and incubated at 25°C. Plates were observed under a Leica™ inverted microscope at 40X magnification. Images were obtained at intervals of 46, 70 and 94 hours.

4.4 Results

4.4.1 Growth quantification

Figures 4.1 – 4.4 show the results from the calculations of the fractional areas (represented as bar graphs) for each medium used in this study with the respective values of standard deviation. Values are obtained from the average of six replicate experiments. Although not a particular trend can be deducted regarding the choice of the inoculum size resulting in the lowest variation, it can definitely be considered that the most suitable media, in terms of reproducibility upon different replicates, are the PDA and YED for all the fungi, even though YED shows the lowest variability in the major part of the cases.
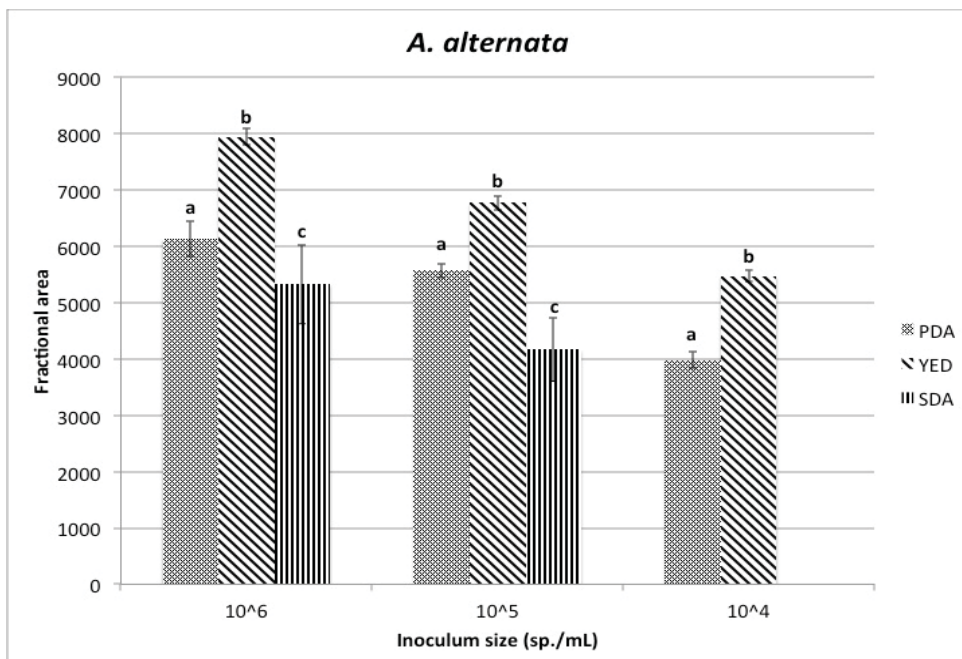
Figure 4.1 *Fractional areas of A. alternata for each medium and inoculum. Different letters show the results of the statistical analysis (t-test) performed between different media.*
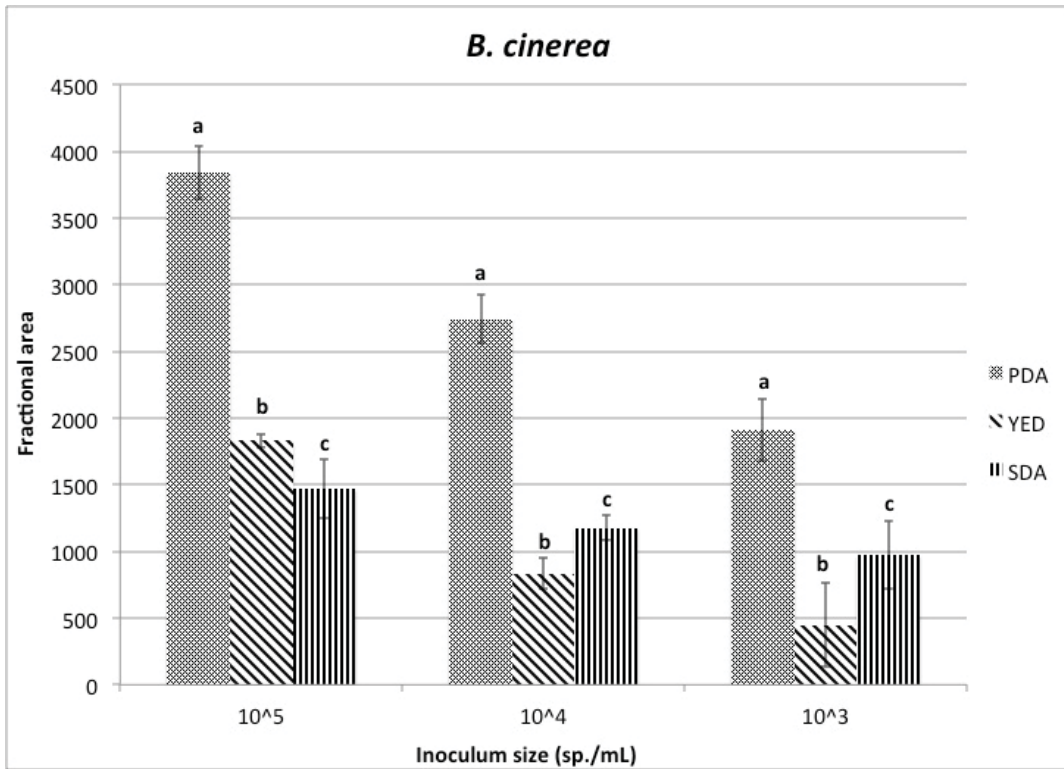
Figure 4.2 *Fractional areas of B. cinerea for each medium and inoculum. Different letters show the results of the statistical analysis (t-test) performed between different media.*
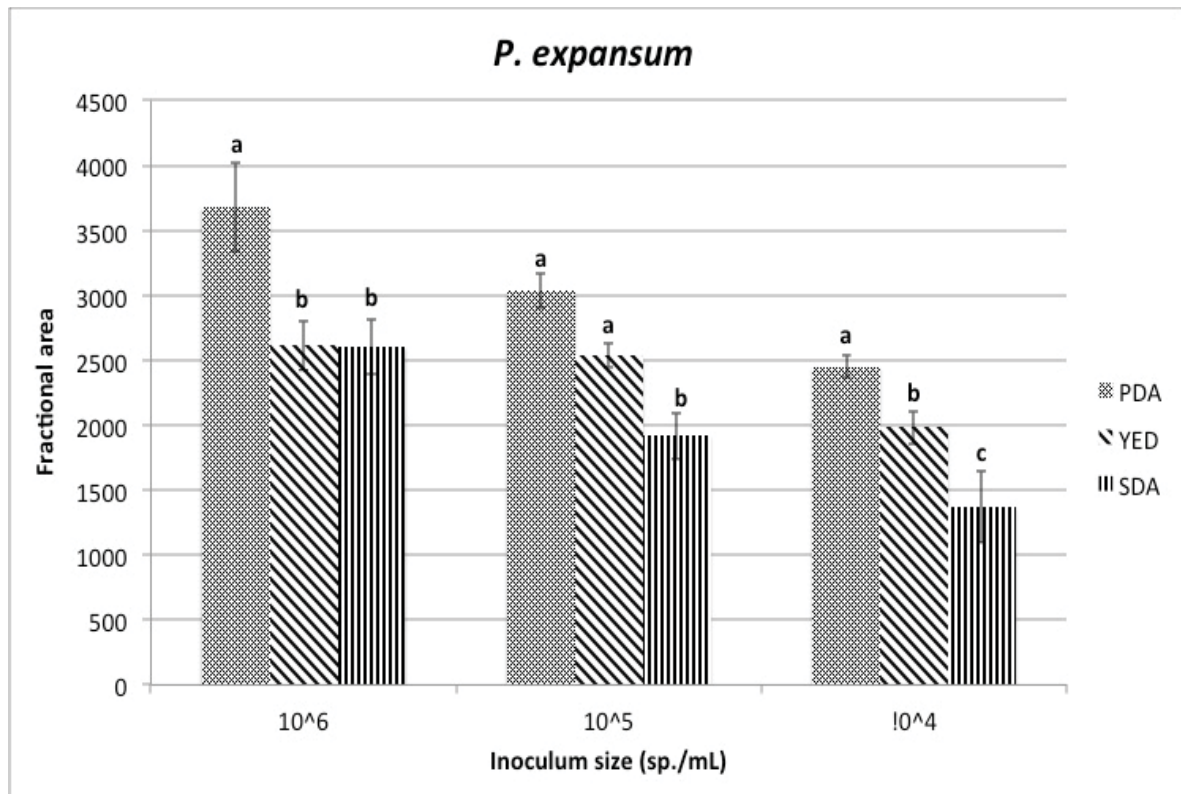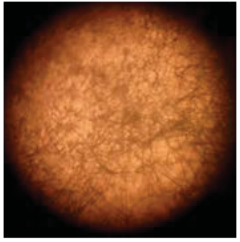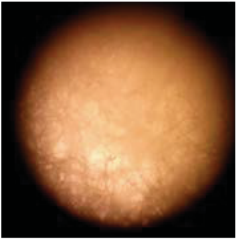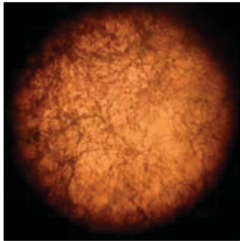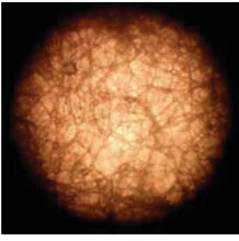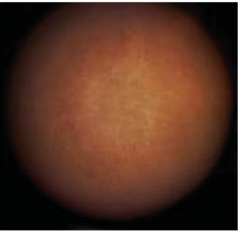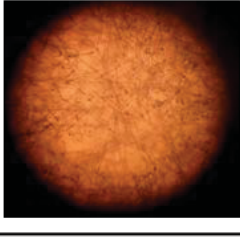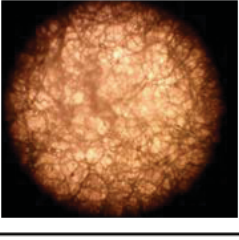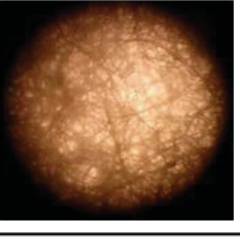
Figure 4.3 *Fractional areas of P. expansum for each medium and inoculum. Different letters show the results of the statistical analysis (t-test) performed between different media.*
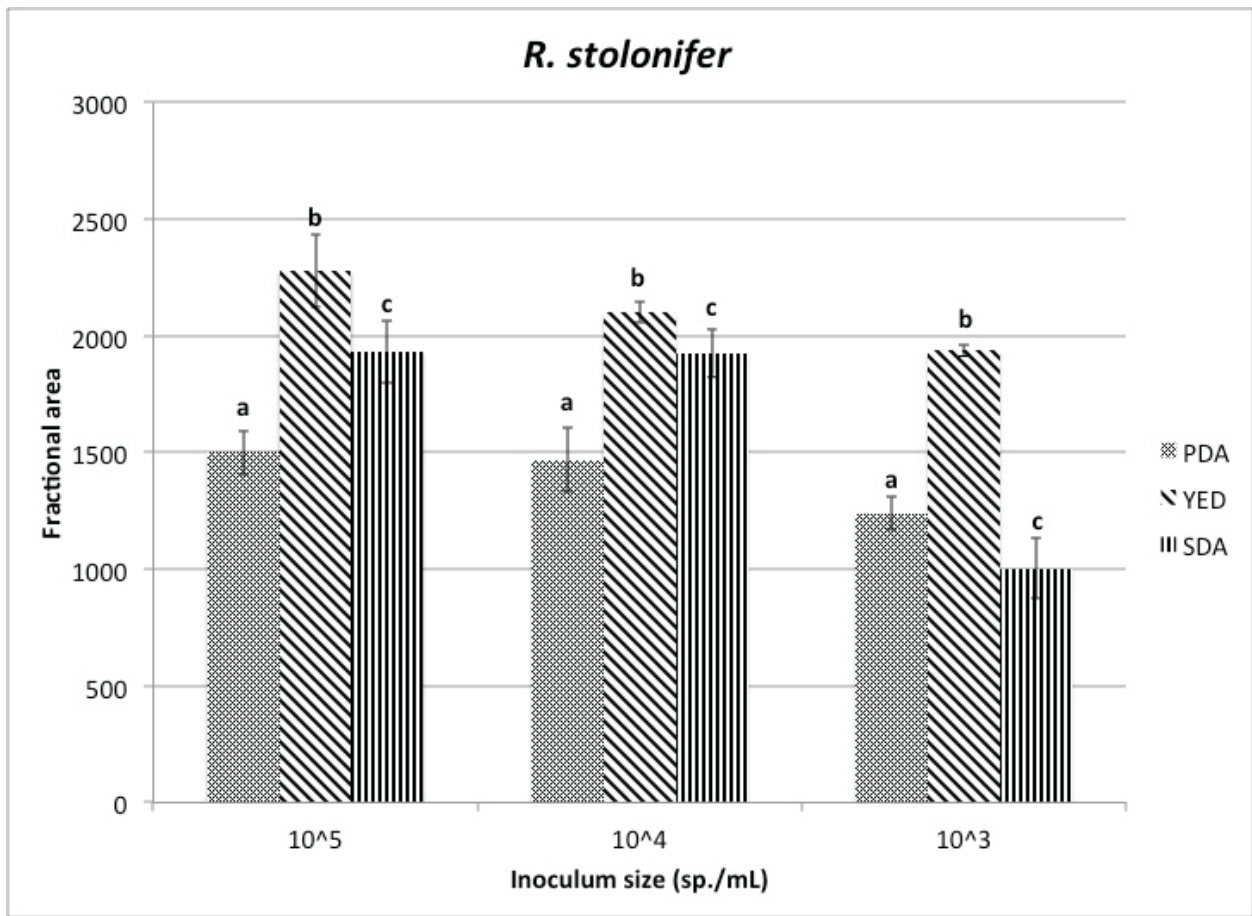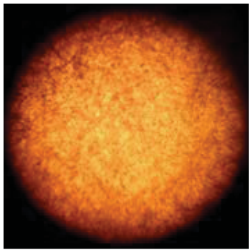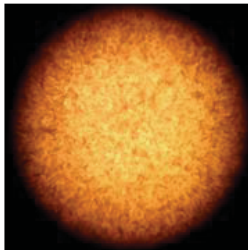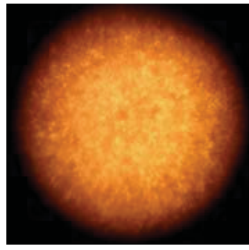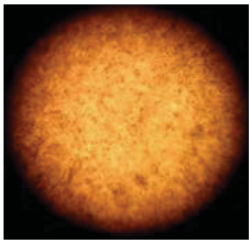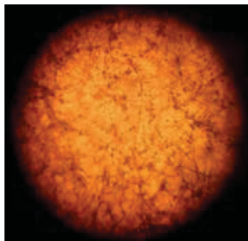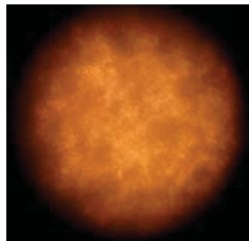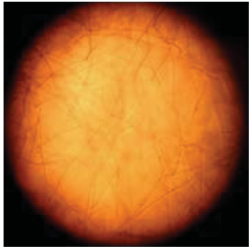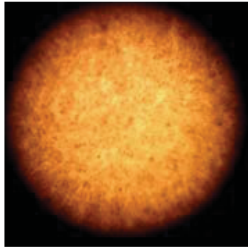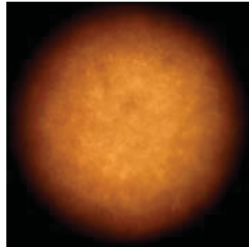
Figure 4.4 *Fractional areas of R. stolonifer for each medium and inoculum. Different letters show the results of the statistical analysis (t-test) performed between different media.*

4.4.2 Microscopic examination

Images from the microwells of the culture of *Alternaria alternata* are shown in Figs. 4.5-4.7. In Fig. 4.5, images from PDA microwells show that, from 46 to 70 hours, the growth proceeds quite homogeneously with few exceptions where there is a higher hyphal concentration on the edge of the well (46 hrs, 10^5 sp./mL). At 70 hours for the 10^6 sp./mL inoculum size, an abundant growth occurs which makes the well opaque. This phenomenon increases at 94 hours except for the lowest inoculum size (10^4). Similar results can be observed for the YED microwells in Fig. 4.6, although the growth appears more homogeneous than in PDA, especially for the 10^6 inoculum size. This is also the only case when the well does not turn opaque throughout the growth. In the case of SDA, as shown in Fig. 4.7, a big mycelial growth develops already at 46 hours for the 10^6 sp./mL inoculum size and the well turns opaque after 70 hours.

Figure 4.5. *Images of each microwell from the culture of A. alternata on PDA at different inoculum size and time intervals.*

Figure 4.6. *Images of each microwell from the culture of A. alternata on YED at different inoculum size and time intervals.*

	SDA		
	46 hrs	**70 hrs**	**94 hrs**
10^6			
10^5			
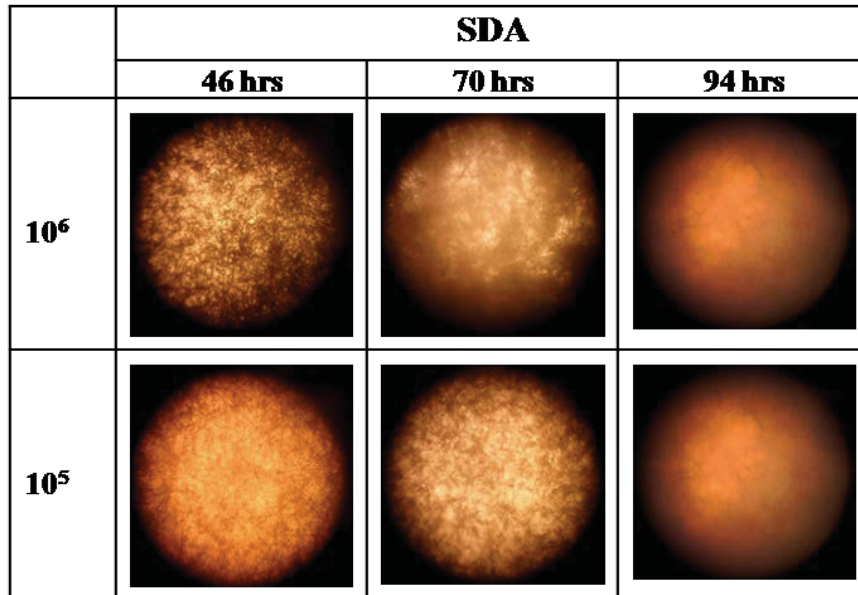
Figure 4.7. *Images of each microwell from the culture of A. alternata on SDA at different inoculum size and time intervals.*

4.5 Discussion

The growth of filamentous fungi consists of complex microscopic differentiation resulting in various visible appearances (Grimm et al., 2005; Kossen, 2000). Such processes involve different cell types leading from conidia, over germ-tubes, to hyphae. In our microscopic examination we could clearly see how the fungi were developing from small hyphal formations in the early growth stages, into more complex and dense structures with a consistent spore germination after 70 hours of incubation, especially on YED medium (Figure 4.6). Variation in turbidity, associated to morphological changes, has been established as a parameter to predict and quantify fungal growth in submerged cultures (Morris and Nicholls, 1978; Trinci, 1972). However, since fungi produce mycelial biomass, whose weight increases exponentially only during the early growth stage (Koch, 1975), as well as the fact they are not unicellular and can spread in three-dimensions, quantification and modelling of growth becomes difficult (Dantigny et al., 2005;

Medina et al., 2012; Meletiadis et al., 2001). Furthermore, most mycelial pellets can sediment rapidly thus preventing accurate measurement of turbidity (Calam, 1969). In order to overcome these limitations, different parameters involved in turbidimetric protocols, such as agar concentration, inoculum size and nutrients' composition need to be optimized. In our assay semi-solid (0.125%) agar formulations was used since it has been shown (Medina et al., 2012) to have the appropriate consistency for fungal spore germination and growth initiation. This particular composition is able to retain the spores in the three dimensional space of the microwells thus preventing them to settle in the bottom and resulting in a more uniform development of the hyphal network (Medina et al., 2012) as was also shown in the current research (Figures 4.5-4.7). When the effect of different inoculum sizes has been assessed, it was found that, although there is not a specific trend, inocula concentrations comprised between 10^6 and 10^3 sp./mL, were able to give consistent results. The selection of the inoculum levels included those of a previous turbidimetric study (Medina et al., 2012) where it has been shown that spores' concentrations of 10^5 or 10^6 spores/mL give the best reproducible results in the case of *Aspergillus flavus*. Hitherto there is no consensus about the choice of the optimal nutrient medium for turbidimetric assays. Nevertheless, by definition, a nutrient medium must be able to support adequate growth of the fungus and must result in reproducible results (Meletiadis et al., 2001). Such assumptions are of fundamental importance for the appropriate use of the turibidimetric assay, since it has been mainly used as an antifungal susceptibility test. Meletiadis et al., (2001) demonstrated (Meletiadis et al., 2001) that the choice of a poor medium in which fungi grow slowly or a medium that provides high variability in the growth rate may produce unclear and misleading results in antifungal testing, especially in terms of MIC estimation. An optimal nutrient medium should therefore provide the best possible growth in order to allow moulds to develop without

restrictions and to express all phenotypes (Meletiadis et al., 2001). Colony morphology is also affected by the nutrients composition of the medium (G. Sharma & Pandey, 2010), despite the fact that it has been poorly investigated with regards to the turbidimetric assay. However, a macroscopic morphological study about the growth of the fungus *Curvularia lunata* has been performed onto three different liquid media (Lanisnik Rizner & Wheeler, 2003). The authors have shown that the fungal morphology could vary from branched hyphae, dispersed throughout the medium, to star-like compact pellets. Furthermore, different carbon and nitrogen sources could also affect mycelial mass as well as pigment production (Tea & Romih, 2007). In this study we show that both YED and PDA are suitable media to assess the growth dynamics of filamentous fungi in the turbidimetric assay giving reproducible and consistent results upon repeated experiments. However, knowing that the appropriateness of a medium for filamentous fungi should never be implicitly postulated (Meletiadis et al., 2001), appropriate selection should always bemade. From one hand YED gave the lowest variation and the most homogeneous colony morphology, on another hand PDA's outcomes were not significantly different. Additionally, we here prepared PDA from fresh potatoes in order to get a more satisfactory nutrients' composition (Pitt and Hocking, 2009) than dehydrated powders. Furthermore, the preparation of PDA from fresh potatoes is listed by the U.S. Food and Drug Administration as an approved laboratory method to help ensure food safety (BAM Media M127) (FDA, 2001), while YED preparation from fresh yeast extract is not present in such list.

4.6 Conclusions

An automated turbidimetric assay has been successfully developed to investigate the different growth characteristics of four filamentous fungi in microtitration plate cultures. Semi-solid YED and PDA appear to be the most suitable media for fungal growth investigation. If compared to other techniques for fungal growth estimation, the turbidimetric assay shows several advantages, such as the possibility to analyze up to 96 samples per time, the minimal amount of substances required and the automated processing of the data. This work provides essential support to further studies aimed at assessing fungal growth by means of turbidimetric protocols, especially in the case when the efficacy of an antifungal compound needs to be investigated in a rapid, reliable and quantitative way.

Chapter 5: Assessing the efficacy of ZnO nanoparticles against postharvest fungal isolates by automated turbidimetric analysis

5.1 Introduction

5.1.1. Assessing the efficacy of novel antifungal compounds

Studies aimed at assessing the antifungal properties of compounds involve several bioassays commonly used in microbiology, such as agar disk-diffusion test (Banoee et al., 2010) and colonies diameters measurement (He et al. 2009; Savi et al. 2013) (refer also to Appendix 1 regarding the optimization of the protocols to assess the efficacy of ZnO NPs as antifungal agent). Such techniques come from the protocols generally used to assess the fungal growth but with the addition of an antifungal agent that needs to be tested. For instance, colony diameter measurement can be modified by incorporating the antifungal agent or extract into the molten agar at a desired concentration and mixed well (Balouiri et al., 2016). The medium is then poured in Petri dishes and the diameter of the fungal growth on the plates is measured as usual. When testing an antifungal compound, this technique is also known as "Poisoned food method" (Balouiri et al., 2016). However, as extensively shown in Chapter 3, among all the available protocols to investigate the fungal growth, turbidimetry is an interesting and promising technique since it has the advantage of being automated, not destructive and to correlate culture absorbance with fungal biomass (Meletiadis et al., 2003). In recent years, there has been a growing interest in researching and developing new antifungal agents from various sources (reference to biological control strategies is made in Appendix 2 where the evaluation of the interactions between *Erwinia persicina*'s biofilms and fungal isolates are reported) to fight against resistance

phenomena or to replace toxic and potentially carcinogenic compounds, therefore great attention must be paid to antifungal activity screening and evaluating methods. Nanotechnology has brought great opportunities and alternative solutions for the development of new antifungal agents (Espitia et al., 2012), such as metal nanoparticles. Amongst the currently available metal nanoparticles (previously illustrated in Chapter 2), zinc oxide nanoparticles (ZnO NPs) possess superior durability, lower production cost at industrial scale, greater selectivity and heat resistance, if compared to copper and silver nanoparticles (He et al., 2011).Furthermore, silver nanoparticles have some risks as the exposure to silver can cause agyrosis (Rai et al., 2009) and it is toxic to mammalian cells (Gong et al., 2007) unless if used in minute concentrations. Unfortunately, copper compounds may also be toxic to fish and other organisms and they may also cause environmental hazards. Therefore, direct use of copper and copper compounds in high doses should be avoided (Ingle et al., 2014). Few studies have focused on the toxicological impact of ZnO nanoparticles as well as studies about biotransformation and elimination routes (Espitia et al., 2012). However, ZnO is currently one of the five zinc compounds that are listed as a generally recognized as safe (GRAS) substance by the U.S. Food and Drug Administration (FDA, 2016).

Turbidimetric assays found their first applications long time ago (Joslyn & Galbraith, 1950) for determining antibiotic strength of experimental preparations. At this time, the technique was not yet automated and was not performed on multiwell plates for microtitration. Throughout the years, turbidimetry protocols have been improved and automated by computerized processing of the data (Broekaert et al., 1990; Skytta et al., 1991) thus successfully used for screening the antibacterial activity of a large variety of compounds (Casey et al., 2004; Rainard, 1986; Sarker et al., 2007; Teh et al., 2017; Vijayakumar & Muriana, 2015) including nanoparticles (Martins et

al., 2011; Raghupathi et al., 2011; Salem et al., 2015). However, turbidimetric studies in mycology are quite limited (Medina et al., 2012; Meletiadis et al., 2003; Rossi-Rodrigues et al., 2009; Wilson et al., 1997) and, hitherto, far fewer studies (Kim et al., 2012; Pereira et al., 2014) are available about the antifungal screening of metal nanoparticles, and more specifically about ZnO nanoparticles.

5.2 Objective

The objective of this study was to assess the antifungal activity of ZnO NPs against *Penicillium expansum*, *Botrytis cinerea*, *Alternaria alternata* and *Rhizopus stolonifer* performing a turdidimetric assay. Fungal responses were compared based on the quantification of the surface areas extracted from the OD measurements. Furthermore, the Minimum Inhibitory Concentration (MIC) and Non Inhibitory Concentration (NIC) were estimated for *P. expansum* by predictive mycology tools.

5.3 Materials and methods

5.3.1. Preparation of the medium

This study (which was developed based on the revised protocol of Chapter 4) was carried out on semi-solid Potato Dextrose Agar (PDA) prepared from raw potatoes in order to get a more satisfactory potato infusion than commercially dehydrated forms (Pitt & Hocking, 2009). As per Chapter 4, agar content was 0.125% w/v to allow the development of a homogeneous hyphal network thus reducing light crossing the well in a way that is proportional to hyphal growth and, at the same time, preventing pellet sedimentation onto the bottom of the wells (Medina et al.,

2012). Medium preparation has been therefore performed by following the protocol illustrated in Section 4.3.2 for semi-solid PDA.

5.3.2. Antifungal screening

A turbidimetric assay was performed to investigate the antifungal activity of ZnO nanoparticles. ZnO nanopowder (<50 nm particles size, Sigma Aldrich, St. Louis, U.S.A.) was suspended into 100 mL of semi-solid PDA to reach the final concentrations of 0 mM, 6 mM, 12 mM and 15 mM for *A. alternata*, *B. cinerea* and *R. stolonifer*, while a wider concentration range (see Table 5.1) was chosen for *P. expansum* to allow MIC and NIC estimation. Media with nanoparticles were then placed into an ultrasonicating bath at 37 kHz sonicating frequency (Elmasonic S60, Elma,Singen, Germany) for 30 min in order to break nanoparticles' aggregations. An additional medium without ZnO was used as a control. Hereafter, 150 µl of the medium and 20 µl of the inoculum suspension were decanted and mixed into a standard 96-well flat-bottom plate for microtitration (Thermo Scientific, Denmark).Non-inoculated media with and without nanoparticles were also prepared and used as negative controls. The plate was incubated at 25ºC into a Tecan Sunrise™ microtitre reader (Tecan, Salzburg, Austria). O.D. was read at 600 nm automatically every 20 min without shaking. It is important to indicate that a reading at 600 nm is far away from the absorbance peak of ZnO (370 nm), so that light scattering due to Tyndall effect is negligible. Sequential O.D. measurements were performed to generate O.D .curves for each sample at least in triplicate. Each time the corresponding positive controls were also collected.

5.3.3. Quantitative assessment of the inhibitory concentrations

For this study, the area under the *O.D. versus time* was calculated by the trapezoidal method in Microsoft Excel®. Firstly a comparatively assessment was performed between the fungi. Hereafter, *Penicillium expansum* was chosen for estimating its MIC, NIC values. Selection was made considering it as the most common postharvest fungal disease. For the MIC studies, the ratios of the areas, or fractional areas (*fa*), with and without ZnO nanoparticles, referred to as A_c and A_{c0} respectively, where then calculated as follows (Guiller, Nazer, & Dubois-Brissonnet, 2007):

$$fa(c) = \text{Ac}/\text{A}_{c0} \tag{1}$$

where *c* is the concentration of ZnO. The updated version (Lambert & Lambert, 2003) of the Lambert-Pearson model (LPM) based on a Gompertz function (Lambert & Pearson, 2000) was then used to model the observed fractional areas:

$$fa(c) = \exp\left[-\left(\frac{c}{p_1}\right)^{p_2}\right] \tag{2}$$

where, p_1 is the concentration at maximum slope and p_2 is a slope parameter. The regression analysis was performed by using the Generalised Reduced Gradient (GRG) algorithm (Excel solver) and the least squares optimisation where the objective function is expressed as a sum of squares. For *P. expansum*, the minimum inhibitory concentration (MIC), defined as the concentration above which no growth is observed relative to the control and the non-inhibitory concentration (NIC) defined as the concentration below which normal visible growth is observed

(Chorianopoulos et al., 2006), were estimated from the LPM as follows (Chorianopoulos et al., 2006; Guiller et al., 2007):

$$\text{MIC} = p_1 \exp\left(\frac{1}{p_2}\right) \tag{3}$$

$$\text{NIC} = p_1 \exp\left(\frac{1-e}{p_2}\right) \tag{4}$$

5.4 Results

5.4.1. Antifungal effect of ZnO nanoparticles

ZnO NPs are able to inhibit the growth of the studied fungi at different levels (Figure 5.1). A significant shift in the growth is already visible at 6 mM ZnO NPs concentration for all the three isolates. *A. alternata* and *B. cinerea* do not show a significant difference in the level of inhibition at 15 mM, while *R. stolonifer* shows the highest inhibition at the same concentration. Results obtained are consistent as they were showing low variation among at least three replicate experiments thus demonstrating that PDA is a suitable medium for this type of studies and that turbidimetry is a suitable technique to assess the efficacy of ZnO NPs as an antifungal agent.
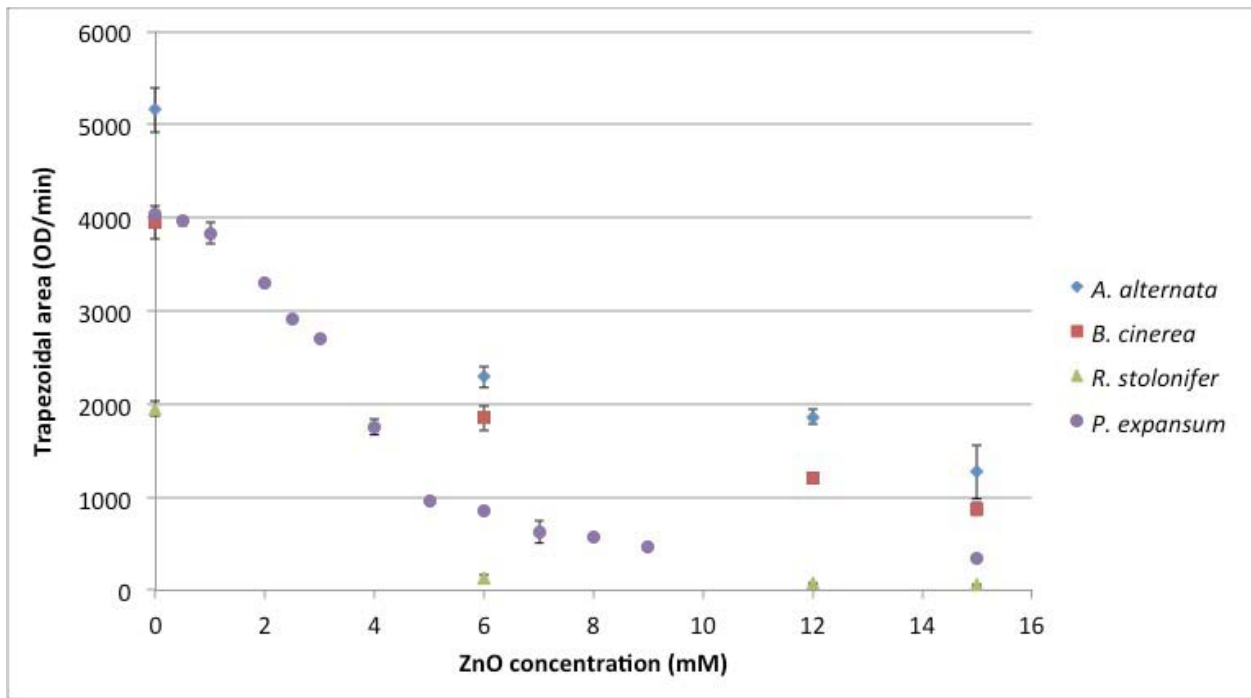
Figure 5.1. *Trapezoidal area vs ZnO NPs concentrations comparative plot for A. alternata, B. cinerea, R. stolonifer and P. expansum.*

5.4.2. Full inhibitory profile of *P. expansum*

Figure 5.2 shows the growth curves for a representative replicated experiment *with P. expansum*. The inhibitory effect of ZnO nanoparticles (C_1 to C_{12}) against the control (C_0) is already evident from the lowest concentration of ZnO (C_1). Samples inoculated with C_{12} were completely inhibited and resulted in an almost flat curve. Two significant shifts in the growth trends are present between C_2-C_3 and C_5-C_6. The corresponding ZnO NPs concentrations are listed in Table 5.1.
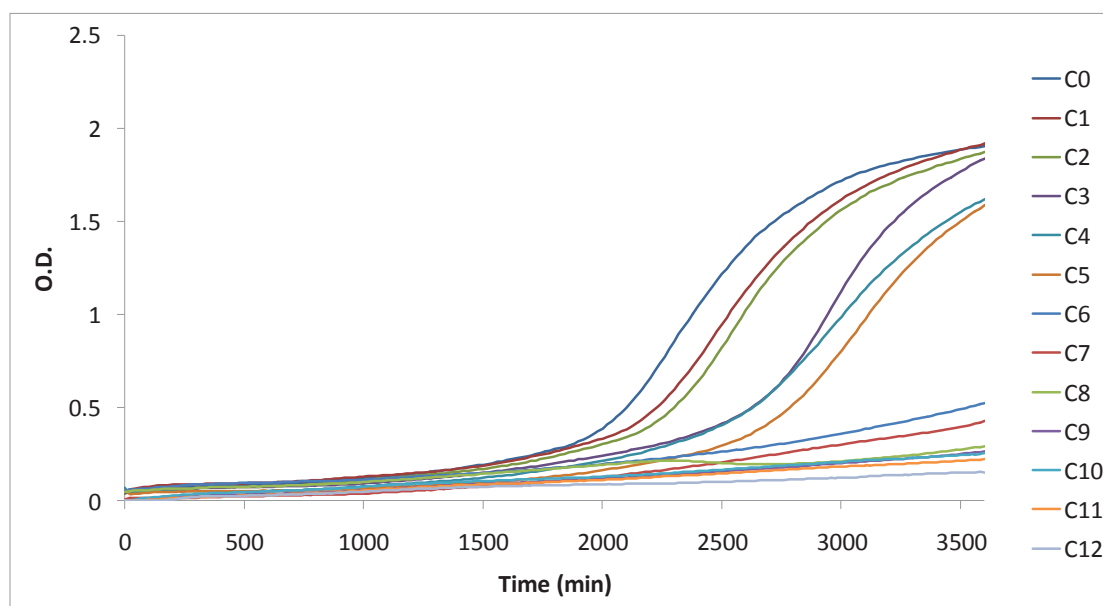
Figure 5.2. *Growth curves for P. expansum inoculated without ZnO (C$_0$) and with concentrations ranging from 0.5 mM up to 15 mM (C$_1$ - C$_{12}$).*

Table 5.1. *List of all the tested concentrations of ZnO nanoparticles for P. expansum. Range starts from a concentration of 0.5 mM corresponding to 40.70 ppm (C$_1$) up to 15 mM corresponding to 1221.12 ppm (C$_{12}$).*

	mM	ppm
C$_0$	0	0
C$_1$	0.5	40.70
C$_2$	1	81.41
C$_3$	2	162.82
C$_4$	2.5	203.52
C$_5$	3	244.22

C$_6$	4	325.63
C$_7$	5	407.04
C$_8$	6	488.45
C$_9$	7	569.86
C$_{10}$	8	651.26
C$_{11}$	9	732.67
C$_{12}$	15	1221.12

The dependent (*fa*) and independent variables (logarithm of the ZnO concentration expressed in log ppm) of equation 2 where plotted in a graph (Figure 5.3). A non-linear regression analysis of equation 2 was performed to estimate p_1 and p_2 and MIC and NIC were then calculated by the equations 3 and 4. MIC and NIC were found to be 9.8 mM and 1.8mM (798 ppm and 147 ppm), respectively.
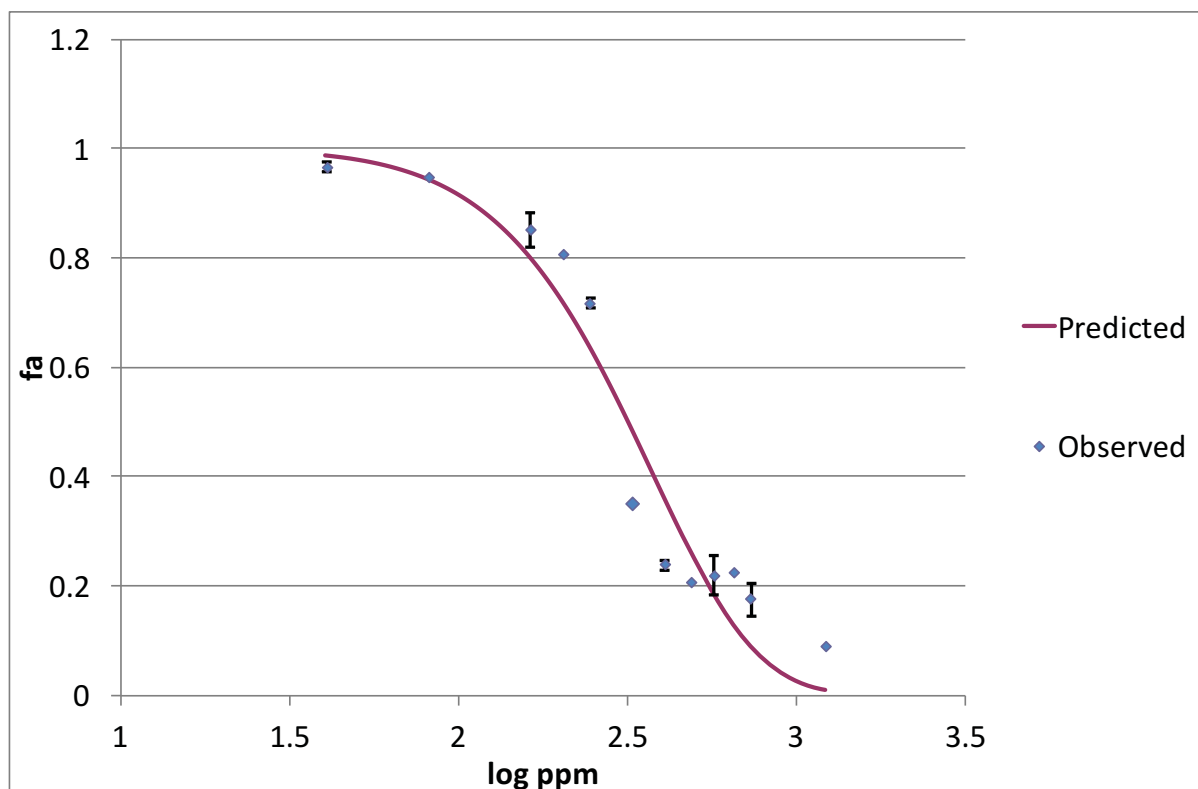
Figure 5.3. *Inhibition profile of ZnO nanoparticles against P. expansum. Scattered points represent the averages of the observed values of estimated fractional area, continuous line represents the predicted values obtained from the LPM. The Mean Squared Error (MSE) was 0.08.*

5.5 Discussion

Current results indicate that ZnO nanoparticles with sizes < 50 nm possess a significant antifungal activity against *Penicillium expansum*, the causative agent of blue mould, known as the most common postharvest decay of apples and pears (Sardella et al., 2016; Sutton et al., 2014). The inhibitory capacity of ZnO nanoparticles was also evident against *Alternaria alternata*, *Botrytis cinerea* and *Rhizopus stolonifer*. ZnO has already been shown to be effective

against filamentous fungi in several studies (He et al., 2011; Savi et al., 2013; J. Sawai, 2003) using conductimetry and growth diameters measurements. He et al. investigated the antifungal effect of ZnO nanoparticles with sizes of 70±15 nm in concentrations ranging from 0 up to 12 mM against *P. expansum* (He et al., 2011). Their results indicated that concentrations of ZnO nanoparticles higher than 3 mM could significantly inhibit the radial growth of *P. expansum* onto Petri dishes, but not lower concentrations in the range between 0 mM and 3 mM were investigated. The current results show that concentrations even lower than 3 mM (in the case of *P. expansum*) may also exhibit a clear antifungal effect for nanoparticles with sizes <50 nm. Furthermore, the MIC and NIC were estimated by performing non-linear regression analyses on the obtained data which allows for a quantitative and accurate antifungal activity assessment. Other researchers (J. Sawai & Yoshikawa, 2004) evaluated the antifungal activity of ZnO bulk powder against *Saccaromyces cerevisiae, Candida albicans, Aspergillus niger* and *Rhizopus stolonifer* using an indirect conductimetric assay. This technique is based on the changes in electrical conductivity of an alkaline solution produced by CO_2 absorption from fungal metabolism. Conductimetric data were processed by the authors using the growth inhibition kinetic model proposed by Takahashi (Takahashi, 1990) for the estimation of the MIC which was reported to be ≈1.2 M, thus suggesting a lower antifungal activity of bulk ZnO formulations compared to nanoparticles presented in the current study. When Savi et al. compared the effect of different Zn-compounds treatments against *Fusarium graminearum*, *Penicillium citrinum* and *Aspergillus flavus* concluded that $ZnSO_4$ and $Zn(ClO_4)$ showed better antifungal activity than nano and bulk ZnO (Savi et al., 2013).It is therefore evident that appropriate selection of the form of ZnO or Zn salts should be made depending on the specific applications.

Nutrients' availability plays also a fundamental role for the capacity of the fungi to recover from the antagonistic effect of the nanoparticles. The medium used in the current study, prepared from fresh potatoes, contains a richer source of nutrients than dehydrated media, as also stated by Pitt and Hocking (2009). Commercially available powders should therefore be carefully used while assessing antifungal compounds for fresh-food pathogens as they may lead to an overestimation of antifungal activity and provide non-realistic results. Future studies should be performed, in which the effect of the media on the antifungal properties of specific nanoparticles is assessed.

5.6 Conclusions

The development of a quantitative, rapid and reliable antifungal assay is nowadays crucial in food mycology as the necessity of testing novel antifungal compounds is recently arising. As a consequence, a method that can allow accurate results for filamentous fungi by automated monitoring represents an attracting option (Medina et al., 2012). In this study, a turbidimetric assay for the screening of ZnO nanoparticles against postharvest filamentous fungi was developed and optimised in order to obtain reliable and reproducible results. In comparison with other methods for antifungal activity testing, the turbidimetric assay has the advantage of being monitored automatically allowing rapid multiple data collection and the opportunity of being implemented by mathematical models.

Chapter 6: Physiological effects and mode of action of ZnO nanoparticles against postharvest fungal contaminants

6.1 Introduction

6.1.1. Mode of action of nanoparticles

The exact mechanism of the antimicrobial activity of nanoparticles still needs to be elucidated (Moritz & Geszke-Moritz, 2013). One of the possible cytotoxic mechanisms may result from the uptake of nanoparticles by bacterial cells since they are able to penetrate their cell wall (Martínez-Gutierrez et al., 2012). Other cytotoxicity mechanisms may derive from the release of ions from the NPs surface as it happens in the case of AgNPs (Rai et al., 2009) where the exposure of bacterial cells to silver ions induces changes in cell membrane leading to the enhancement of its permeability and consequent damage (Barani et al., 2012). Nanoparticles may also generate reactive oxygen species (ROS) inducing membrane lipid peroxidation and consequent cell damage. These mechanisms are also connected to the NPs' toxicity to biological systems, including eukaryotic cells (Bondarenko et al., 2013), therefore the extent of the *in vivo* use of nanoparticles as antimicrobial agent needs to be limited in a way to still preserve the antimicrobial activity but also to avoid undesired damage to non-target eukaryotic systems (Seil & Webster, 2012). In the case of fungi, Savi et al. (2013) investigated the antifungal properties of Zn-compouds against the mycotoxin-producing fungi *Fusarium graminearum*, *Penicillium citrinum* and *Aspergillus flavus* with their possible mechanism of action by scanning electron microscopy (SEM) and detection of the produced ROS. In their study, they observed deformed fungal hyphae with ruptures and unusual bulges after Zn-compounds treatment. Such morphological aberrations were associated with cell damage due to an increase in the production

of ROS, thus leading fungal cells to death (Savi et al., 2013). ZnO NPs, with an average diameter of 70 ± 15 nm, were also found to succesfully inhibit the grow of *B. cinerea* and *P. expansum* by affecting their cellular functions and inducing fungal hyphae distortion (He et al., 2011). Nevertheless, no information is available in literature about the morphological aberrations occurring on fungal spores, which are the main cause of cross-contamination during postharvest storage. Furthermore, to the knowledge of the authors, there are no morphological studies investigating the effect of ZnO NPs treatment against *Rhizopus stolonifer* and *A. alternata*, despite the former being of the most rampant and fast-growing fruit rot fungus (Pitt and Hocking, 2009) and the latter a fungus producing toxigenic metabolites that can accumulate in food thus becoming a hazard to human health (Pose et al., 2009). Evidently, more studies are required in order to assess the responses of a series of fungal contaminants in presence of ZnO nanoparticles and the role of Zn^{2+} ions in their efficacy. These studies will need to be carried *in vitro* before considering further *in vivo* or *in situ* assessments.

6.2. Objective

The objective of the current study was to investigate the antifungal activity of ZnO nanoparticles against the postharvest fungi of *P. expansum*. *B. cinerea*, *R. stolonifer* and *A. alternata*. The responses of these fungi, in the presence of ZnO, were quantitatively and qualitatively assessed while ions chelation studies were performed in order to elucidate the possible mechanisms responsible for antifungal activity.

6.3 Materials and Methods

6.3.1. Inoculum preparation

Postharvest disease fungi *Penicillium expansum*, *Botrytis cinerea*, *Rhizopus stolonifer* and *Alternaria alternata* used in this study were kindly provided by the fungal collection of the Postharvest Pathology group of IRTA (Spain). Fungal spores were harvested from 7-day old Malt Extract Agar (MEA) (Biolife, Milano, Italy) cultures by flooding the plates with a 0.05% Tween-80 solution and by scraping off the plates' surface with a sterile bent rod. The resulting suspension was aseptically filtered through a 4-layer sterile gauze to remove any mycelial contamination. Final spores' concentration was adjusted to 10^5 spores/mL with a haemocytometer for all the fungi.

6.3.2. Nanoparticles' suspensions preparation

ZnO nanopowder (<50 nm particles size, > 97%, Sigma Aldrich, U.S.A.) was suspended into 100 mL of sterile water. The nanoparticles' suspensions were then placed into an ultrasonicating bath at 37 kHz sonicating frequency (Elmasonic S60, Elma, Singen, Germany) for 30 min in order to break nanoparticles' aggregations.

6.3.3. Medium preparation

This study was carried out on Potato Dextrose Agar (PDA) prepared from raw potatoes following the procedure shown by Pitt and Hocking (2009) in order to get a more satisfactory potato infusion than commercially dehydrated forms (Pitt & Hocking, 2009; Rinaldi, 1982). The refraction index of the potato infusion was measured with a refractometer (Atago, Japan) and

was found to be n_D= 1.3340±0.0001 at 25ºC.The autoclaved PDA medium, was cooled down to ≈55°C, poured into sterile 9-cm Petri dishes and then mixed, by an orbital shaker, with ZnO NPs suspensions in order to reach the final concentrations of 3, 6, 12 and 15 mM in a final volume of 20 mL per each plate. An additional batch of plates filled with PDA without ZnO NPs was also prepared as control. Finally, four perpendicular diameters were drawn onto the plates' surface for performing the fungal growth testing.

6.3.4. Diameter extension measurement

All the PDA plates were inoculated in the center with 10 µl of the previously obtained spores' suspension (10^5 sp./mL) of each fungus (see 6.3.1). After drying, plates were enclosed into sterile polyethylene bags to prevent medium desiccation and incubated at 25°C. Growth diameters were measured twice a day. Results were plotted into graphs of diameters against time and then fitted to a linear model in order to estimate the fungal growth rate for to the different nanoparticles' concentrations. A linear model was selected (over Baranyi) based on previous reports by Gougouli & Koutsoumanis (2012). All tests were performed at least in triplicate.

Estimated growth rate were then correlated by using a three-parameter model (Judet-Correia et al., 2011)which reads as follow:

$$\frac{\mu}{\mu_{opt}} = \frac{1}{1 + \left(\frac{ZnO}{ZnO_{50}}\right)^d}$$

where μ is the diameter growth rate [cm/h], μ_{opt} the diameter optimal growth rate [cm/h] at [ZnO]=0 mM, ZnO the concentration of the nanoparticles (mM) and ZnO_{50} the concentration at which $\mu = \mu_{opt}/2$ while d is a design parameter.

6.3.5. SEM imaging

For the scanning electron microscopy, two batches of PDA plates with 0 mM and 12 mM ZnO concentration, respectively, were prepared as described before. Agar plugs of about 0.5 cm were excised with a scalpel from 72-hour-old cultures in the case of *P. expansum*, *B. cinerea* and *A. alternata* and 48-hour-old cultures in the case of *R. stolonifer*. Plugs were immersed into 5 cm Petri dishes initially filled with a modified Karnovsky's fixative and afterwards with osmium tetroxide for post-fixation (Alves et al., 2013). Samples were finally coated with gold in a sputter and kept into a desiccator until observation. Images were taken from the samples using an environmental scanning microscope operating in high vacuum (Merlin, Carl Zeiss Optic, Germany).

6.3.6. Assay with EDTA

A chemical assay with EDTA (Labbox, Spain),a well-known metal ion chelating agent (Hart, 2011; Patton et al., 2004)has been performed to verify the importance of ions release from nanoparticles for their antifungal activity mechanism. Two batches of plates were prepared, one filled with20 mL of PDA mixed with ZnO NPs (final concentration: 12 mM) and another one

with 20 mL of ZnO NPs (same concentration as previous) + EDTA (final concentration: 10.5 mM). Additionally, two batches of PDA plates prepared from sterile water and an EDTA only (same concentration as previous) solution were also used as controls. Prior to mixing with the agar, the pH of each suspension was checked and adjusted to the same value as the 12 mM ZnO NPs suspension (pH = 7.0±0.2). Four perpendicular diameters were drawn onto the plates' surface and mycelium growth was measured. Statistical significance of data was assessed by a *t-test*. Additionally, absorbance spectra of ZnO NPs alone and in combination with EDTA were obtained by an UV-2600 spectrophotometer (Shimadzu, Japan).

6.4 Results

6.4.1 Diameter extension measurement

Figure 6.1 illustrates the diameter growth rates, previously obtained from the linear regression of the diameter kinetic studies, as a function of the nanoparticles' concentration. Parameters values estimated by the model are also listed in Table 6.1. From Figure 6.1, is clear that the most significant decrease in the growth rate occurs in *R. stolonifer*. Furthermore, *R. stolonifer*'s growth was completely inhibited at ZnO NPs concentration as high as 15 mM. Table 6.1 shows that the fungus with the lowest ZnO_{50} value was *R. stolonifer*, followed by *P. expansum*, *A. alternata* and finally by *B. cinerea*
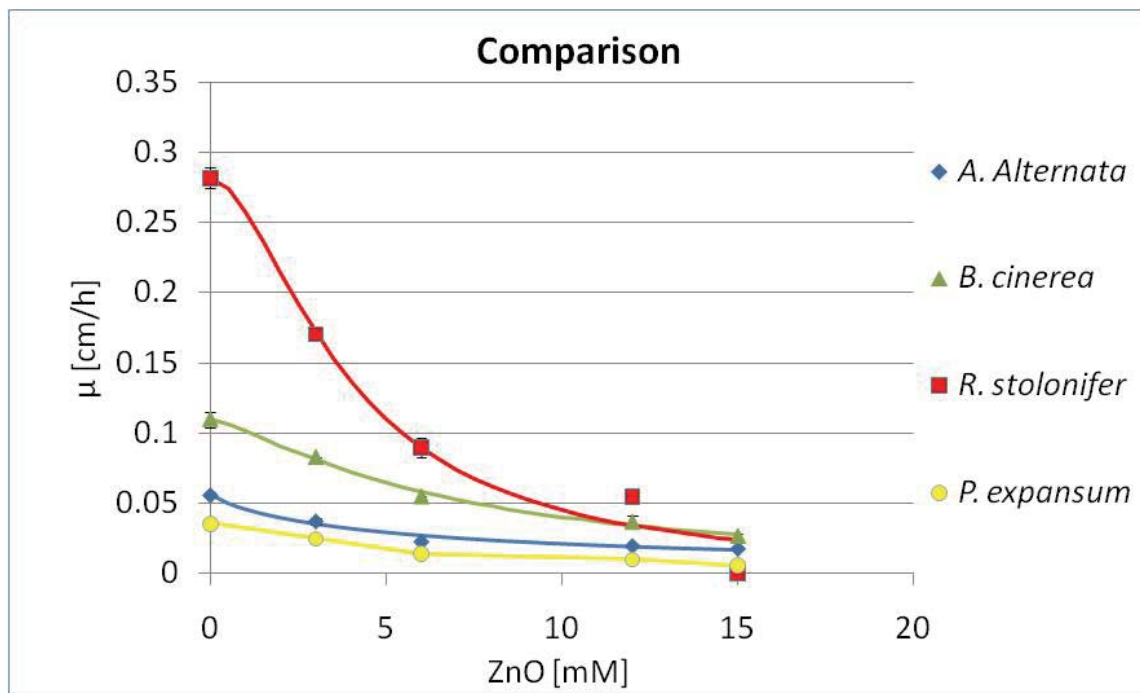
Figure 6.1. *Growth rate μ vs ZnO concentration graph for all the studied fungi. Scattered points represent the results deriving from the linear regression analysis performed on the observed values. Continuous lines represent the values estimated by the model.*

Table 6.1. *List of the parameters estimates for all the fungi following the prediction model. The concentration at which the growth rate was equal to half the optimum growth rate (ZnO_{50}) is highlighted in bold.*

	ZnO_{50} *(mM)*	μ_{opt} *(cm/h)*	*d*
A. alternata	**5.49**	0.05	0.85
B. cinerea	**6.54**	0.11	1.31
R. stolonifer	**3.88**	0.03	1.34
P. expansum	**5.08**	0.28	1.74

6.4.2. Scanning electron microscopy

In order to investigate the damages induced by ZnO NPs to the selected fungal isolates, SEM analysis was performed to examine the structural changes occurring due to the treatment with nanoparticles. In Figure 6.2a), c), e), g) SEM pictures from control plates of *P. expansum*, *A. alternata*, *B. cinerea* and *R. stolonifer* are shown. Fungal spores are clearly visible and their structure appears to be intact in all the cases. On the contrary, Figure 6.2b), d), f), h) shows the fungi, in the same order as listed before, after the growth onto plates with 12 mM ZnO NPs. Different morphological aberrations are clearly visible in all the samples. In Figure 6.2b, spores from *P. expansum* appear to be seriously damaged and, in some cases, broken as a consequence

of swelling. *A. alternata* (Figure 6.2d) seems to grow like an amorphous mass where the single fungal structures can barely be distinguished, while the structures of *B. cinerea* (Figure 6.2f) show several punches. Finally, spores of *R. stolonifer* (Figure 6.2h) are evidently crushed and crumpled.
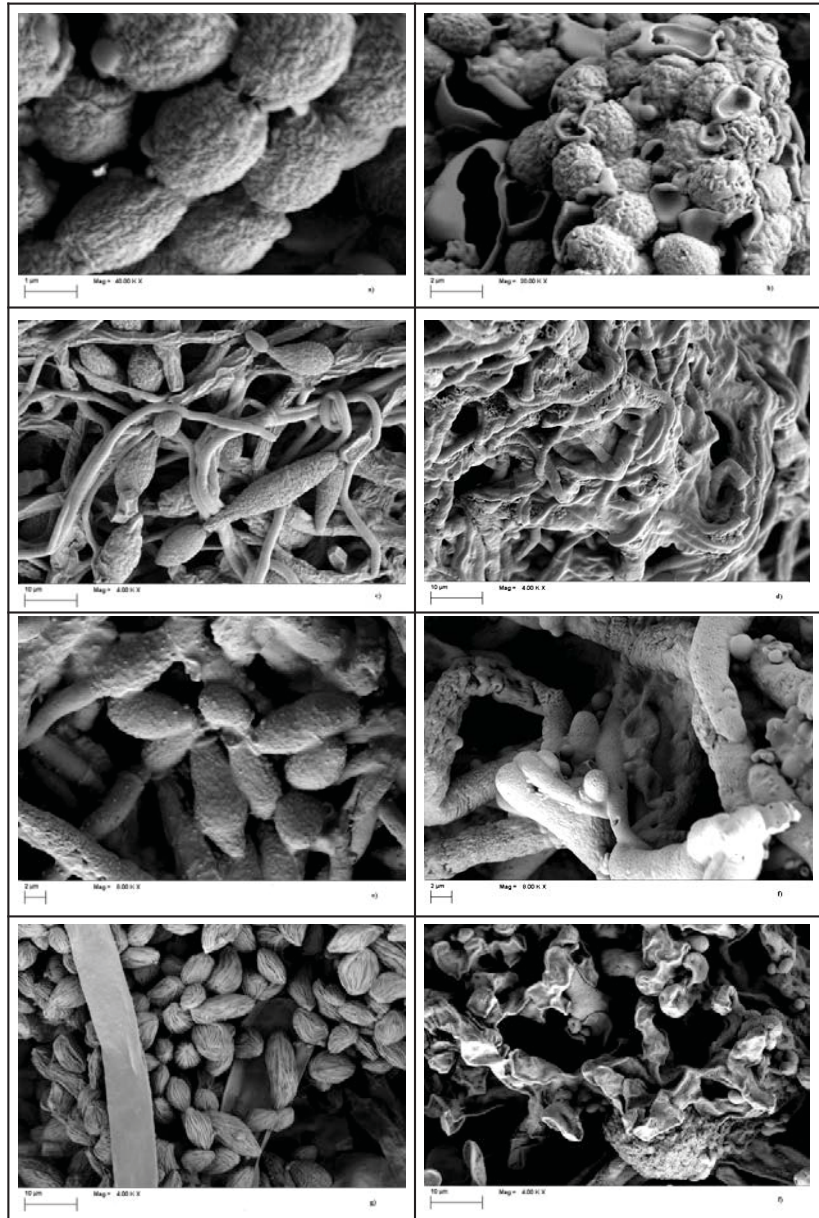
Figure 6.2. *SEM images of P. expansum, A. alternata, B. cinerea and R. stolonifer without (a,c,e,g) and with (b,d,f,h) ZnO NPs respectively. Samples were inoculated onto PDA plates with a final concentration of 12 mM ZnO NPs. Morphological aberrations are evident in all the treated samples.*

6.4.3. Assay with EDTA

This assay showed that, whenever EDTA was mixed with ZnO NPs, a significant reduction of their antifungal activity was observed, as shown in Figure 6.3 for *P. expansum*. EDTA alone also showed antifungal activity, even though lower than ZnO NPs (Figure 6.3). The combination of EDTA+ZnO NPs resulted in a deleterious effect to the nanoparticles' activity also in the case of the other fungi, as summarized in Table 6.2. The statistical relevance of the data provided in Table 6.2 was also confirmed by a *t-test* . As a matter of fact, addition of EDTA resulted in a significant reduction of suspended ZnO NPs as can be deducted from Figure 6.4 which shows the absorbance spectrum of ZnO NPs, with the characteristic peak at 360 nm (Khorsand Zak et al., 2011), and the spectrum of ZnO NPs treated with EDTA. The lower absorption of the latter indicates a decrease of the NPs' quantity. It is known that within the pH region $6.6 < pH < 7.7$, the zinc species that are present in the ZnO NPs suspension are $Zn^{2+}_{(aq)}$ and $ZnO(OH)^{+}_{(aq)}$ which are in equilibrium with the surface hydroxide $Zn(OH)_{2\ (s)}$ (Fatehah et al., 2014) and that EDTA forms very strong complexes with almost every divalent metal ion. This may indicate that the NPs are acting as a source of Zn^{2+} ions which are known to have *per se* an antimicrobial effect (Seil & Webster, 2012).
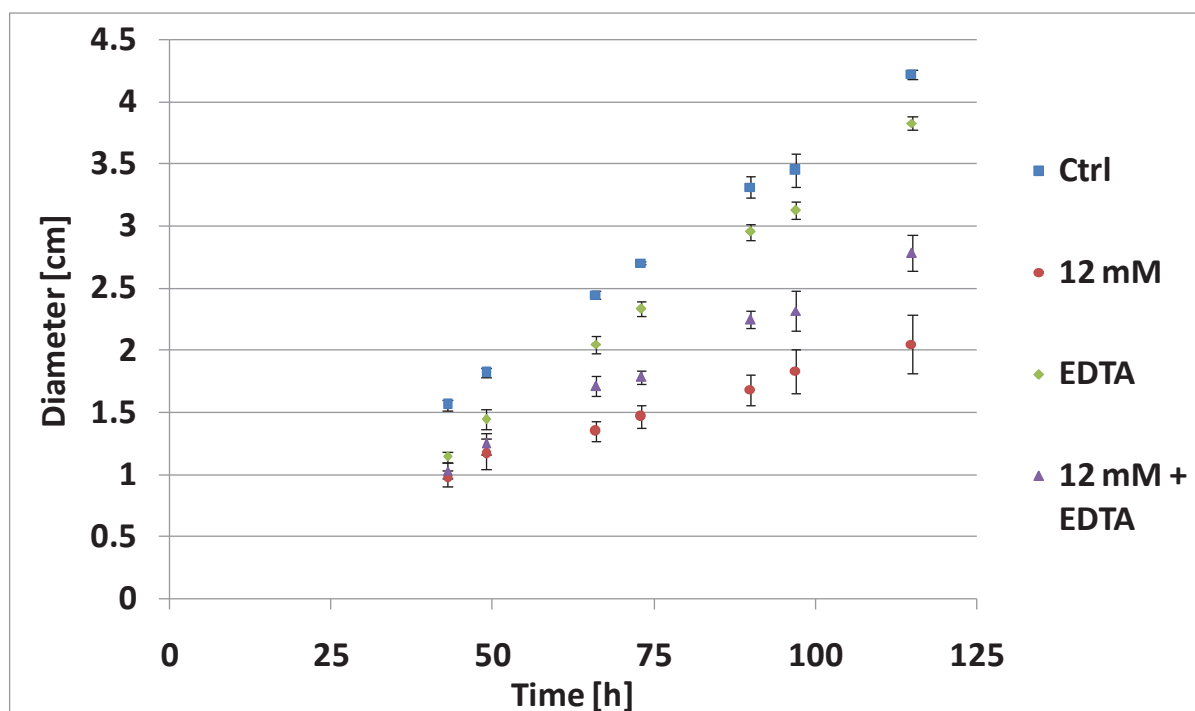
Figure 6.3. *Diametric increase of P. expansum on PDA only (Control), PDA with ZnO NPs (12 mM), PDA with ZnO NPs + EDTA (NPs+EDTA) and PDA with EDTA only. Each spot represents the average from at least 3 replicates.*

Table 6.2. *Growth rates (cm/h) for all the fungal samples with EDTA, ZnO NPs and ZnO NPs+ EDTA. Data were obtained by linear regression analysis on the raw diametrical measurements. Small characters show statistical analysis results (t-test) performed between different samples for the same fungi.*

	Control	ZnO NPs	ZnO NPs + EDTA
A. alternata	$0.056\pm1.042 \times 10^{-3\ a}$	$0.022\pm2.447 \times 10^{-3\ b}$	$0.053\pm2.690 \times 10^{-3\ a}$
B. cinerea	$0.081\pm0.484 \times 10^{-3\ a}$	$0.021\pm0.533 \times 10^{-3\ b}$	$0.072\pm2.029 \times 10^{-3\ c}$
R. stolonifer	$0.263\pm6.133 \times 10^{-3\ a}$	$0.069\pm7.501 \times 10^{-3\ b}$	$0.230\pm2.059 \times 10^{-3\ c}$
P. expansum	$0.036\pm1.086 \times 10^{-3\ a}$	$0.014\pm0.488 \times 10^{-3\ b}$	$0.023\pm0.984 \times 10^{-3\ c}$
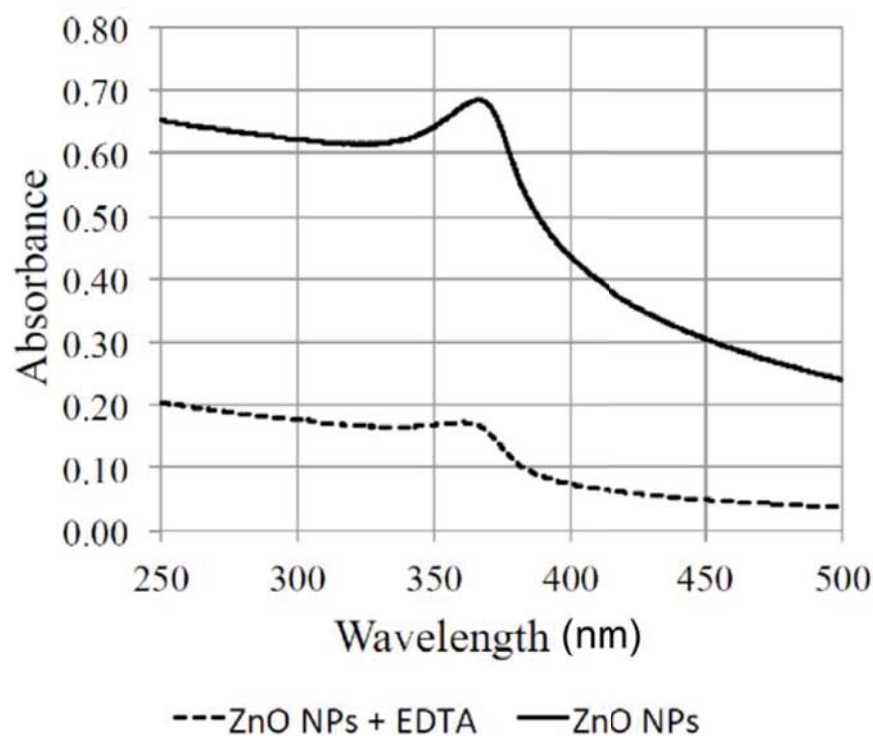
Figure 6.4. *Absorbance spectra of ZnO NPs (continuous line) and of ZnO NPs treated with EDTA (fragmented line). The characteristic peak at 360 nm is evident for the ZnO NPs. The dilution rate of each measured sample was 1:8 from the neat suspensions used in the assay.*

6.5 Discussion

We here confirm the efficacy of ZnO NPs against postharvest fungal isolates by diameter extension technique. Previous studies of diameter extension measurements on PDA plates (He et al., 2010) reported that, ZnO NPs with sizes of 70±15 nm and at concentrations greater than 3 mM, could significantly inhibit the growth of *P. expansum* and *B. cinerea*. Furthermore, the authors concluded that *P. expansum* was more sensitive to ZnO NPs than *B. cinerea*, as also shown by the present study. However, our study has been performed with a lower size ZnO nanoparticles than He et al. as we considered the fact that ZnO NPs antimicrobial activity

decreases with the increase of their size (Sirelkhatim et al., 2015). Colonies diameters measurements were also preformed in a study about the investigation of the antifungal activity of ZnO NPs, with a mean diameter of 30 nm and at concentrations ranging from 10 mM up to 100 mM, against *Fusarium graminearum*, *Aspergillus flavus* and *Penicillium citrinum* (Savi et al., 2013). Amongst the three fungal isolates, *P. citrinum* was the most sensitive to the ZnO NPs being the only one which could be completely inhibited at high ZnO NPs concentrations (Savi et al., 2013).However, in the above mentioned studies, no data modelling was performed on the obtained results in order to estimate growth parameters such as the *ZnO$_{50}$*and no information was provided by the authors about the nature of the growth medium, whether it was a dehydrated formulation or it was prepared by raw ingredients. Knowing that media prepared from raw materials provide a more satisfactory nutrients' composition than synthetic ones (Pitt and Hocking, 2009), commercially available powders should be carefully used while assessing antifungal compounds for fresh-food pathogens as they may lead to an overestimation of antifungal activity and provide non-realistic results.

The irreversible morphological aberrations observed with the SEM imaging, are a clear proof that ZnO NPs have fungicide and not fungistatic activity. In a previous study (He et al., 2010), hyphal distortion due to treatment with ZnO NPs, has been also observed in *P. expansum* and *B. cinerea*. However, no information about the spores' morphology was provided by the authors. Similarly, hyphal alterations in filamentous fungi due to ZnO NPs treatment were also reported by Savi et al.(2013). In our study we show that ZnO NPs can also efficiently compromise fungal sporulation with clearly irreversible damages. Similar SEM studies aimed at qualitatively investigate the effect of other categories of antifungal agents, have also highlighted that morphological aberrations occur as a result of antifungal treatment. Changes in hyphal

morphology due to chitosan treatment were observed for *A. alternata*, *B. cinerea*, *P. expansum* and *R. stolonifer* by de Oliveira et al., (2012)as well asfor *Candida albicans* cells exposed to a combination of allicin and amphotericin B, which showed noticeable morphological changes with burst or collapsed membranes in a study by Kim et al. (2012). Still, different plant extracts tested against *Aspergillus niger*, *Fusarium oxysporum* and several *Botrytis* and *Penicillium* species, induced in these fungi ultrastructural aberrations responsible for hyphae's viability loss (Pârvu & Pârvu, 2011).

Finally, the current study provides additional support to previous studies suggesting that metal ions release plays a crucial role in the antifungal mechanism of nanoparticles (Dimkpa et al., 2013). The antimicrobial properties of Zn^{2+} ions have also been emphasized by Pasquet et al. (2014). In their study, the authors show that the partial dissolution of ZnO particles releases Zn^{2+} ions in aqueous suspension thus contributing to the antimicrobial activity of ZnO particles by facilitating their diffusion to microbial cells (Pasquet et al., 2014). Although these studies, aimed at investigating the mechanism of ZnO NPs antimicrobial activity, have successfully identified Zn^{2+}ions release and ROS production as favourite candidates, the actual role of ions in the chemical equilibrium of ZnO NPs has never been verified by ions depletion with the introduction of a chelating agent so to exclude other potential interactions responsible for antifungal activity. Additionally, the precise mechanisms of action of ZnO NPs are yet considered in literature under debate (Sirelkhatim et al., 2015). Another important aspect that deserves to be highlighted, since there are several studies assessing the synergistic effect of either ZnO NPs or EDTA with other antimicrobial compounds (Banoee et al., 2010; Casalinuovo et al., 2017; Robertson et al., 2012), is that we here show that ZnO NPs cannot be used in concomitance with EDTA to enhance their activity due to the importance of Zn^{2+} ions release. The outcomes from the interactions between

two compounds should never be implicitly postulated as results may be different from what expected.

6.6 Conclusions

In our study we show that ZnO NPs with an average diameter size lower than 50 nm possess strong antifungal activity which makes them a potential candidate to be used as a routine antifungal compound for fruit spoilage prevention. Mathematical modelling of data allowed us to quantify the effect of ZnO NPs against each of the studied fungal isolates and to establish a sensitivity scale. SEM analysis revealed that ZnO NPs induce serious physical damages to the fungal structures which can be assumed to be irreversible. The assay with EDTA provides further support to previous studies which indicate ions release as one of the potential mechanism of ZnO NPs antifungal activity.

Chapter 7. Assessing the air filtration efficacy of compressed and uncompressed polyurethane foams.

7.1. Introduction

7.1.1 Air decontamination in fruit storage facilities

Fresh fruits can bring large economic benefits when they undergo a proper postharvest life. Storage of fruits for several weeks or months before marketing may cause disease problems if good postharvest handling procedures are not accomplished. Debilitating or contaminated environments should be avoided and life-shortening injuries prevented or at least minimized. At the same time, procedures must limit, directly or indirectly, the activity of pathogens (Sommer, 1989). Postharvest management is a set of post-production practices, which include: cleaning, washing, selection, grading, disinfection, dumping, packing and storage (El-Ramady et al., 2013). Such practices aim at eliminating undesirable elements and improving product quality as well as ensuring that the product complies with established quality standards. Postharvest practices include the management and control of variables such as temperature and relative humidity, the selection and use of packaging and the application of fungicides (FAO, 2009). While fruit and vegetable storage warehouses go through great lengths to control the environmental conditions within them (Labavitch, 2016) and a lot of emphasis is laid on controlled atmosphere storage and fungicides application onto the fruit (Suslow, 2005), poor attention is paid to the quality of the air in terms of circulating particulate matter, even though it has been shown that the presence of spores in the air inside these facilities affects the quality of the product negatively (Brincat et al., 2016; Ocón et al., 2011). Highly resistant fungal spores can

cause spoilage of fruit and foodstuffs in storage facilities, therefore their presence must be controlled.

The most common way to eliminate bioaerosols from the internal environment of facilities is by air filtration (Brincat et al., 2016). The most used air filtration systems to reduce the abundance of fungal spores in such environments are High Efficiency Particulate Air (HEPA) filters as they are known to be amongst the most efficient filters available for particles trapping. In these devices, the material which is trapped by the filter forms a "cake". As soon as the thickness of the cake increases, the path that particles are forced to travel through becomes longer and more contorted. This increases the filter's efficiency but also the pressure drop so that, at some point, the filter needs to be replaced (Brincat et al., 2016; Novick et al., 1992). Specifically, HEPA filters need to be replaced on a yearly basis and their pressure drop increases with continual use (Novick et al., 1992), thus making them a very expensive solution for food storage environments. A good alternative to HEPA filters is represented by polyurethane (PU) foams. PU foams, like HEPA filters, trap particles on the surface of their fibres. As particles travel through the foam, which has a very elevated internal surface area, they are likely to adhere to it (Brincat et al., 2016). Each foam has a nominal number of Pores Per Inch (PPI), the larger the PPI value the smaller the pores. The PPI and the thickness of the foams (i.e., the length) is usually adjusted in order to find an optimal balance between trapping efficiency and pressure drop (Brincat et al., 2016; Roesler, 1966).

Further to a previous study (Briffa et al., 2017), whose aim was to assess the air filtration (vis-à-vis fungal spores) capability of PU foams differing for PPI and thickness, in this study we aim at assessing the change in fungal spore filtration efficacy when conventional polyurethane foam is compressed to different ratios, effectively reducing the pore size.

7.2 Objective

The aim of this study was to assess the change in fungal spore filtration efficacy when a conventional polyurethane foam is compressed to different ratios, thus effectively reducing its pore size.

7.3. Materials and methods

7.3.1. Production of polyurethane foams

90 PPI polyurethane foam samples (Articoli Resine Espanse, Italy) were cut to 30 mm and 50 mm thickness. Furthermore, different samples of 30 mm thickness were compressed to 5 mm and 25 mm. In order to achieve this, 30 mm foam was introduced into a custom designed press where two plates were moved to the desired thickness. This setup was then introduced into an oven at 180°C and the foams were heated for one hour in the compressed state. Afterwards, they were cooled down to room temperature and removed from the press. When removed, the foams kept their compressed state.

7.3.2 Air filtration system

Outer environmental air of the area of Msida in Malta (site of the Faculty of Health Sciences) was selected as source of fungal spores. A filtration manifold with 3 ports was attached to an air flow meter connected to a vacuum pump. Acrylonitrile butadiene styrene (ABS) plastic adapters, generated by 3D printer were designed in a way to allow their insertion into the manifold ports while providing a platform into which any foam under assessment could be placed. Sterile cellulose nitrate membrane filters (pore size 0.45μm) were placed by flamed forceps onto the

base of each manifold port. The whole setup was sealed with parafilm M sealing film (Bemis NA, Neenah, Wisconsin) and paraffin wax so as to ensure that the setup was thoroughly air-tight.

Foams were fit into the adapters which were sealed to the three manifold ports by means of further sheets of parafilm. The air sampling occurred as the vacuum pump was switched on. Air was drawn through foams supported by the adapters in the manifold ports and spores were trapped onto the membrane filters. A control with no foams into the adapters was also run at each replicate experiment. The necessary volume of air was sampled by running the vacuum pump for a period of time while the flow rate was measured by an air flow meter. A volume of at least 400 L of air was sampled each time (Briffa et al., 2017).

7.3.3 Microbial analysis

For the controls, the volume of air filtered was split between the 3 manifold ports so that CFUs of the control would be obtained by adding the CFUs grown on the membrane filters of each individual manifold port. Foam samples were inserted in one manifold port with the other two closed. This was done to obtain a CFUs count between 10 and 150 as recommended by the Food and Drug Administration BAM (FDA, 2001). After the air sampling, the membranes were removed from the apparatus and placed onto Dichloran Rose Bengal with Chloramphenicol (DRBC) agar plates under subdued light and plates were incubated at 25°C for 5 days in darkness(Chilvers et al., 1999; FDA, 2001). Afterwards, the number of colony forming units (CFUs) present on the membrane filter was counted. All the experiments were performed on at least 3 separate days by running triplicates each time and during the summer season.

The percentage of fungal spores eliminated from the air by the foam on each day was calculated using the following formula:

$$Percentage\ Efficiency = 100 - \left(\frac{AverageCFU/Lfoam\ analysis}{AverageCFU/L\ of\ control}\right)\%$$

The Percentage Efficacy corresponds to the % of CFUs eliminated from the air.

7.3.4 Scanning electron microscopy (SEM) imaging

Micrographs of the polyurethane foams used in this study were captured using a Carl Zeiss Merlin Field emission scanning electron microscope (SEM). The foam samples were cut in cubes having a length of approximately 5 mm. The sample was then introduced in the SEM. The magnification used was 100, with a scan speed of 8, probe current of 65 pA and an EHT of 1.2 kV.

7.4. Results

An increase in the thickness of the foams used (each obtained from the same supplier and having the same porosity i.e. 90 PPI) generally speaking results in a higher percentage of filtration

efficacy, as clearly shown in Figure 7.1. However, a saturation effect (i.e. no observable change in the filtration efficiency of the foam) develops when the foam thickness is increased from 30 mm up to 50 mm.
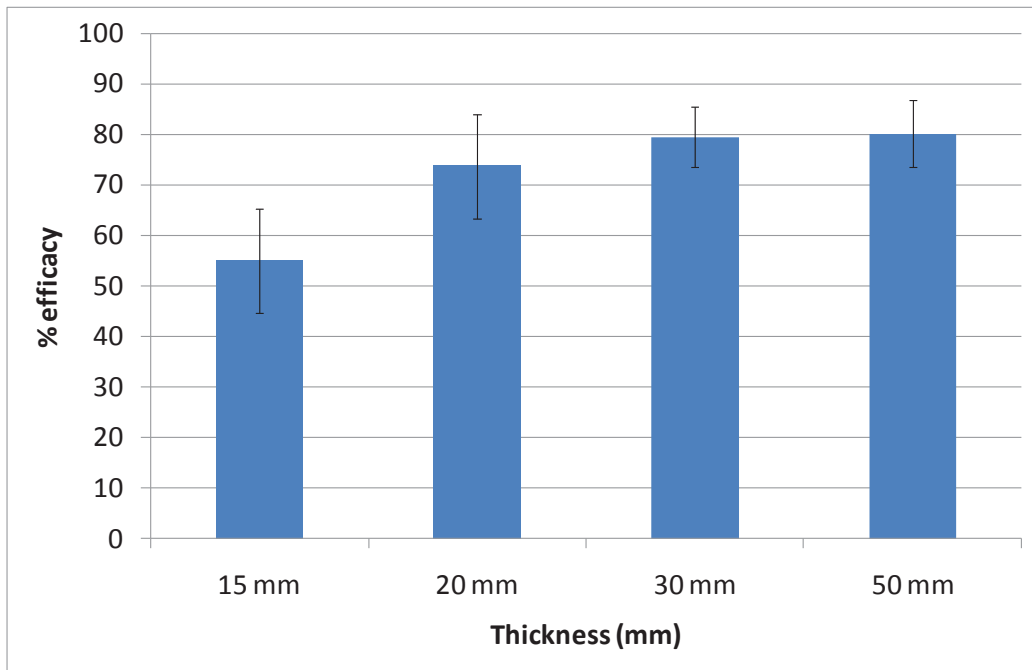
Figure 7.1. *Comparison of the percentage efficacy of uncompressed foams.*

In view of this, in order to further reduce the pore size of the foam filters used, compression was applied to the foam. Referring to Figure 7.2, it is evident that pore size may be effectively controlled using compression. In the case of the uncompressed foam, the pore size is very large when compared to fibres' diameter. On the other hand, referring to Figure 7.2b, this difference is not so large in the case of the compressed foam. Compression of the foam results in a more sinuous path for the air passing through the foam, which means that the air has to travel in a more non-laminar fashion something which as expected results in an increase in air filtration efficiency. In fact, as shown in Figure 7.3, high compression (compression of 83%) results in an

increase of circa 10% in efficiency when compared to the uncompressed foam filter. Also as expected, low compression of the foam (17 %) does not seem to exert a big effect on the trapping efficacy, since there is not a big change in the sizes of the pores. Additionally, uncompressed foams had a pressure drop of 0.3 kPa at an air speed of 2 m/s. Compression of the foam is not expected to have a large effect on the pressure drop of the foam filter: this is because changes in pore size do not affect the pressure drop to a high extent when the fibre diamters are large (Wang et al., 2008).
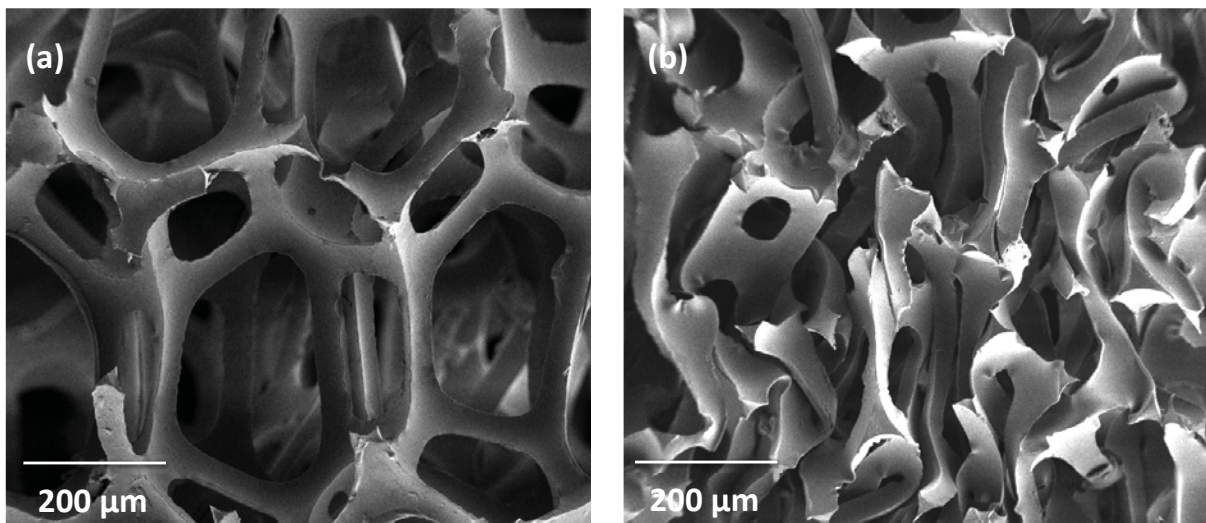
Figure 7.2. *SEM micrographs of the 90 ppi foam used (a) the original uncompressed foam and (b) 30 mm foam compressed to 5 mm foam.*
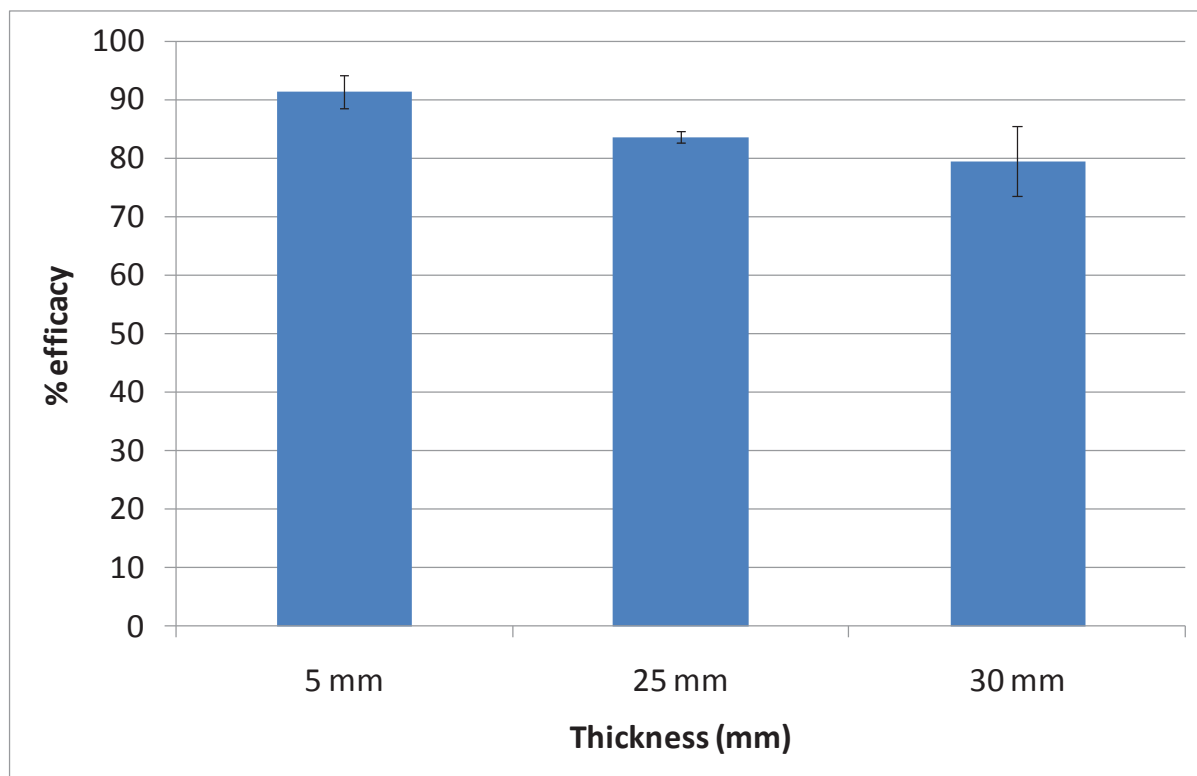
Figure 7.3. *Comparison of the percentage efficacy between uncompressed foams (30 mm) and compressed ones (5 mm and 25 mm).*

7.5 Discussion

At a first glance, the saturation effect may seem something strange since an increase in the thickness of the foam results in an increase in the path that air has to travel through the foam. This should result in more particles and spores being retained by the filter. The latter argument is true when testing the efficiency of the foam filter against a particular spore/particle size, however, in environmental air, numerous spores of different fungal species are present with average sizes ranging between 1 and 10 μm (Samson et al., 2000). This means that the efficiency of the foam filter will be different for different micro-organisms. Thus the nearly equal filtration

efficiency obtained for the foam filters having a thickness of 30 mm and 50 mm may be due to the fact that large spores are nearly all trapped by the foam filter having a thickness of 30 mm, whilst smaller fungal spores are passing from both the 30mm and 50 mm foam filters due to the low filtration efficiency of the foam filter for small spore sizes. This means that polyurethane foams are a good candidate for "primary" air filtration, generally used to protect the mechanical items of air movement systems from gross contamination (Wirtanen et al., 2002). Furthermore, the use of polyurethane foams allows a wide range of collection efficiencies in the respirable range (Roesler, 1966) with the possibility of fine-tuning to a certain extent the trapping ability of the foam filter by choosing the proper combination of thickness and porosity (PPI) of the foam (Brincat et al., 2016). A higher foam porosity corresponds to a higher ability to trap small particles and foams with the same porosity but different thickness show different trapping abilities (Roesler, 1966). The increase in efficiency after high compression is probably due to an increased filtration efficiency for smaller spore sizes. This is in agreement with previous studies carried out on non-woven filters where it was shown that filter efficiency increases with a decrease in porosity, and with a decrease in fibre diameter (Wang et al., 2008). Furthermore, compression of the foam is not expected to have a large effect on the pressure drop of the foam filter. This is because in the case of non-woven filters, it was shown that changes in pore size do not affect the pressure drop to a high extent when the fibre diameters are large (Wang et al., 2008). It is also important to point out that in the case of this study, a thermo-mechanical process was used to produce the compressed foam filters. It has been recently reported (Boba et al., 2016; Gatt et al., 2011) that polyurethane foams have a shape memory effect so that, when heated, they will return to their original shape after a plastic deformation. This means that such compressed foams filters can be easily uncompressed by heating them above the glass transition

temperature of the polymer, something which will result in the uncompressed foam. The uncompressed foam would then be easily cleaned from any trapped material as pores will become very large. The uncompressed foam could then once again be subjected to the thermo-mechanical process to produce the compressed foam filter, which can be easily re-used.

Noticeably, such foam filters may find practical applications in the food industry whereby consumer protection is essential. This is due to the fact that food contamination can have hazardous effects on human health. Airborne dust particles not only introduce foreign matter into the product, but also add microbial contamination (Ljungqvist and Reinmuller, 1993). Airborne contamination can be composed of multiple families of microorganisms which can be dispersed in the air as aerosols, such as bacteria, yeasts and mould spores (Parret et al., 2000). The size of aerosols particles is generally in the range of 0.5-50 μm (Wirtanen et al., 2002)and particle size is the major factor influencing their aerodynamic behaviour (Kang, Y.J., Frank, 1989). Compressed foam filters thus present a possible way to cheaply control the particle content in the air (dust and microorganisms) thus limiting the risk of product contamination and hence contribute to safe food manufacture (Klemetti et al., 2006). For example, fruits are stored for up to 12 months after harvest and are subject to attack by numerous postharvest pathogens. Despite modern fungicides and storage facilities, occasional losses of 15-25% are still reported (Sutton et al., 2014). The use of an air filter with optimised performance able to minimise the presence of fungal spores in postharvest warehouses, which also does not imply the use of toxic compounds, would be the ideal candidate as an alternative solution for postharvest disease management. A compressed polyurethane foam-based filtration system would be, for instance, suitable for pear and/or apple postharvest warehouses, where the most important decay pathogens of these fruits are *Penicillium, Botrytis* and *Alternaria* species. This is due to the fact that *Penicillium* has

spherical spores with size ranging from 4.5-5 µm while *Alternaria* has elliptical spores with sizes ranging up to 9-18 µm for the minor elliptical axis and 20-63 µm for the major elliptical and *Botrytis* 8 -14 x 6-9 µm (Samson et al., 2000; Sutton et al., 2014). This indicates that such spores can potentially be easily trapped by the compressed foam proposed in this study.

7.6 Conclusion

In our study we show that compression is a valid procedure to enhance the air filtration efficacy of polyurethane foams. Compression, by reducing the pore size of the foam, allows a more sinuous path for the air passing through the foam thus resulting in an increase in its trapping ability. Due to their low production cost on industrial scale, compressed foam filters represent a possible way to cheaply control the particle content in the air. Such foam filters may find practical applications in the food industry whereby consumer protection is essential, for instance in fruit postharvest warehouses. Further studies will be needed in order to assess the efficacy of such foams directly in the postharvest chambers and to investigate *in vivo* the effects on the stored fruits.

Chapter 8. General discussion, conclusions and future perspectives

Postharvest management aims at preventing fruit spoilage and ensuring that the product complies with established quality standards. Maintaining fruit quality begins with cooling it soon after harvest, therefore almost all pears are currently placed in cold storage facilities within hours of harvest and cooled to 0-4°C. However, postharvest disease fungi might adapt, by mutation and selection, to grow at abnormally low temperatures. In the study performed in Chapter 3 of this thesis, the low values (below zero) of T_{min} estimated by the CMI, comply with the assumption that all these fungi possess the potential of surviving to cold-storage temperatures. Additionally, *R. stolonifer* was identified as the most aggressive fungus in terms of growth rate, a result which is also supported by previous comparative studies (see Section 3.5.1) showing that isolates from the genus *Rhizopus* have high growth rates if compared to other genera. We also showed that the prediction model (CMI) and the synthetic medium (SDA), used for the study in Chapter 3, were suitable to describe the *in vitro* mycelium growth as a function of the temperature for all the fungal isolates. On the other hand, the validation on a simulated pear medium showed that predictions were realistic for almost all the isolates with some deviation in the case of *R. stolonifer* and *B. cinerea*. Nevertheless, when the same isolates were grown on a real food matrix at the predicted optimal temperatures, with the only exception of *P. expansum*, significant different growth rates were obtained between pears and pear pulp agar medium. We can therefore conclude that nutrient substrate has a big influence on the fungal growth rate and that a simulated medium may provide results which are distant from what happens on food. Such limitation must always be considered in predictive mycology studies and implemented by accuracy and/or correction factors in order to develop the most accurate and precise predictive models.

The growth of filamentous fungi consists of complex microscopic differentiations resulting in various visible appearances and depending on several parameters. In Chapter 4, parameters like nutrient medium and inoculum size, were optimized to obtain a turbidimetric protocol suitable for the assessment of fungal growth. Microscopic examination of fungal cultures, inside the wells of the microtitration plates, allowed us to see how fungi were developing from small hyphal formations into more complex and dense structures with a consistent spore germination, especially on YED medium. When the effect of different inoculum sizes was investigated, it was found that, although there was not a specific trend, inocula concentrations comprised between 10^6 and 10^3 sp./mL, were able to give consistent results. Hitherto there is no consensus about the choice of the optimal nutrient medium for turbidimetric assays. Nevertheless, by definition, a nutrient medium must be able to support adequate growth of the fungus and must result in reproducible results. In Chapter 4 we showed that both YED and PDA were suitable media to assess the growth dynamics of filamentous fungi in the turbidimetric assay, giving reproducible and consistent results upon repeated experiments. Nevertheless, the final choice of the medium, that was subsequently used for the turbidimetric antifungal assay performed in Chapter 5, fell onto PDA prepared from fresh potatoes since it provides a more satisfactory nutrients' composition and it is listed by the U.S. Food and Drug Administration as an approved laboratory method to help ensure food safety, while YED preparation from fresh yeast extract is not present in such list.

Due to the arising necessity of testing novel antifungal compounds for postharvest disease control, the development of a quantitative, rapid and reliable antifungal assay is nowadays crucial in food mycology. As a consequence, a method that can allow accurate results for filamentous fungi by automated monitoring represents an attracting option. For these reasons,

the turbidimetric assay was used in Chapter 5 for the screening of ZnO nanoparticles against the selected fungal isolates. Reliable and reproducible results were obtained showing that ZnO NPs, with an average diameter size lower than 50 nm, possess strong antifungal activity thus making them a potential candidate as a routine antifungal compound against postharvest disease fungi. Furthermore, data modelling allowed us to estimate the MIC and NIC for the fungus *P. expansum* (Chapter 5) and to quantify the effect of ZnO NPs against each of the studied fungal isolates in order to establish a sensitivity scale (Chapter 6). Minimal concentrations of ZnO NPs were needed to obtain a 50% reduction of the growth rate of the studied postharvest pathogens (Section 6.4.1). SEM analysis revealed that ZnO NPs induce serious physical damages to the fungal structures which can be assumed to be irreversible. The assay with EDTA provides further support to previous studies which indicate ions release as one of the potential mechanism of ZnO NPs antifungal activity.

Finally, we also show that compression is a valid procedure to enhance the air filtration efficacy of polyurethane foams (Chapter 7). Compression, by reducing the pore size of the foam, allows a more sinuous path for the air passing through the foam thus resulting in an increase in its trapping ability. Due to their low production cost on industrial scale, compressed foam filters represent a possible way to cheaply control the particle content in the air. These foam filters may be another practical solution for the food industry whereby consumer protection is essential, for instance in fruit postharvest warehouses.

Novel postharvest disease management solutions, such as ZnO nanoparticles and compressed polyurethane foams, are expected to increase the safety and the quality of pear fruit. This will provide the pears producers' sector with a powerful marketing advantage and give a concrete response to the society's demand for healthier food and environmental protection. Furthermore,

the results from this research work, will provide an essential support to pear producers in complying the new EU legislations.

Further studies will be needed in order to assess the efficacy of ZnO nanoparticles in potential *in vivo* applications, for instance as a fruit coating agent. Such studies should be carried out in greenhouses, orchards or in the postharvest chambers to investigate the effects of the ZnO NPs directly onto the fruits. Furthermore, such studies should be supplemented by performing appropriate toxicological assessments to ensure the final consumers' safety of the coated products. Additionally, ZnO NPs may also be embedded into polyurethane foam filters thus adding, to their trapping ability, also the capacity of inactivating the trapped fungal spores.

Appendixes

This section presents additional studies that were performed during the period of this Ph.D. Although these studies focused on different fungi and intervention approaches, they contributed to the final development of the experimental protocols that are presented in Chapters 4-6.

Appendix 1: Optimizing protocols to assess the efficacy of ZnO nanoparticles as antifungal agents against *Aspergillus* spp.

A1.1 Introduction

Aspergillus species are among the most abundant fungi worldwide (Krijgsheld et al., 2011). They can grow over a wide range of temperature (6-55°C) and at relatively low humidity. *Aspergilli* are predominantly found on complex plant polymers (Bennett, 2010) and are considered to be common food spoilage fungi (Krijgsheld et al., 2011). *Aspergillus niger* is the most common *Aspergillus* species responsible for postharvest decay of guavas, lichtis, mangoes, papayas, pineapples, pomegranates, apples, pears and grapes (Pitt & Hocking, 2009). *A. niger* is responsible for dry rot of sweet potato, the third most important tuber crop of Sub-Saharan Africa (Agu, Okigbo, & Ngenegbo, 2015) and there has also been a report of *A. niger* causing postharvest rot on cherry fruit (Thomidis and Exadaktylou, 2012). Another important member of the genus *Aspergillus* is *Aspergillus terreus*. *A. terreus* is a common soil saprophyte that has been isolated from desert soil, grasslands and stored corn, barley and peanuts (Balajee, 2009). Every year, it causes severe losses to important crops worldwide destroying over 125 million tons of rice, wheat, maize, soybean as well as potatoes, where it is responsible for foliar blight (Louis et al., 2014). Several studies have identified different pesticides which can control diseases caused by *Aspergillus* spp. (Bellí et al., 2006; Serey et al., 2007; Valero et al., 2007). However, the development of resistance phenomena by *A. niger* against some azole compounds (Howard et al., 2011) as well as concerns about safety due to the proved toxicity of most of the above mentioned compounds (Elskus, 2012), requires the identification of alternative solutions in postharvest disease control. In recent years, nanoparticles (NPs) have received increased interest thanks to their unique physical and chemical properties (Rai et al., 2009; He et al., 2011),

their higher stability (Espitia et al., 2012) and lower toxicity towards mammalian cells (Moritz & Geszke-Moritz, 2013). Studies aimed at assessing the antimicrobial properties of NPs involved several bioassays commonly used in microbiology, such as agar disk-diffusion and colonies diameters measurement (He et al., 2011; Savi et al., 2013; Balouiri et al., 2016). An interesting technique which can also be used for screening antifungal compounds is turbidimetry, since it correlates culture absorbance with fungal biomass (Meletiadis et al., 2003). Turbidimetry protocols have been improved and automated by computerized processing of the data (Broekaert et al., 1990; Skytta et al., 1991) thus successfully used for screening the antibacterial activity of a large variety of compounds (Rainard, 1986; Casey et al., 2004; Sarker et al., 2007; Teh et al., 2017) including nanoparticles (Martins et al., 2011; Raghupathi et al., 2011; Salem et al., 2015). However, turbidimetric studies in mycology are quite limited (Wilson et al., 1997; Meletiadis et al., 2003; Droby et al., 2009; Rossi-Rodrigues et al., 2009; Medina et al., 2012) and, hitherto, far fewer studies (Pereira et al., 2014) are available about the antifungal screening of metal nanoparticles.

A1.2. Objective

The main objective of this study was to assess the antifungal activity of ZnO nanoparticles against *A. niger* and *A. terreus* by i) disk diffusion test, ii) colonies diameter measurements and iii) turbidimetry assays. The experimental design of these three techniques was revised and complemented by using predictive mycology tools. Furthermore, the final aim of this work was to identify and discuss the limits of each technique.

A1.3. Materials and methods

A1.3.1 Inoculum preparation

Spores suspensions of *Aspergillus niger* and *Aspergillus terreus*, harvested from 5-day old MEA plates, were adjusted to a concentration of 10^5 spores/mL for both the isolates. Three 10-fold sequential dilutions were then prepared from the neat suspension. The concentration range from 10^2 to 10^5 spores/mL was used as inoculum for the modified disc-diffusion test, while for the mycelium growth inhibition and the turbidimetric assay, only the concentration of 10^5 spores/mL was used.

A1.3.2. Medium preparation

Potato Dextrose Agar (PDA) was prepared from raw potatoes as described by Pitt and Hocking (2009). The refraction index of the potato infusion was nD= 1.3340±0.0001 at 25°C. For the turbidimetric assay, agar content was modified to 0.125% w/v since this concentration has shown to give reproducible and consistent results upon repeated experiments (Medina et al., 2012).

A1.3.3. Modified disk-diffusion test

Filter paper (Whatman nº1) was cut into 15-mm diameter discs to fit the bottom of each well of 24-well flat-bottom microplates. Discs were impregnated with different ZnO NPs (< 50 nm diameter) suspensions in propan-2-ol with the following concentrations: 0 mM, 2 mM, 4 mM, 6 mM, 8 mM, 9 mM, 12 mM, 15 mM, 18 mM, 22 mM and 30 mM. After drying, 500 μl of PDA were decanted into each well and left to solidify. Wells were then inoculated with the spores'

suspensions of *A. niger* and *A. terreus*. Plates were finally incubated at 35°C for 48 hours and results were reported as binary response, i.e., growth/no growth (Tassou et al., 2009; Decelis et al., 2017). Additionally, pictures of microwells were taken by a Nikon digital camera. Fungal colonies were scooped out from each well and separated from the paper discs. Samples were mounted as fresh material (Alexopoulos and Beneke, 1962) and observed under a Leica™ inverted microscope at 100X and 400X.

A polynomial logistic equation was developed to describe the probability of growth/no growth of the studied fungi. The model incorporated the effect of the inoculum size (*ino*) and the nanoparticles' concentration (NPs). The b_i represent parameters of the equations to be estimated during the logistic regression analysis while *p* is the probability of recovery with logit(*p*) = ln (*p*/(*1-p*)).

$$\text{logit}(p) = b_1 + b_2 \cdot (NPs) + b_3 \cdot (ino) + b_4 \cdot (NPs \cdot ino) + b_5 \cdot (NPs)^2 + b_6 \cdot (ino)^2$$

The most significant parameters were selected (p < 0.001) based on a stepwise algorithm of the logistic regression (in Matlab™). Predicted interfaces for *p* = 0.1, 0.5, 0.9 were calculated and plotted.

A1.3.4. Mycelium growth inhibition

PDA medium was poured into sterile Petri dishes at 55°C and mixed with different ZnO NPs suspensions in order to reach final concentrations of 0, 5, 9, 12, 15 and 30 mM for *A. niger* and 0, 5, 9, 15, 18, 22 and 30 mM for *A. terreus*. All the plates were inoculated in the center with 10 µl of spores' suspension of each fungus and incubated at 35°C. Growth diameters were measured

twice a day and results were plotted into graphs of diameters against time. Linear regression analysis was performed to estimate the mycelium growth rate:

$$d(t) = d_o + \mu(t - \lambda)$$

d(t) is the diameter of the mycelium at time *t*([h]), $d_0$is the diameter of the inoculation suspension drop ([cm]). μ is the diameter growth rate ([cm/h]). λ is the lag phase ([h]). The lag phase was obtained from the extrapolation of the straight line and the estimation of the time at which *d(t) = d_0.*

A1.3.5. Turbidimetric assay

150 µl of semi-solid PDA and 20 µl of the inoculum suspensions were decanted and mixed into each well of standard 96-well flat-bottom plates for microtitration. Non-inoculated media, with and without nanoparticles, were also prepared and used as negative controls. Plates were incubated at 35°C into a Tecan Sunrise™ microtitre reader. O.D. was read at 600 nm automatically every 20 min without shaking. Sequential O.D. measurements were performed to generate O.D. curves for each sample, at least in quadruplicate. Each time the corresponding positive controls were also collected. Hereafter, the area under the curve was calculated by the trapezoidal method (Chorianopoulos et al., 2006).

A.1.4 Results and discussion

A1.4.1 Modified disk-diffusion test

A modified version of the common agar disk-diffusion test has been performed to investigate the complete inhibitory effect of ZnO nanoparticles against the selected isolates. Growth/no growth

probabilities were obtained for *A. niger*, while this was not possible to achieve for *A. terreus* since not enough samples showed a complete inhibition to be considered as "negative response".

Figure A1 shows the growth/no growth boundaries of *A. niger* after 48 hours of incubation. Black and white dots represent samples where growth and no growth, respectively, was observed for all the replicates. Grey shaded dots represent results where a growth/no growth variability was observed among different replicates. It can be immediately deducted that the higher the concentration of the NPs, the higher the inhibitory potential. A minimum of 12mM will be needed to achieve complete inhibition. No logistic regression was performed for *A. terreus* as the majority of responses were positive.
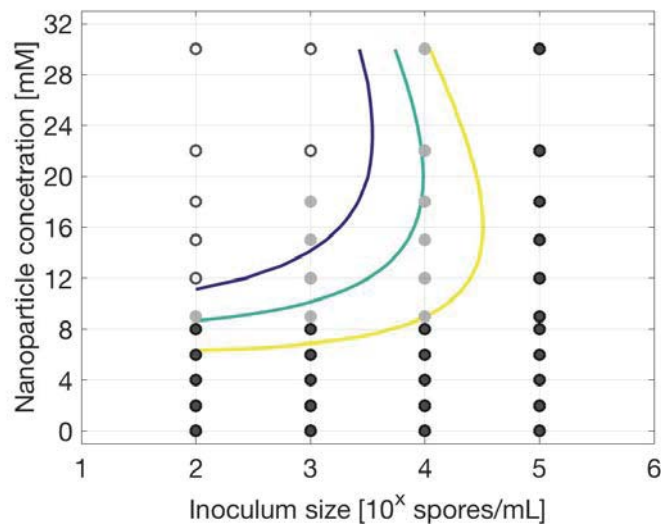
Figure A1. *Growth prediction curves for A. niger at different inoculum sizes and under different nanoparticles concentrations. The blue, the light blue and the yellow lines represent the predicted probability of growth p=0.1 , p=0.5 and p=0.9, respectively. The black, the white and the grey dots represent positive, negative and positive/negative responses respectively.*

Pictures from the microwells highlighted that both the fungi, even if at a different extent, were sensitive to the inhibitory effect of ZnO. Photos from 30 mM ZnO NPs concentration were especially selected to show that, although the samples had been reported to have a positive binary response (e.g., *A. terreus*), there was still a significant inhibition of the fungal growth. Comparisons between controls and samples treated with ZnO nanoparticles of *A. niger* and *A. terreus* are shown in Figure A2 and Figure A3 respectively.
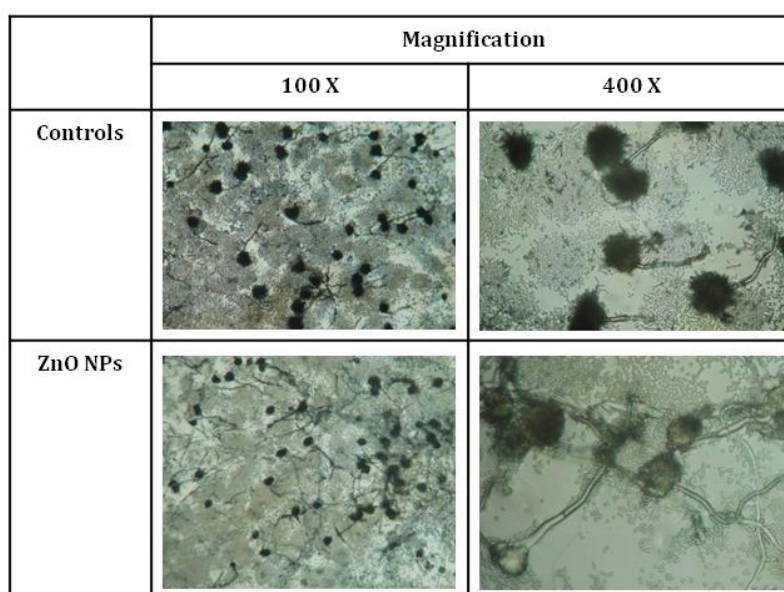
Figure A2. *Pictures from microwells with A. niger. Inoculum size is 10^5 sp./mL for each sample (control and 30 mM NPs).*

	Magnification	
	100 X	400 X
Controls		
ZnO NPs		
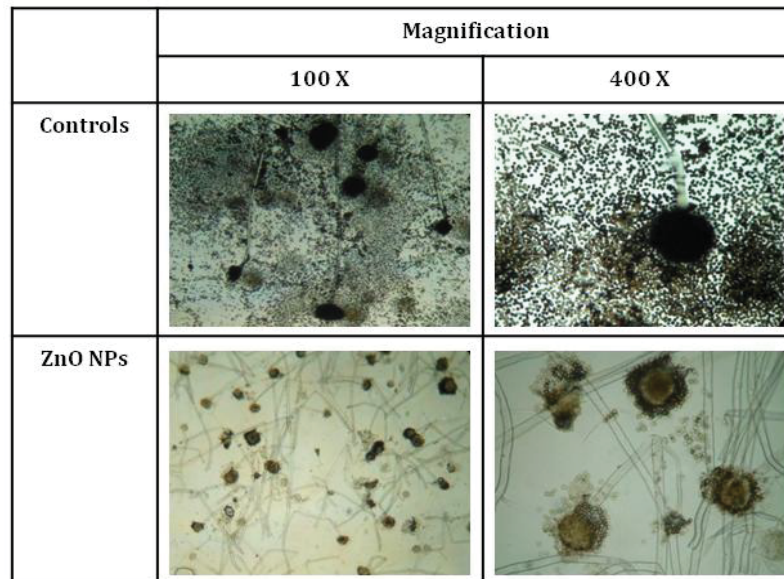
Figure A3. *Pictures from microwells with A. terreus. Inoculum size is 10^5 sp./ml for each sample (control and 30 mM NPs).*

A1.4.2 Mycelium growth inhibition

Results from diameter extension measurements showed that both the fungi were sensitive to the inhibitory effect of ZnO nanoparticles. Figure A4 shows the diameter increase rate as a function of ZnO concentration for both. *A. niger* appears to be the fungus which is more sensitive to the antagonistic effect of the nanoparticles. Nevertheless, significant antifungal activity against both *A. niger* and *A. terreus* was found already at concentrations as low as 5 mM. As the concentrations increased up to 30 mM, the efficacy of the ZnO treatment was enhanced.
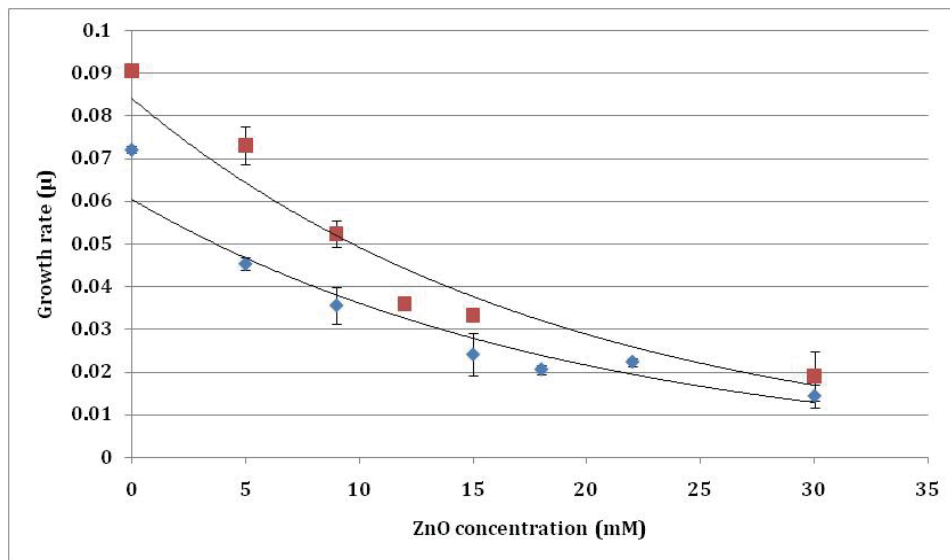
Figure A4. *Comparison of the growth ratios against ZnO concentrations for A. niger (red) and A. terreus (blue)*

As confirmed by our study, measurement of colony diameter is a very direct technique and offers the possibility to perform regression analyses thus correlating colony diameter increase with time (Sonia Marín et al., 2008). However, it should be considered with caution as it does not take into account the three-dimensional growth of fungi and it is not directly correlated with fungal biomass (Taniwaki et al., 2006; Medina et al., 2012).

Turbidimetric assay

In the case of turbidimetry, a significant inhibitory effect started to be clear from the concentration of 9 mM for *A. niger* and 5 mM for *A. terreus*. Furthermore, a significant shift in the growth is visible for *A. niger* from 5 mM to 9 mM, while from concentrations higher than 9 mM, both the fungi show comparable inhibition extents.
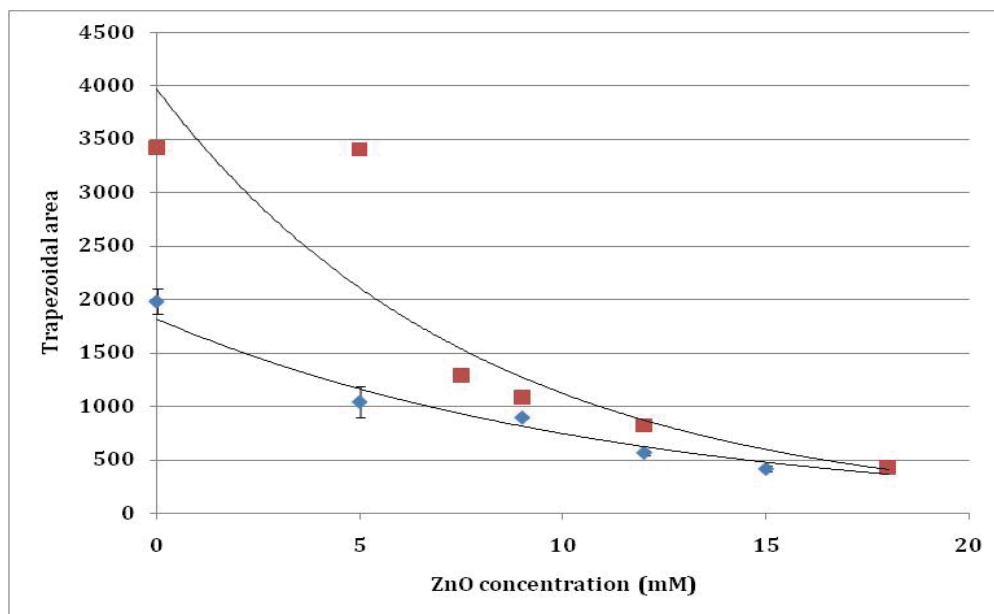
Figure A5. Comparison of the fractional areas values against ZnO concentrations for *A. niger(red) and A. terreus (blue).*

Optical density measurement is a common method to quantify various parameters like cell concentration, biomass and changes in morphology. The use of turbidimetry became popular for measuring the growth of bacterial cultures, although with the proper adjustements of parameters like medium composition and agar content, this technique can be suitable for fungi. In our study we used as growth substrate PDA prepared from raw potatoes in order to get a more satisfactory nutrients' concentration than dehydrated preparations (Rinaldi, 1982; Pitt and Hocking, 2009). Attention must be therefore paid while using commercially available powders for assessing antifungal compounds against postharvest fruit pathogens as they may lead to an overestimation of antifungal activity and provide non-realistic results. Additionally, we adjusted the agar content to 0.125% to get a semi-solid consistance of the medium. This particular agar precentage

allows the development of a homogeneous hyphal network in the three dimensions thus reducing the light crossing the well in a way that is proportional to hyphal growth and, at the same time, preventing pellet sedimentation onto the bottom of the wells (Medina et al., 2012), which are the main limitations of turbidimetric assays.From our study we can deduct that, although all the techniques are able to describe the antifungal effect of ZnO nanoparticles, there is a discrepancy in the quantification of such effect. As a matter of fact, no primary standard exists for the quantification of fungal growth, as it happens for bacteria, (Pitt & Hocking, 2009) and all the currently available techniques show some limitations and drawbacks. Mycelium growth inhibition and turbidimetry allowed to obtain more quantitative results than the modified agar disc-diffusion test. Nevertheless, the modified disc-diffusion test provided results after only 48 hours of incubation without needing to be followed up for at least 4-5 days, as instead for the mycelium growth inhibition. The modified disc-diffusion test may be therefore useful in some cases as a preliminary screening, prior to more quantitative investigations. On the other hand, turbidimetry like the mycelium growth inhibition, is a good quantitative approach and, as reported in literature, it also shows good correlation with fungal biomass (Meletiadis et al., 2003; Medina et al., 2012). Additionally, very small amounts of samples are required and the possibility for automated computerized processing of data is available.

Appendix 2: Evaluation of the interactions between *Erwinia persicina's* biofilms and fungal isolates

A2.1. Introduction

A2.1.1. Bacterial-fungal interactions

The successful establishment of an association between bacteria and fungi has deep consequences for both the organisms which can vary from case to case (Frey-Klett et al., 2011). There are instances where bacteria provide fungi with compounds that enhance fungal virulence while in other cases bacteria may repress fungal pathogenesis (Wargo & Hogan, 2006). Early evidence of antagonistic effect towards fungal pathogenicity performed by bacteria was provided by Blakeman and Fraser (1971) who found a bacterial community living on *Chrysantemum* leaves that was able to inhibit the sporulation of *Botrytis cinerea*. More recent studies showed that bacterial degradation of oxalic acid produced by *B. cinerea* can reduce the fungus' pathogenicity (H. Schoonbeek, Jacquat-Bovet, Mascher, & Métraux, 2007) or that certain *Pseudomonas* isolates, producing phenazine antibiotics, induce the expression of several ABC transporter genes in *B. cinerea* thus protecting it against their antagonistic effect (H.-J. Schoonbeek, Raaijmakers, & De Waard, 2002). In most natural environments, microorganisms are mainly present as biofilms rather than as planktonic or free cells (Douglas, 2003; El-Azizi, Starks, & Khardori, 2004; Shirtliff, Peters, Jabra-rizk, Program, & Sciences, 2009). Microbial communities are attached to natural or abiotic surfaces embedded into an exopolymeric matrix consisting of single microbial species or a mixture of bacterial and fungal species (Costerton and Montanaro, 2005; Douglas, 2003; Lewis et al., 2001; Lynch and Robertson, 2008; Shirtliff et al., 2009; Wargo and Hogan, 2006). Studies about biofilm development and species interactions are focused largely on bacterial species or on bacterial-fungal interactions within biofilms produced by human fungal pathogens such as *Candida albicans* (Costerton and Montanaro, 2005; Jenkinson and Douglas, 2002; Gupta et al., 2005; Hogan and Kolter, 2002; Kerr, 1994; Sardi et al., 2013).

A2.1.2 Biological control

Bacterial-fungal interactions have also been extensively investigated in postharvest disease-related microorganisms in order to identify putative biological antagonists able to replace conventional chemical treatments used to control fruit decay (Nunes, 2012; Spadaro & Droby, 2016). As a result of these studies, several biocontrol agents, mainly yeasts, have been successfully identified even if still few studies are available on bacterial biofilm-fungi interactions (Calvo-Garrido et al., 2014; Droby et al., 2009; W. J. Janisiewicz & Korsten, 2002; Lahlali, Hamadi, guilli, & Jijakli, 2011; Liu, Sui, Wisniewski, Droby, & Liu, 2013). The introduction of microbial antagonists is more effective in controlling postharvest diseases of fruits and vegetables than other means of biological control (R. R. Sharma, Singh, & Singh, 2009). The success of these studies on both laboratory scale and in packing houses, has generated interest in the production of microbial antagonists for the control and the prevention of postharvest diseases (R. R. Sharma et al., 2009). Although, the mechanisms of microbial antagonism have not been yet fully clarified, competition for nutrients and space is one of the most accredited modes of action (Ippolito et al., 2000; Sharma et al., 2009; Wilson et al., 2005). Additionally, antibiosis and parasitism are other modes of action of microbial antagonists (W. Janisiewicz, 2003; Wilson & Wisniewski, 1989).

Erwinia persicina is a phytopathogenic biofilm-forming bacterium belonging to the genus *Erwinia* which comprises both pathogenic and epiphytic plant-associated bacteria (Gehring & Geider, 2012). *E. persicina* has been found on common bean (González et al., 2005) and pea (González et al., 2007). It has also been isolated from tomato, banana, apple, melon, pear and cucumber (Diánez et al., 2009; Hao et al., 1990; Zhang and Nan, 2014) as well as from biofilms

located on Palaeolithic rock paintings (Kiessling et al., 2005). Interestingly, some non-pathogenic species of *Erwinia*, such as *E. cypripedii*, showed antagonistic activity, primarily by competing for nutrients, against various isolates of *Erwinia carotovora subsp. carotovora*, the causal agent of soft rot of carrots, tomatoes and pepper (Moline, 1991).

A2.1.3. *A. niger* and *P. expansum*

Aspergillus niger and Penicillium expansum are two important postharvest disease fungi. *A. niger* is the causative agent of black mould in grapes and it's a common contaminant of food (Samson et al., 2001) . *P. expansum* is responsible for blue mould, the most common postharvest disease of apple and pear. (Sutton et al., 2014).

A. niger and *P. expansum* are also known to produce several mycotoxins such as Ochratoxin A (OTA) for the former, and patulin and citrinin for the latter. OTA has various nephrotoxic, carcinogenic, immunotoxic and teratogenic effects (CAST, 2003) and it is an ubiquitous toxin contained in improperly stored food products (Kizis, Natskoulis, Nychas, & Panagou, 2014; Pfohl-Leszkowicz & Manderville, 2007). Patulin is found especially in apples infected by blue mould but also in other fruits, grains, and vegetables (Hopmans, 1997; S Marín, Morales, Hasan, Ramos, & Sanchis, 2006). Finally, citrinin-producing strains of *P. expansum* can produce metabolites which are able to inhibit *Bacillus cereus* and *Bacillus subtilis* (Viñas, Dadon, & Sanchis, 1993). Both citrinin and patulin could also elicit similar to OTA toxic responses in humans and animals (CAST, 2003).

A2.2 Objective

The aim of the present study was to evaluate *in vitro* the interactions of *Erwinia persicina* when co-cultured with *A. niger* and *P. expansum*. Furthermore, the indirect biofilm formation of *Erwinia persicina*, when co-existing with the aforementioned fungi was assessed, as well as toxin formation by the fungi.

A3. Materials and methods

A3.1 Media preparation

Czapek Yeast Agar (CYA) and Pear Pulp Agar (PPA) were used in this study. CYA composition was the same as in Pitt and Hocking (2009), while Pear Pulp Agar (PPA) was prepared following the procedure illustrated by the same authors for Potato Dextrose Agar but by replacing potatoes with "Abate Fetel" pears. After autoclaving, media were poured into sterile Petri dishes and two perpendicular diameters were drawn onto the plates' reverse sides to allow growth diameter measurement. The water activity (a_w) of each medium was measured with an *AquaLab LITE* water activity meter (Degacon, *USA*) and was found to be $a_w = 0.99$ for both of them.

A3.2 Preparation of cultures and growth studies

Fungal spores were harvested from 7-day old Malt Extract Agar (MEA) cultures by adding 10 ml of a 0.05% Tween-80 solution and by scraping off the plate's surface with a sterile bent rod. The resulting suspension was aseptically filtered through 4-layer sterile gauze to remove any mycelial contamination. Fungal spores were then counted with a haemocytometer. The stock cultures for *Erwinia persicina* stored in vials at −80°C and were activated after adding 10 μl to 10 ml of Tryptone Soy Broth (TSB; LabM) and incubated at 25°C for 24 hours. A 10 μl portion of the activated culture was transferred to 10 ml of fresh TSB and incubated at 25 °C for 24 h. Bacteria were harvested after centrifugation at 5000g for 10 min at 4 °C (Multifuge 1S-R, Thermo

Electron Corporation). The cell pellet was washed twice in 10 ml of 1/4 Ringer solution (Ringer's Solution Tablets, LabM) and re-suspended in 10 ml of 1/4 Ringer Solution and further diluted in quarter-strength Ringer solution to yield inocula of *E. persicina* of approximately 10^4 CFU ml^{-1} to be used for the assays.

A total volume of 100 µl for *E. persicina* (final concentration ca 10^3 CFU ml^{-1}) was spread homogeneously onto the plates' surface and afterwards, when plates were dry, an appropriate volume of the initial fungal spores' suspension was inoculated in the centre of the plates so that the final amount of spores was in the range of 10^3. *Erwinia persicina* was co-inoculated with both the fungi. Two controls with *E. persicina* alone and each fungus alone were also prepared. Plates were closed into polyethylene sterile bags to prevent media desiccation and incubated at 25°C for 7 days.

A3.3 Sample preparation for fluorescence microscopy analysis

A batch of sterile test tubes was filled with Pear Pulp Broth (PPB). PPB was prepared as for the growth studies but without adding agar. A stainless steel coupon was inserted into each tube in order to provide abiotic surface enhancing the biofilm formation. Tubes were filled with 4.5 ml of broth and mixed with the previously prepared fungal spores' suspensions in order to reach a final concentration of 10^3 spores ml^{-1} for both the fungi. 500 µl of *E. persicina* bacterial suspension (final concentration ca 10^3 CFU ml^{-1}) were also added to the tubes. Similar to the previous assays, control samples of *E. persicina* alone and the fungi alone were also prepared. Finally, tubes were incubated for 7 days at 25°C. After the incubation, the stainless steel coupons were removed from the tubes, stained with orange acridine, washed with absolute methanol and

rinsed with distilled water prior to observation under fluorescence microscope (N-400FL, OPTIKA, Italy) at 1000× magnification.

A3.4 Assessment of toxin production

The production of patulin and citrinin by *P. expansum* and of ochratoxin A (OTA) by *A. niger* were investigated. A preliminary assessment was performed by growing the fungi onto Coconut Cream Agar (CCA) plates in order to detect the production of citrinin by *P. expansum* and OTA by *A. niger*. CCA was prepared as follows according to Heenan et al. but without adding chloramphenicol (Heenan et al., 1998). After autoclaving, medium was shaken vigorously before pouring it into the plates to allow a better homogenisation. Plates were incubated as for the previous experiments at 25°C for 7 days. Afterwards, plates were observed from the reverse side under long wavelength (365 nm) UV light (Dyer, 1994; Heenan et al., 1998; Mohamed et al., 2013) and pictures were collected.

Patulin and OTA production from *P. expansum* and *A. niger* respectively, have been quantified by processing the samples by HPLC. For the toxins' extraction, *A. niger* and *P. expansum* were grown onto CYA plates with and without *E. persicina*, following the same inoculation scheme of the previous sections, and incubated at 25°C for 7 days. The whole content of each Petri dish (medium and mycelium) was weighted in order to express OTA and patulin production per g of substrate and extraction took place with 100 ml of an 80:20 methanol:water solution of HPLC grade purity (Kizis et al., 2014). The weighted substrates were blended with the solutions for 2 min, left for a total of 30 min before being filtered, first through a Whatman N°1 filter paper and subsequently through a Millex® nylon membrane syringe-driven filter of 0.2 mm pore size (EMD Millipore Corp. Billerica, USA), and finally kept at 4°C until analysis. The quantification of OTA and patulin performed by reversed-phase HPLC methods in accordance with the

European Standards EN 14177 and EN 14133, while detection levels were 2 and 1 ppb for patulin and OTA, respectively (CEN, 2003a; CEN, 2003b).

A4. Results and discussion

A4.1 Growth diameters measurements

The co-culture of *A. niger* with *E. persicina* on PPA (Fig. A2.1a) showed an antagonistic effect due to the presence of the bacterium. On the contrary, such antagonism was not evident on CYA (Fig. A2.1b) where the two combinations showed comparable growth results. In the case of *P. expansum,* a growth delay appeared from 50 till 150 hours of co-culture on PPA (Fig. A2.1c), while no significant difference was observed in the same co-culture on CYA (Fig. A2.1d) plates. These results show that there is an antagonistic effect onto the fungal growth due to the co-presence of the bacterium. *P. expansum* was inhibited only in the initial stage of the growth, regardless substrate, while *A. niger* has shown not to be significantly influenced by the bacterium's presence on CYA. There was a significant discrepancy between results on CYA and PPA plates, as significant antagonistic effect was shown only on the latter. Different factors can contribute to trigger antagonistic effect during bacterial-fungal interactions. These could be assigned to the nutrients' composition as well as the carbon/nitrogen sources availability (Ajdari et al., 2011; Engelkes, Nuclo, & Fravel, 1997; Rajderkar, 1966; Timnick, Lilly, & Barnett, 2015) which can explain the difference observed between CYA and PPA. Therefore, nutrients' availability and competition for their uptake should be considered when assessing biofilm-fungi interactions by using in vitro model systems that represent realistic conditions. However, it is also known that the competition can be advantageous for the fungi if they have the opportunity to establish before the bacteria thus gaining higher biomass (Mille-Lindblom, Fischer, & Tranvik, 2006).
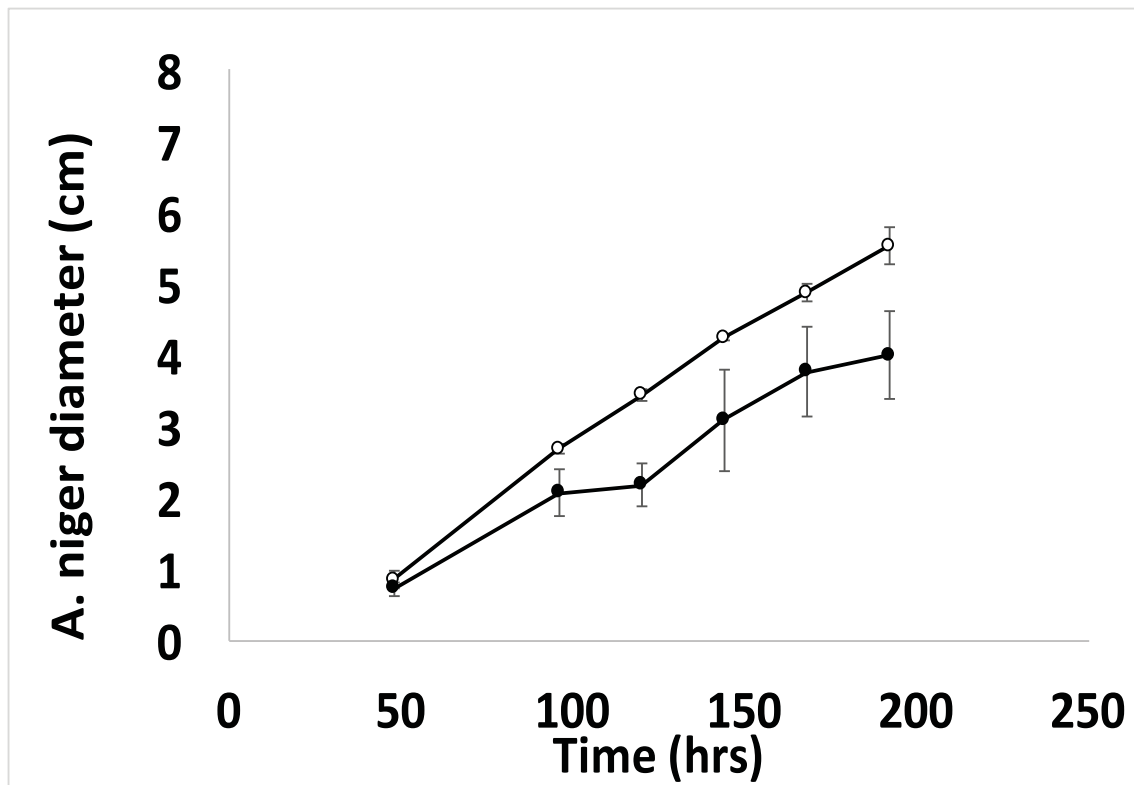
Figure A2.1: Diametric increase of *A. niger* and *P. expansum* alone (○) and during co-culturing with *E. persicina* (●) at 25°C on PPA (a, c) and CYA (b, d). Data are mean values with standard error bars of growth diameters against time. Each point represents an average of triplicate measurements.

A4.2 Fluorescence microscopy

Fluorescence microscopy allowed the investigation of the biofilm's behaviour during the co-cultures with the fungi. Figure A2.2(a) shows a control with *E. persicina*'s biofilm growing alone, appearing like a consistent orange mass of cells. Samples with *P. expansum* showed variable results as there were some areas of the coupons where the two microorganisms co-existed but both in a reduced size (Fig. A2.2b) and some others where the fungal growth was predominant onto the biofilm (Fig. A2.2c). Microscopy studies revealed filamentation of *A. niger* alone (Fig A2.2d)*,* while in co-culture with *E. persicina* fungal colonization was eliminated due to extensive bacterial attachment onto fungal hyphae (Fig. A2.2e, f).

Fluorescence microscopy pictures revealed that there was a reciprocal antagonistic effect occurring during the bacterial biofilm-fungi interactions as it was also observed in the growth diameter studies, especially on PPA. In the case of *A. niger*, the biofilm's structure was compromised, even though bacterial cells were able to adhere and grow onto the fungal hyphae. This phenomenon was not observed with *P. expansum*, where *E. persicina* was growing mostly as isolated colonies near the fungal cells. Hyphal attachment by antagonists is a phenomenon which has been already described in other studies. Wisniewski et al. (1991) observed that *Pichia guilliermondii* cells had the capacity to attach to the hyphae of *Botrytis cinerea*. After *Pichia*'s cells were dislodged from the hyphae, the hyphal surface appeared to be concave and there was a partial degradation of the cell wall of *Botrytis cinerea* at the attachment sites. Furthermore, *Candida saitona* was also shown to attach strongly to the hyphae of *Botrytis cinerea* thus causing swelling (El-Ghaouth, Wilson, & Wisniewski, 1998). Attachment of the antagonists to a site enhances their potential activity for the utilization of nutrients at the invasion site and it partly affects the access of the pathogen to the nutrients as well (R. R. Sharma et al., 2009).

126
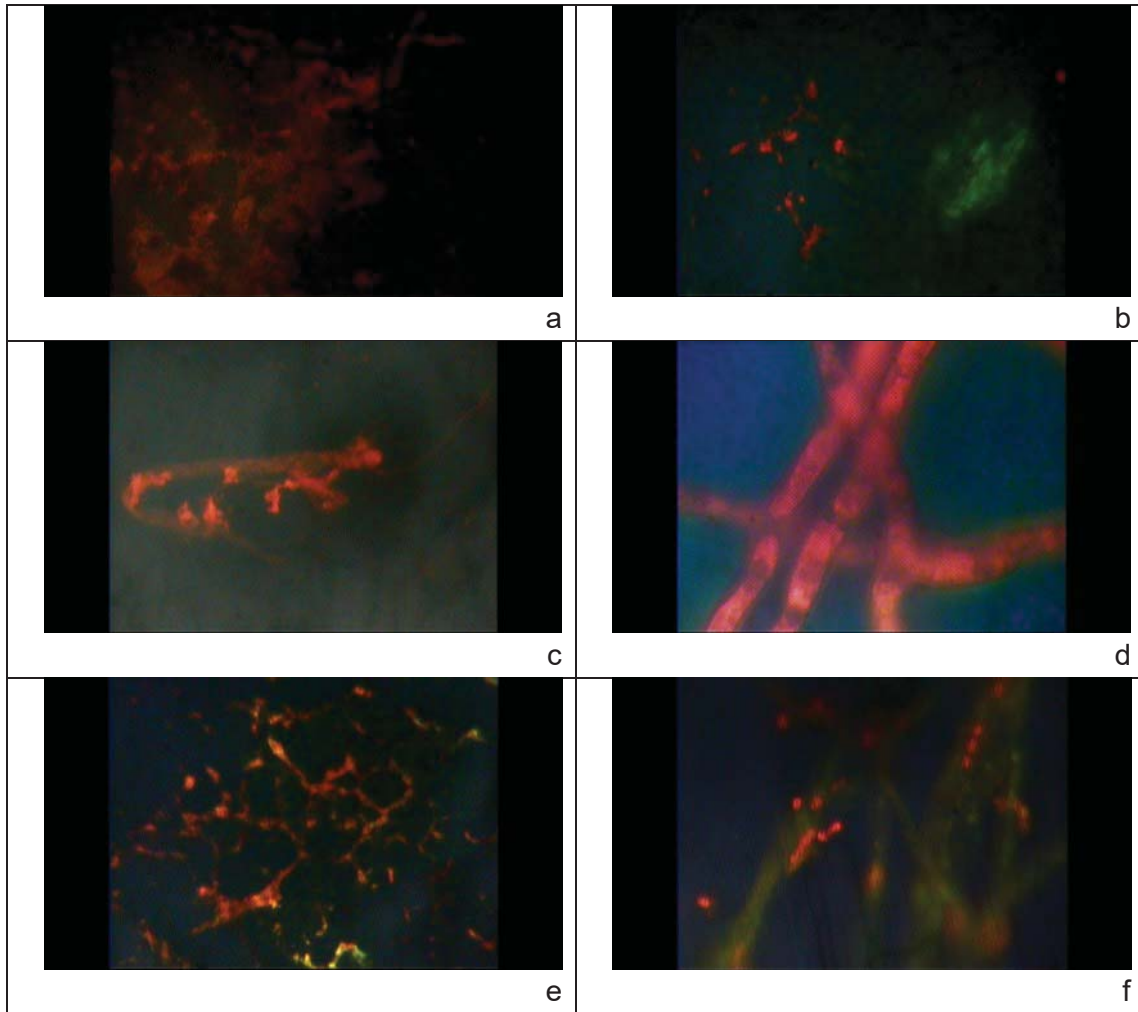
Figure A2.2*: a) Bacterial biofilm of *E. persicina* growing alone in PPB; b) and c) Different fields of view of the same sample of *P. expansum* growing with *E. persicina* in PPB; d) Fungal hyphae of *A. niger* growing alone in PPB; e) and f) Fungal hyphae of *A. niger* covered by *E. persicina*'s cells.

A4.3 Toxins detection

Figure A3.3 shows the CCA plates emitting fluorescence under long wavelength UV light. Plates with *E. persicina* alone showed a weak and barely visible greenish fluorescence in the centre of the plate (Fig A3.3a). Plates of *A. niger* grown with *E. persicina* (Fig A3.3b) and alone (Fig A3.3c) both showed a yellow-greenish fluorescence. Plates with *P. expansum* showed a central round yellow-greenish fluorescence which was more extensive for the samples of *P. expansum* grown alone (Fig A3.3e) than those co-cultured with *E. persicina* (Fig A3.3d). HPLC analyses have shown that *A. niger* produced 54.84 ppb of OTA when grown alone and 34.03 ppb of OTA when co-cultured with *E. persicina*. No patulin was detected in any of the tested samples.

The ability of certain microorganisms to produce toxins and/or a multitude of low molecular weight molecules can affect, positively or negatively, the growth of the neighbouring ones (Frey-Klett et al., 2011; Schroeckh et al., 2009). Results from the current study show that there is a production of citrinin by *P. expansum* and of OTA by *A. niger*. Both the toxins are present in higher quantity when the fungi are grown alone as shown by the more intense fluorescence signal onto the CCA plates (for both citrinin and OTA) and as confirmed, in the case of the OTA, by HPLC quantification. Evidently, this is another antagonistic effect of the co-culture with *E. persicina*. Patulin detection was instead negative for all the fungi by HPLC analyses. *E. persicina* was also emitting a weak fluorescence on CCA which, to the knowledge of the authors, cannot be assigned to any toxins production for this bacterium (Diánez et al., 2009).
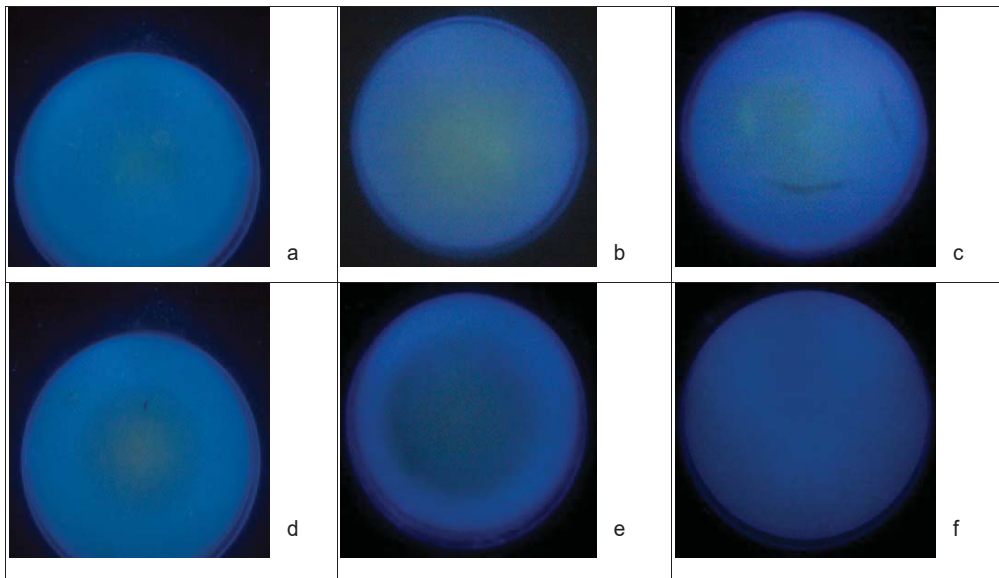
Figure A3: a) *E. persicina* grown alone on CCA; b) Co-culture of *E. persicina* and *A. niger*; c) *A. niger* grown alone; d) *P. expansum* grown with *E. persicina*; e) *P. expansum* grown alone; f) Uninoculated plate filled with CCA only, used as control.

A5. Conclusions

This study investigates the interactions between bacterial biofilm and filamentous fungi. Evidences of a mutual antagonistic effect between the biofilm-forming bacterium *E. persicina* and the fungi *A. niger* and *P. expansum* are identified. Nutrients uptake competition, fungal filamentation and toxins production are factors playing a critical role in establishing the observed antagonistic effects. Understanding the mode of action of antagonist microorganisms is nowadays important for the development of biological control agents and for providing support to genetic manipulation studies in the area of crop protection. Genetic manipulation may result in new biocontrol strains, with increased production of toxic compounds and lytic enzymes, improved space and nutrients competence or else non-virulent mutants where unwanted genes

might be deleted (Janisiewicz, 2003; Spadaro & Gullino, 2005).

References

AbuQamar, S.F., Moustafa, K., Tran, L. S. P. (2016). Omics and Plant Responses to Botrytis cinerea. *Frontiers in Plant Science*, *7*:1658.

Agu, K. C., Okigbo, I. C. C., Ngenegbo, U. C. (2015). Fungi Associated with the Post-Harvest Loss of Sweet Potato. *International Journal of Research Studies in Biosciences. 3*(9), 33–38.

Ajdari, Z., Ebrahimpour, A., Abdul Manan, M., Hamid, M., Mohamad, R., Ariff, A. B. (2011). Nutritional requirements for the improvement of growth and sporulation of several strains of monascus purpureus on solid state cultivation. *Journal of Biomedicine and Biotechnology*, (2011). *2011*, 1-9.

Alexopoulos, C.J., Beneke, E.S. (1962). *Laboratory Manual for INTRODUCTORY MYCOLOGY*. Minneapolis: Burgess Publishing Company.

Alexopoulos, C.J. Mims, C. W. (1979). *Introductory mycology*. John Wiley & Sons, Inc.

Alves, E., Lucas, G.,C., Pozza, E.,A., de Carvalho Alves, M. (2013). Scanning Electron Microscopy for Fungal Sample Examination. In G. Gupta, K.V. and Tuohy, M. (Ed.), *Laboratory Protocols in Fungal Biology*.

Aponiene, K., Rasiukeviciute, J., Viskelis, A., Valiuskaite, P., Viskelis, P., Uselis, N., Luksiene, Z. (2015). First attempts to control microbial contamination of strawberries by ZnO nanoparticles. In *Interanational Nonthermal Processing Workshop, Athens, Greece*. p.143.

Arbi, B. El, Idrissi, E. L., Brahim, S., Issam, M. K., Lahoucine, H., Abderraouf, H. (2014). Screening of actinomycete bacteria producing antifungal metabolites which could be used in biological control against a phytopathogenic fungus (Rhizopus stolonifer). *Open Science. 2*(4), 84–89.

Arciniegas-Grijalba, P. A., Patiño-Portela, M. C., Mosquera-Sánchez, L. P., Guerrero-Vargas, J. A., Rodríguez-Páez, J. E. (2017). ZnO nanoparticles (ZnO-NPs) and their antifungal activity against coffee fungus Erythricium salmonicolor. *Applied Nanoscience*, *7*(5), 225–241.

Baert, K., Valero, A., De Meulenaer, B., Samapundo, S., Ahmed, M. M., Bo, L., Devlieghere, F. (2007). Modeling the effect of temperature on the growth rate and lag phase of Penicillium expansum in apples. *International Journal of Food Microbiology*, *118* (2), 139–150.

Balajee, S. A. (2009). *Aspergillus terreus* complex. *Medical Mycology*, *47*(s1), S42–S46.

Balouiri, M., Sadiki, M., & Ibnsouda, S. K. (2016). Methods for in vitro evaluating antimicrobial activity: A review. *Journal of Pharmaceutical Analysis*, *6*(2), 71–79.

Banoee, M., Seif, S., Nazari, Z. E., Jafari-Fesharaki, P., Shahverdi, H. R., Moballegh, A., Shahverdi, A. R. (2010). ZnO nanoparticles enhanced antibacterial activity of ciprofloxacin against Staphylococcus aureus and Escherichia coli. *Journal of Biomedical Materials Research - Part B Applied Biomaterials*, *93*(2), 557–561.

Barani, H., Montazer, M., Samadi, N., Toliyat, T. (2012). In situ synthesis of nano silver/lecithin on wool: Enhancing nanoparticles diffusion. *Colloids and Surfaces B: Biointerfaces*, *92*, 9–15.

Bellí, N., Marín, S., Sanchis, V., Ramos, J. (2006). Impact of fungicides on Aspergillus carbonarius growth and ochratoxin A production on synthetic grape-like medium and on grapes. *Food Additives and Contaminants*, *23*(10), 1021–9.

Bennett, J. W. (2010). An Overview of the Genus Aspergillus, pp. 1-17. In: Aspergillus molecular Biology and Genomic. M. Machida and K. Gomi (eds.), Caister Academic Press, Norfolk, Uk.

Bizukojc, M., Ledakowicz, S. (2006). A kinetic model to predict biomass content for Aspergillus niger germinating spores in the submerged culture. *Process Biochemistry*, *41*(5), 1063–1071.

Blakeman, J. P., Fraser, A. K. (1971). Inhibition of Botrytis cinerea spores by bacteria on the surface of chrysanthemum leaves. *Physiological Plant Pathology*, *1*(1), 45–54.

Boba, K., Bianchi, M., McCombe, G., Gatt, R., Griffin, A. C., Richardson, R. M., Grima, J. N. (2016). Blocked Shape Memory Effect in Negative Poisson's Ratio Polymer Metamaterials. *ACS Applied Materials & Interfaces*, *8*(31), 20319–20328.

Bondarenko, O., Juganson, K., Ivask, A., Kasemets, K., Mortimer, M., Kahru, A. (2013). Toxicity of Ag, CuO and ZnO nanoparticles to selected environmentally relevant test organisms and mammalian cells in vitro: A critical review. *Archives of Toxicology*, *87*(7), 1181–1200.

Briffa, M., Decelis, S., Brincat, J. P., Grima, J. N., Gatt, R., Valdramidis, V. (2017). Evaluation of polyurethane foam materials as air filters against fungal contamination. *Food Control*, *73*, 91–100. 8

Brincat, J. P., Sardella, D., Muscat, A., Decelis, S., Grima, J. N., Valdramidis, V., Gatt, R. (2016). A review of the state-of-the-art in air filtration technologies as may be applied to cold storage warehouses. *Trends in Food Science and Technology*. *50*, 175-185. Elsevier Ltd.

Broekaert, W. F., Franky R.G. Terras, Vanderleyden, J. (1990). An automated quantitative assay for fungal growth inhibition. *Fems Microbiology Letters*, *69*, 55–60.

Brooks, C., Cooley, J. S. (1928). Time-Temperature relations in different types of peach-rot infection. *Journal of Agricultural Research*, *37*(9), 507–543.

Brooks, F. T., Hansford, C. G. (1923). Mould growths upon cold-store meat. *Transactions of the British Mycological Society*, *8*(3), 113–142. Calam, C. T. (1969). The culture of micro-organisms in liquid medium. *Methods in Microbiology*, *1*, 255-326.

Calvo-Garrido, C., Viñas, I., Usall, J., Rodríguez-Romera, M., Ramos, M. C., Teixidó, N. (2014). Survival of the biological control agent Candida sake CPA-1 on grapes under the influence of abiotic factors. *Journal of Applied Microbiology*, *117*(3), 800–811.

Casalinuovo, I.A., Sorge, R., Bonelli, G., Di Francesco, P. (2017). Evaluation of the antifungal effect of EDTA, a metal chelator agent, on Candida albicans biofilm. *European Review for Medical and Pharmacological Sciences. 21*(6):1413–1420.

Casey, J. T., O'Cleirigh, C., Walsh, P. K., O'Shea, D. G. (2004). Development of a robust microtiter plate-based assay method for assessment of bioactivity. *Journal of Microbiological Methods*, *58*(3), 327–334.

CAST, (Council for Agricultural Science and Technology). (2003). *Mycotoxins: Risks in Plant, Animal, and Human Systems*.

CEN (Comité Européen de Normalisation), 2003a, Foodstuffs - Determination of ochratoxin A in wine and beer - HPLC method with immunoaffinity column clean-up, EN14133:2003. European Committee for Standardization, Brussels, pp. 1-19.

CEN (Comité Européen de Normalisation), 2003b, Foodstuffs - Determination of patulin in clear and cloudy apple juice and puree - HPLC method with liquid/liquid partition clean-up, EN14177:2003. European Committee for Standardization, Brussels, pp. 1-26.

Chilvers, K. F., Reed, R. H., Perry, J. D. (1999). Phototoxicity of rose bengal in mycological media--implications for laboratory practice. *Letters in Applied Microbiology*, *28*(2), 103–7.

Chorianopoulos, N. G., Lambert, R. J. W., Skandamis, P. N., Evergetis, E. T., Haroutounian, S.

A., Nychas, G. J. E. (2006). A newly developed assay to study the minimum inhibitory concentration of Satureja spinosa essential oil. *Journal of Applied Microbiology*, *100*(4), 778–786.

Cioffi, N., Torsi, L., Ditaranto, N., Tantillo, G., Ghibelli, L., Sabbatini, L., Traversa, E. (2005). Copper nanoparticle/polymer composites with antifungal and bacteriostatic properties. *Chemistry of Materials*, *17*(21), 5255–5262.

Coates, L., Johnson, G., Dale, M. (1997). Postharvest diseases of fruit and vegetables. In H. Brown, J., Ogle (Ed.), *Plant pathogens and plant diseases*.

Costerton, J.W., Montanaro, L., (2005). Biofilm in implant infections: its production and regulation. *International Journal of Artificial Organs*, *28*, 1062–1068.

Cousin, M. A. (1996). Chitin as a Measure of Mold Contamination of Agricultural Commodities and Foods. *Journal of Food Protection*, *59*(1), 73–81.

D'Enfert, C. (1997). Fungal Spore Germination: Insights from the Molecular Genetics of Aspergillus nidulans and Neurospora crassa. *Fungal Genetics and Biology*, *21*(2), 163–172.

Dantigny, P., Guilmart, A., Bensoussan, M. (2005). Basis of predictive mycology. *International Journal of Food Microbiology*, *100*(1–3), 187–196.

Dean, R., Van Kan, J. A. L., Pretorius, Z. A., Hammond-Kosack, K. E., Di Pietro, A., Spanu, P. D., Foster, G. D. (2012). The Top 10 fungal pathogens in molecular plant pathology. *Molecular Plant Pathology*, *13*(4), 414–430.

Decelis, S., Sardella, D., Triganza, T., Brincat, J.P., Gatt, R., Valdramidis, V. P. (2017). Assessing the Anti-fungal Efficiency of Filters Coated with Zinc Oxide Nanoparticles. *Royal Society Open Science*, *4. 16032*.

Diánez, F., Santos, M., Font, I., de Cara, M., Tello, J. C. (2009). New host for the enterobacterial

phytopathogen Erwinia persicina. *Current Research Topics in Applied Microbiology and Microbial Biotechnology,* 78–82. II International Conference on Environmental, Industrial and Applied Microbiology. University of Seville, Spain, 28th November - 1st December 2007.

Dimkpa, C. O., McLean, J. E., Britt, D. W., Anderson, A. J. (2013). Antifungal activity of ZnO nanoparticles and their interactive effect with a biocontrol bacterium on growth antagonism of the plant pathogen Fusarium graminearum. *BioMetals*, *26*(6), 913–924.

Douglas, L. J. (2003). Candida biofilms and their role in infection. *Trends in Microbiology*, *11*(1), 30–36.

Droby, S., Wisniewski, M., Macarisin, D., Wilson, C. (2009). Twenty years of postharvest biocontrol research: Is it time for a new paradigm? *Postharvest Biology and Technology*, *52*(2), 137–145.

Dutta, R. K., Nenavathu, B. P., Gangishetty, M. K., Reddy, A. V. R. (2012). Studies on antibacterial activity of ZnO nanoparticles by ROS induced lipid peroxidation. *Colloids and Surfaces B: Biointerfaces*, *94*, 143–150.

Dyer, S. (1994). Detection of toxigenic isolates of Aspergillus flavus and related species on coconut cream agar. *Journal of Applied Microbiology*, *76*(1964), 75–78.

El-Azizi, M. A., Starks, S. E., Khardori, N. (2004). Interactions of Candida albicans with other Candida spp. and bacteria in the biofilms. *Journal of Applied Microbiology*, *96*(5), 1067–1073.

El-Ghaouth, A., Wilson, C. L., Wisniewski, M. E. (1998). Ultrastructural and Cytochemical Aspects of the Biological Control of Botrytis cinerea by Candida saitoana in Apple Fruit. *Phytopathology*. *88*, 282–291.

El-Kazzaz, M. K. (1983). Ethylene Effects on In Vitro and In Vivo Growth of Certain Postharvest Fruit-Infecting Fungi. *Phytopathology*, *73*(7), 998.

El-Ramady, H. R., Domokos-szabolcsy, É., Abdalla, N. A., Taha, H. S., Fári, M. (2013). Sustainable Agriculture and Climate Changes in Egypt. *Sustainable Agriculture Reviews. 12*, 41-95.

Elskus, A. A. (2012). *Toxicity, Sublethal Effects, and Potential Modes of Action of Select Fungicides on Freshwater Fish and Invertebrates*. Reston, Virginia.

Engelkes, C. A., Nuclo, R. L., Fravel, D. R. (1997). Effect of carbon, nitrogen, and C:N ratio on growth, sporulation, and biocontrol efficiency of Talaromyces flavus. *Phytopathology*, *87*(5), 500–505.

Eskandari, M., Haghighi, N., Ahmadi, V., Haghighi, F., Mohammadi, S. R. (2011). Growth and investigation of antifungal properties of ZnO nanorod arrays on the glass. *Physica B: Condensed Matter*, *406*(1), 112–114.

Espitia, P. J. P., Soares, N. de F. F., Coimbra, J. S. dos R., de Andrade, N. J., Cruz, R. S., Medeiros, E. A. A. (2012). Zinc Oxide Nanoparticles: Synthesis, Antimicrobial Activity and Food Packaging Applications. *Food and Bioprocess Technology*, *5*(5), 1447–1464.

FAO. (2009). Course on agribusiness management for producers' associations. Module 4 – Post-harvest and marketing. In T. F. Santacoloma P, Roettger A (Ed.), *Training materials for agricultural management, marketing and finance*. Rome.

Fatehah, M. O., Aziz, H. A., Stoll, S. (2014). Stability of ZnO Nanoparticles in Solution. Influence of pH, Dissolution, Aggregation and Disaggregation Effects. *Journal of Colloid Science and Biotechnology*, *3*(1), 75–84.

FDA. (2016). Part 182—substances generally recognized as safe. Washington DC, USA: Food

and drug administration. Retrieved from https://www.accessdata.fda.gov/scripts/cdrh/cfdocs/cfcfr/CFRSearch.cfm?fr=182.8991

FDA BAM Media M127. January 2001. https://www.fda.gov/food/foodscienceresearch/laboratorymethods/ucm063519.htm (Last access: 25/09/2017).

FDA. (2001). BAM Media M183: Dichloran rose bengal chloramphenicol (DRBC) agar. Retrieved September 21, 2017, from https://www.fda.gov/Food/FoodScienceResearch/LaboratoryMethods/ucm064266.htm

Feng, W., & Zheng, X. (2007). Essential oils to control Alternaria alternata in vitro and in vivo. *Food Control*, *18*(9), 1126–1130.

Fieira, C., Oliveira, F., Calegari, R. P., Machado, A., Coelho, A. R. (2013). In vitro and in vivo antifungal activity of natural inhibitors against Penicillium expansum Inibidores naturais no controle in vitro e in vivo de Penicillium expansum. *Food Science and Technology*. *33*(1), 40–46.

Food and Agriculture Organization of the United Nations (FAO). (2014). FAOSTAT. Retrieved from http://www.fao.org/faostat/en/#data/QC

Frey-Klett, P., Burlinson, P., Deveau, A., Barret, M., Tarkka, M., Sarniguet, A. (2011). Bacterial-Fungal Interactions: Hyphens between Agricultural, Clinical, Environmental, and Food Microbiologists. *Microbiology and Molecular Biology Reviews*, *75*(4), 583–609.

Gatt, R., Attard, D., Manicaro, E., Chetcuti, E., Grima, J. N. (2011). On the effect of heat and solvent exposure on the microstructure properties of auxetic foams: A preliminary study. *Physica Status Solidi (B) Basic Research*, *248*(1), 39–44.

Gehring, I., Geider, K. (2012). Identification of Erwinia species isolated from apples and pears

by differential PCR. *Journal of Microbiological Methods*, *89*(1), 57–62.

Ghule, K., Ghule, A. V., Chen, B.-J., & Ling, Y.-C. (2006). Preparation and characterization of ZnO nanoparticles coated paper and its antibacterial activity study. *Green Chemistry*, *8*(12), 1034.

Gkana, E. N., Natskoulis, P. I., Nychas, G. J. E., Panagou, E. Z. (2016). Effect of Initial Inoculum and Substrate Composition on Growth and Biofilm Formation of Aspergillus carbonarius in Microtiter Plates. In *IAFP's conference*, 11th-13th May 2016, Athens, Greece.

Gong, P., Li, H., He, X., K, W., Hu, J., Tan, W. (2007). Preparation and Antibacterial Activity of Fe3O4@Ag Nanoparticles. *Nanotechnology*, *18*, 604–11.

González, A. J., Tello, J. C., de Cara, M. (2005). First report of Erwinia persicina from Phaseolus vulgaris in Spain. *Plant Disease*, *89*, 109.

González, A. J., Tello, J. C., Rodicio, M. R. (2007). Erwinia persicina causing chlorosis and necrotic spots in leaves and tendrils of Pisum sativum in southeastern Spain. *Plant Disease*, *91*, 460.

Gougouli, M., Kalantzi, K., Beletsiotis, E., Koutsoumanis, K. P. (2011). Development and application of predictive models for fungal growth as tools to improve quality control in yogurt production. *Food Microbiology*, *28*(8), 1453–1462.

Gougouli, M., Koutsoumanis, K. P. (2012). Modeling germination of fungal spores at constant and fluctuating temperature conditions. *International Journal of Food Microbiology*, *152*(3), 153–161.

Grimm, L. H., Kelly, S., Krull, R., Hempel, D. C. (2005). Morphology and productivity of filamentous fungi. *Applied Microbiology and Biotechnology*, *69*(4), 375–384.

Guiller, L., Nazer, A. I., Dubois-Brissonnet, F. (2007). Growth Response of Salmonella

Typhimurium in the presence of natural and synthetic antimicrobials : Estimation of MICs from Three Different Models. *Journal of Food Protection*. *70*(10), 2243–2250.

Gupta, N., Haque, A., Mukhopadhyay, G., Narayan, R. P., Prasad, R. (2005). Interactions between bacteria and Candida in the burn wound. *Burns*, *31*(3), 375–378.

Hao, M.V., Brenner, D.J., Stigerwat, A.G., Kosako, Y., Komagata, K. (1990). Erwinia persicinus, a new species isolated from plants. *International Journal of Systematic Bacteriology*. 40(4): 379-383.

Harper, K. A., Beattie, B., Pitt, J. I., Best, D. J. (1972). Texture changes in canned apricots following infection of the fresh fruit with Rhizopus stolonifer. *Journal of the Science of Food and Agriculture*, *23*, 311–320.

Hart, J. R. (2011). Ethylenediaminetetraacetic Acid and Related Chelating Agents. *Ullmann's Encyclopedia of Industrial Chemistry*, 547–572.

He, L., Liu, Y., Mustapha, A., & Lin, M. (2011). Antifungal activity of zinc oxide nanoparticles against Botrytis cinerea and Penicillium expansum. *Microbiological Research*, *166*(3), 207–215.

Heenan, C.N., Shaw, K.J., Pitt, J. I. (1998). Ochratoxin A production by Aspergillus carbonarius and A. niger isolates and detection using coconut cream agar. *Journal of Food Mycology*, *1*(2), 67–72.

Henriquez, J. L., Sugar, D., Spotts, R. (2004). Etiology of bull's eye rot of pear caused by Neofabraea spp. in Oregon, Washington, and California. *Plant Disease*, *88*(10), 1134–1138.

Henriquez, J. L., Sugar, D., Spotts, R. (2008). Effects of Environmental Factors and Cultural Practices on Bull's Eye Rot of Pear. *Plant Disease*, *92*(3), 421–424.

Hogan, D. A., & Kolter, R. (2002). Pseudomonas-Candida Interactions: An Ecological Role for

Virulence Factors. *Science*, *296*(5576), 2229-2232.

Hopmans, E. (1997). Patulin: a Mycotoxin in Apples. *Perishables Handling Quarterly Issue. 91*, 5–6.

Howard, S. J., Harrison, E., Bowyer, P., Varga, J., Denning, D. W. (2011). Cryptic species and azole resistance in the Aspergillus niger complex. *Antimicrobial Agents and Chemotherapy*, *55*(10), 4802–4809.

Hurley, P. M., Hill, R. N., Whiting, R. J. (1998). Mode of carcinogenic action of pesticides inducing thyroid follicular cell tumors in rodents. *Environmental Health Perspectives*, *106*(8), 437–445.

Gorny, J. R. (2001). *A summary of CA and MA requirements and recommendations for fresh cut (minimally processed) fruits and vegetables.* Postharvest Horticulture Series n. 22A, pp. 95 - 145, University of California Davis.

Ingle, A. P., Duran, N., Rai, M. (2014). Bioactivity, mechanism of action, and cytotoxicity of copper-based nanoparticles: A review. *Applied Microbiology and Biotechnology*, *98*(3), 1001–1009.

Ippolito, A., El Ghaouth, A., Wilson, C. L., Wisniewski, M. (2000). Control of postharvest decay of apple fruit by Aureobasidium pullulans and induction of defense responses. *Postharvest Biology and Technology*, *19*(3), 265–272.

Jackson, John, E. (2003). *Biology of apples and pears*. Cambridge University Press.

Janisiewicz, W. (2003). Control Of Postharvest Diseases Of Fruits Using Microbes. In *Fungal Biotechnology in Agricultural, Food, and Environmental Applications*. CRC Press.

Janisiewicz, W. J., Korsten, L. (2002). Biological control of postharvest diseases of fruits. *Annual Review of Phytopathology*, *40*(1), 411–441.

Jenkinson, HF.; Douglas, L. (2002). Candida interactions with bacterial biofilms. In J. Brogden, KA.; Guthmiller (Ed.), *Polymicrobial Infections and Disease* (pp. 357–373). Washington, DC: ASM Press.

Jones, AL, Aldwinckle, HS. (1990). *Compendium of apple and pear diseases*, pp. 53-58. St. Paul, Minnesota: American Phytopathological Society.

Joslyn, D. A., Galbraith, M. (1950). Procedures for Antibiotic, 711–716.

Judet-Correia, D., Bollaert, S., Duquenne, A., Charpentier, C., Bensoussan, M., Dantigny, P. (2010). Validation of a predictive model for the growth of *Botrytis cinerea* and *Penicillium expansum* on grape berries. *International Journal of Food Microbiology*, *142*(1), 106–113.

Judet-Correia, D., Charpentier, C., Bensoussan, M., Dantigny, P. (2011). Modelling the inhibitory effect of copper sulfate on the growth of *Penicillium expansum* and *Botrytis cinerea*. *Letters in Applied Microbiology*, *53*(5), 558–564.

Kairyte, K., Kadys, A., Luksiene, Z. (2013). Antibacterial and antifungal activity of photoactivated ZnO nanoparticles in suspension. *Journal of Photochemistry and Photobiology B: Biology*, *128*, 78–84.

Kang, Y.J., Frank, J. F. (1989). Biological aerosols: a review of airborne contamination and its measurement in dairy processing plants. *Journal of Food Protection*, *52*, 512–524.

Kerr, J. R. (1994). Suppression of Fungal Growth Exhibited by *Pseudomonas aeruginosa*. *Journal of Clinical Microbiology*, *32*(2), 525–527.

Khorsand Zak, A., Razali, R., Abd Majid, W. H., Darroudi, M. (2011). Synthesis and characterization of a narrow size distribution of zinc oxide nanoparticles. *International Journal of Nanomedicine*, *6*(1), 1399–1403.

Kiessling, P., Senchenkova, S. N., Ramm, M., Knirel, Y. A. (2005). Structural studies on the

exopolysaccharide from Erwinia persicina. *Carbohydrate Research, 340*, 1761–1765.

Kim, Y. S., Kim, K. S., Han, I., Kim, M. H., Jung, M. H., Park, H. K. (2012). Quantitative and qualitative analysis of the antifungal activity of allicin alone and in combination with antifungal drugs. *PLoS ONE*, *7*(6), 1–8.

Kizis, D., Natskoulis, P., Nychas, G. J. E., Panagou, E. Z. (2014). Biodiversity and ITS-RFLP characterisation of Aspergillus section Nigri isolates in grapes from four traditional grape-producing areas in Greece. *PLoS ONE*, *9*(4).

Klemetti, I., Lacroix, N., Nakatani, S., Sasia, G. (2006). Guidelines on air handling in the food industry. *Trends in Food Science and Technology*, *17*(6), 331–336.

Koch, a L. (1975). The kinetics of mycelial growth. *Journal of General Microbiology*, *89*(2), 209–16.

Kossen, N. W. (2000). The morphology of filamentous fungi. *Advances in Biochemical Engineering/ Biotechnology*, *70*, 1–33.

Krijgsheld, P., Bleichrodt, R., Veluw, G. J. Van, Wang, F., & Dijksterhuis, J. (2011). Development in Aspergillus. *Studies in Mycology*, *74,* 1–29.

Kuehn, H.H. and Gunderson, M. F. (1963). Psychrophilic and mesophilic fungi in frozen food products. *Appl. Microbiol.*, *11*, 352–356.

Labavitch, J. (2016). Pistachios. *The Commercial Storage of Fruits, Vegetables, and Florist and Nursery Stocks*, (66), 772–776.

Lahlali, R., Hamadi, Y., Guilli, M. El, Jijakli, M. H. (2011). Efficacy assessment of Pichia guilliermondii strain Z1, a new biocontrol agent, against citrus blue mould in Morocco under the influence of temperature and relative humidity. *Biological Control*, *56*(3), 217–224.

Lahlali, R., Serrhini, M. N., Friel, D., Jijakli, M. H. (2007). Predictive modelling of temperature and water activity (solutes) on the in vitro radial growth of Botrytis cinerea Pers. *International Journal of Food Microbiology*, *114*(1), 1–9.

Lambert, R. J. W., Lambert, R. (2003). A model for the efficacy of combined inhibitors, (Mic), *Journal of Applied Microbiology. 95*(4). 734–743.

Lambert, R. J. W., Pearson, J. (2000). Susceptibility testing: accurate and reproducible minimum inhibitory concentration (MIC) and non-inhibitory concentration (NIC) values. *Journal of Applied Microbiology*, *88*(5), 784–790.

Lanisnik Rizner, T., Wheeler, M. H. (2003). Melanin biosynthesis in the fungus Curvularia lunata (teleomorph: Cochliobolus lunatus). *Canadian Journal of Microbiology*, *49*, 110–119.

Lewis, K. I. M., Lewis, K. I. M., Suspects, T. H. E. U., Suspects, T. H. E. U. (2001). Riddle of Bio lm Resistance. *Society*, *45*(4), 999–1007.

Li, Y. C., Bi, Y., An, L. Z. (2007). Occurrence and latent infection of alternaria rot of Pingguoli pear (Pyrus bretschneideri Rehd. cv. Pingguoli) fruits in Gansu, China. *Journal of Phytopathology*, *155*(1), 56–60.

Liu, J., Sui, Y., Wisniewski, M., Droby, S., Liu, Y. (2013). Review: Utilization of antagonistic yeasts to manage postharvest fungal diseases of fruit. *International Journal of Food Microbiology*, *167*(2), 153–160.

Ljungqvist B, Reinmuller B. (1993). Interaction between air movements and the disperion of contaminants: clean zones with unidirectional air flow. *Journal of Parenteral Science and Technology*, *47*(2), 60–69.

Louis, B., Waikhom, S. D., Roy, P., Bhardwaj, P. K., Singh, M. W., Chandradev, S. K.,

Talukdar, N. C. (2014). Invasion of Solanum tuberosum L. by Aspergillus terreus: a microscopic and proteomics insight on pathogenicity. *BMC Research Notes*, *7*(1), 350.

Lynch, A. S., Robertson, G. T. (2008). Bacterial and Fungal Biofilm Infections. *Annual Review of Medicine*, *59*(1), 415–428.

Manual, B. A. (2015). BAM : Yeasts , Molds and Mycotoxins, 1–13.

Marín, S., Cuevas, D., Ramos, A. J., & Sanchis, V. (2008). Fitting of colony diameter and ergosterol as indicators of food borne mould growth to known growth models in solid medium. *International Journal of Food Microbiology*, *121*(2), 139–149.

Marín, S., Morales, H., Hasan, H. A. H., Ramos, A. J., Sanchis, V. (2006). Patulin distribution in Fuji and Golden apples contaminated with Penicillium expansum. *Food Additives and Contaminants*, *23*(12), 1316–1322.

Marín, S., Ramos, A. J., Sanchis, V. (2005). Comparison of methods for the assessment of growth of food spoilage moulds in solid substrates. *International Journal of Food Microbiology*, *99*(3), 329–341.

Martínez-Gutierrez, F., Thi, E. P., Silverman, J. M., de Oliveira, C. C., Svensson, S. L., Hoek, A. Vanden, Bach, H. (2012). Antibacterial activity, inflammatory response, coagulation and cytotoxicity effects of silver nanoparticles. *Nanomedicine: Nanotechnology, Biology, and Medicine*, *8*(3), 328–336.

Martins, D., Costa, F. T. M., Brocchi, M., Durán, N. (2011). Evaluation of the antibacterial activity of poly-(d,l-lactide-co-glycolide) nanoparticles containing violacein. *Journal of Nanoparticle Research*, *13*(1), 355–363.

Medina, A., Lambert, R. J. W., Magan, N. (2012). Rapid throughput analysis of filamentous fungal growth using turbidimetric measurements with the Bioscreen C: a tool for screening

antifungal compounds. *Fungal Biology*, *116*(1), 161–169.

Meletiadis, J., Dorsthorst, D. T. A., Paul, E., Verweij, P. E. (2003). Use of turbidimetric growth curves for early determination of antifungal drug resistance of filamentous fungi. *Society*, *41*(10), 4718–4725.

Meletiadis, J., Meis, J. F. G. M., Mouton, J. W. (2001). Analysis of Growth Characteristics of Filamentous Fungi in Different Nutrient Media. *Journal of Clinical Microbiology*, *39*(2),

Mille-Lindblom, C., Fischer, H., Tranvik, L. J. (2006). Antagonism between bacteria and fungi: Substrate competition and a possible tradeoff between fungal growth and tolerance towards bacteria. *Oikos*, *113*(2), 233–242.

Mille-Lindblom, C., von Wachenfeldt, E., Tranvik, L. J. (2004). Ergosterol as a measure of living fungal biomass: persistence in environmental samples after fungal death. *Journal of Microbiological Methods*, *59*(2), 253–262.

Mislivec, P.B., Tuite, J. (1970). Temperature and relative humidity requirements of species of Penicillium isolated from yellow dent corn kernels. *Mycologia*, *62*, 75–88.

Mohamed, S., Flint, S., Palmer, J., Fletcher, G. C., Pitt, J. I. (2013). An extension of the coconut cream agar method to screen Penicillium citrinum isolates for citrinin production. *Letters in Applied Microbiology*, *57*(3), 214–219.

Moline, H. E. (1991). Biocontrol of postharvest bacteria diseases of fruits and vegetables. In E. Wilson, C.L., Chaultz (Ed.), *Biological control of Postharvest Diseases of Fruits and Vegetables* (pp. 114–124). US Department of Agriculture.

Monroe, A. (2009). *Integrated pest management for Australian apples and pears: NSW Industry and Investment Management*. Retrieved from http://www.dpi.nsw.gov.au/__data/assets/pdf_file/0009/321201/ipm-for-australian-apples-

and-pears-complete.pdf

Moritz, M., Geszke-Moritz, M. (2013). The newest achievements in synthesis, immobilization and practical applications of antibacterial nanoparticles. *Chemical Engineering Journal*, *228*, 596–613.

Morris, S. C., Nicholls, P. J. (1978). An Evaluation of Optical Density to Estimate Fungal Spore Concentrations in Water Suspensions. *Phytopathology*, *68*(8), 1240.

Noll, L., Leonhardt, S., Arnstadt, T., Hoppe, B., Poll, C., Matzner, E. Kellner, H. (2016). Fungal biomass and extracellular enzyme activities in coarse woody debris of 13 tree species in the early phase of decomposition. *Forest Ecology and Management*, *378*, 181–192.

Novick, V. J., Monson, P. R., Ellison, P. E. (1992). The effect of solid particle mass loading on the pressure drop of HEPA filters. *Journal of Aerosol Science*, *23*(6), 657–665.

Nunes, C. A. (2012). Biological control of postharvest diseases of fruit. *European Journal of Plant Pathology*, *133*(1), 181–196.

Ocón, E., Gutiérrez, A. R., Garijo, P., Santamaría, P., López, R., Olarte, C., Sanz, S. (2011). Factors of influence in the distribution of mold in the air in a wine cellar. *Journal of Food Science*, *76*(3), 169–174.

Ogawa, JM, English, H. (1991). *Diseases of temperate zone tree fruit and nut crops*. Oakland, California: UCANR Publications.

Oliveira Junior, E. N. de, Melo, I. S. de, Franco, T. T. (2012). Changes in hyphal morphology due to chitosan treatment in some fungal species. *Brazilian Archives of Biology and Technology*, *55*(5), 637–646.

Palou, L., Ali, A., Fallik, E., Romanazzi, G. (2015). GRAS, plant- and animal-derived compounds as alternatives to conventional fungicides for the control of postharvest diseases

of fresh horticultural produce. *Postharvest Biology and Technology*. *122,* 41-52.

Palou, L. Taberner, V. Guardado, A. Montesinos-Herrero, C. (2012). First report of Alternaria alternata causing postharvest black spot of persimmon in Spain. *Australasian Plant Diseases Notes*, *7*, 41–42.

Panasenko, V. T. (1967). Ecology of microfungi. *Botanical Reviews*, *33*, 189–215.

Papagianni, M. (2004). Fungal morphology and metabolite production in submerged mycelial processes. *Biotechnology Advances*, *22*(3), 189–259.

Parret F, Crilly K. (2000). Microbiological air monitoring. *International Food Hygiene*, *10*, 5–7.

Pârvu, M., Pârvu, A. E. (2011). Antifungal plant extracts. *Science Against Microbial Pathogens Communicating Current Research And Technological Advances*, 1055–1062.

Pasquet, J., Chevalier, Y., Pelletier, J., Couval, E., Bouvier, D., Bolzinger, M. A. (2014). The contribution of zinc ions to the antimicrobial activity of zinc oxide. *Colloids and Surfaces A: Physicochemical and Engineering Aspects*, *457*(1), 263–274.

Patton, C., Thompson, S., Epel, D. (2004). Some precautions in using chelators to buffer metals in biological solutions. *Cell Calcium*, *35*(5), 427–431.

Pereira, L., Dias, N., Carvalho, J., Fernandes, S., Santos, C., Lima, N. (2014). Synthesis, characterization and antifungal activity of chemically and fungal-produced silver nanoparticles against Trichophyton rubrum. *Journal of Applied Microbiology*, *117*(6), 1601–1613.

Pfohl-Leszkowicz, A., Manderville, R. A. (2007). Ochratoxin A: An overview on toxicity and carcinogenicity in animals and humans. *Molecular Nutrition and Food Research*, *51*(1), 61–99.

Pierson, CF, Ceponis, M.J., McColloch, L. P. (1971). Market diseases of apples, pears and

quinces. In *Agriculture handbook* (pp. 1–96). Washington DC, USA: Agriculture Research Service, U.S. Department of Agriculture.

Pierson, C. . (1966). Effect of temperature on the growth of Rhizopus stolonifer on peaches and agar. *Phytopathology*, *56*, 276–278.

Pitt, J. I. (1984). The significance of potentially toxigenic fungi in foods. *Food Technol. Aust.*, *36*, 218–219.

Pitt, J. I., & Hocking, A. D. (2009). *Fungi and Food Spoilage* (Third Edit). Springer.

Pose, G., Patriarca, A., Kyanko, V., Pardo, A., Fernández Pinto, V. (2009). Effect of water activity and temperature on growth of Alternaria alternata on a synthetic tomato medium. *International Journal of Food Microbiology*, *135*(1), 60–63.

Pscheidt, J., and Ocamb, C. O. (2014). *Pacific northwest plant disease management handbook*. Corvallis, OR: Oregon State University.

Raghupathi, K. R., Koodali, R. T., Manna, A. C. (2011). Size-dependent bacterial growth inhibition and mechanism of antibacterial activity of zinc oxide nanoparticles. *Langmuir : The ACS Journal of Surfaces and Colloids*, *27*(7), 4020–4028.

Rai, M., Yadav, A., & Gade, A. (2009). Silver nanoparticles as a new generation of antimicrobials. *Biotechnology Advances*, *27*(1), 76–83.

Rainard, P. (1986). Bacteriostatic activity of bovine milk lactoferrin against mastitic bacteria. *Veterinary Microbiology*, *11*(4), 387–392.

Rajderkar, N. R. (1966). The influence of nitrogen nutrition on growth and sporulation of Alternaria solani (Ell. (&) Mart.) jones (&) grout. *Mycopathologia et Mycologia Applicata*, *29*(1), 55–58.

Rinaldi, M. G. (1982). Use of potato flakes agar in clinical mycology. *Journal of Clinical*

Microbiology, *15*(6), 1159–1160.

Robertson, E. J., Wolf, J. M., Casadevall, A. (2012). EDTA inhibits biofilm formation, extracellular vesicular secretion, and shedding of the capsular polysaccharide glucuronoxylomannan by cryptococcus neoformans. *Applied and Environmental Microbiology*, *78*(22), 7977–7984.

Roesler, J. F. (1966). Application of polyurethane foam filters for respirable dust separation. *Journal of the Air Pollution Control Association*, *16*(1), 30–34.

Roselli, M., Finamore, A., Garaguso, I., Britti, M. S., Mengheri, E. (2003). Zinc Oxide protects cultured enterocytes from the damage induced by Escherichia coli. *The Journal of Nutrition*, *133*(12), 4077–4082.

Ross, T. (1996). Indices for performance evaluation of predictive models in food microbiology. *Journal of Applied Bacteriology*, *81*(5), 501–508.

Rossi-Rodrigues, B. C., Brochetto-Braga, M. R., Tauk-Tornisielo, S. M., Carmona, E. C., Arruda, V. M., Chaud Netto, J. (2009). Comparative growth of trichoderma strains in different nutritional sources, using bioscreen c automated system. *Brazilian Journal of Microbiology*, *40*(2), 404–410.

Rosso, L., Lobry, J. R., & Bajard, S. (1995). Convenient Model To Describe the Combined Effects of Temperature and pH on Microbial Convenient Model To Describe the Combined Effects of Temperature and pH on Microbial Growth. *Applied and Environmental Microbiology*, *61*(2), 610–616.

Salem, W., Leitner, D. R., Zingl, F. G., Schratter, G., Prassl, R., Goessler, W., Schild, S. (2015). International Journal of Medical Microbiology Antibacterial activity of silver and zinc nanoparticles against Vibrio cholerae and enterotoxic Escherichia coli. *International*

Journal of Medical Microbiology, *305*(1), 85–95.

Samson RA, Houbraken J, Summerbell RC, Flannigan B, M. J. (2000). *Introduction to food and airborne fungi*. (O. Samson, R.A., Frisvad, J.C., Filtenborg, Ed.) (6th ed.). CBS- Utrecht.

Samson RA, Houbraken J, Summerbell RC, Flannigan B, M. J. (2001). Common and important species of fungi and actinomycetes in indoor environments. In *Microogranisms in Home and Indoor Work Environments* (pp. 287–292). CRC.

Sardella, D., Muscat, A., Brincat, J.P., Gatt, R., Decelis, S., Valdramidis, V. (2016). A Comprehensive Review of the Pear Fungal Diseases. *International Journal of Fruit Science*, *16*(4), 351–377.

Sardi, J. C. O., Scorzoni, L., Bernardi, T., Fusco-Almeida, A. M., & Mendes Giannini, M. J. S. (2013). Candida species: Current epidemiology, pathogenicity, biofilm formation, natural antifungal products and new therapeutic options. *Journal of Medical Microbiology*, *62*(PART1), 10–24.

Sarker, S. D., Nahar, L., & Kumarasamy, Y. (2007). Microtitre plate-based antibacterial assay incorporating resazurin as an indicator of cell growth , and its application in the in vitro antibacterial screening of phytochemicals. *Methods. 42*(4), 321–324.

Savi, G. D., Bortoluzzi, A. J., Scussel, V. M. (2013). Antifungal properties of Zinc-compounds against toxigenic fungi and mycotoxin. *International Journal of Food Science and Technology*, *48*(9), 1834–1840.

Sawai, J. (2003). Quantitative evaluation of antibacterial activities of metallic oxide powders (ZnO, MgO and CaO) by conductimetric assay. *Journal of Microbiological Methods*, *54*(2), 177–182.

Sawai, J., Kojima, H., Ishizu, N., Itoh, M., Igarashi, H., Sawaki, T., Shimizu, M. (1997).

Bactericidal action of magnesium oxide powder. *Journal of Inorganic Biochemistry*, *67*(1–4), 443–443.

Sawai, J., Shoji, S., Igarashi, H., Hashimoto, A., Kokugan, T., Shimizu, M., Kojima, H. (1998). *Hydrogen peroxide as an antibacterial factor in zinc oxide powder slurry. Journal of Fermentation and Bioengineering. 16*(2). 187-194.

Sawai, J., & Yoshikawa, T. (2004). Quantitative evaluation of antifungal activity of metallic oxide powders (MgO, CaO and ZnO) by an indirect conductimetric assay. *Journal of Applied Microbiology*, *96*(4), 803–809.

Schipper, M. A. A. (1984). A revision of the genus Rhizopus. 1. The Rh. stolonifer-group and Rh. oryzae. *Studies in Mycology*, *25*, 1–19.

Schoonbeek, H.J., Raaijmakers, J. M., De Waard, M. A. (2002). Fungal ABC Transporters and Microbial Interactions in Natural Environments. *Molecular Plant-Microbe Interactions*, *15*(11), 1165–1172.

Schoonbeek, H., Jacquat-Bovet, A.-C., Mascher, F., Métraux, J.P. (2007). Oxalate-degrading bacteria can protect *Arabidopsis thaliana* and crop plants against *Botrytis cinerea*. *Molecular Plant-Microbe Interactions*, *20*(12), 1535–1544.

Schroeckh, V., Scherlach, K., Nutzmann, H.-W., Shelest, E., Schmidt-Heck, W., Schuemann, J., Brakhage, A. A. (2009). Intimate bacterial-fungal interaction triggers biosynthesis of archetypal polyketides in Aspergillus nidulans. *Proceedings of the National Academy of Sciences*, *106*(34), 14558–14563.

Seil, J. T., Webster, T. J. (2012). Antimicrobial applications of nanotechnology: Methods and literature. *International Journal of Nanomedicine*, *7*, 2767–2781.

Serey, R. A., Torres, R., Latorre, B. A. (2007). Pre- and post-infection activity of new fungicides

against Botrytis cinerea and other fungi causing decay of table grapes, *34*(3), 215–224.

Sharma, G., Pandey, R. R. (2010). Influence of culture media on growth , colony character and sporulation of fungi isolated from decaying vegetable wastes. *Journal of Yeast and Fungal Research*, *1*(8), 157–164.

Sharma, R. R., Singh, D., Singh, R. (2009). Biological control of postharvest diseases of fruits and vegetables by microbial antagonists: A review. *Biological Control*, *50*(3), 205–221.

Shim, J., Choi, K., Hahn, K., & Lee, J. (2002). Blue mold of pear caused by Penicillium aurantiogriseum in Korea. *Microbiology*, *30*(2), 105–106.

Shirtliff, M. E., Peters, B. M., Jabra-rizk, M. A., Program, I., Sciences, D. (2009). Cross-Kingdom interactions: Candida albicans and bacteria. *FEMS Microbiology Letters*, *299*(1), 1–8.

Siefkes-Boer, H.J., Boyd-Wilson, K.S.H., Petley, M., Walter, M. (2009). Influence of cold-storage temperatures on strawberry leak caused by Rhizopus spp. *New Zealand Plant Protection*, *62*, 243–249.

Silvestre, C., Duraccio, D., Cimmino, S. (2011). Food packaging based on polymer nanomaterials. *Progress in Polymer Science (Oxford)*, *36*(12), 1766–1782.

Sirelkhatim, A., Mahmud, S., Seeni, A., Kaus, N. H. M., Ann, L. C., Bakhori, S. K. M., … Mohamad, D. (2015). Review on zinc oxide nanoparticles: Antibacterial activity and toxicity mechanism. *Nano-Micro Letters*, *7*(3), 219–242.

Skytta, E., Mattila-Sandholm, T. (1991). A quantitative method for assessing bacteriocins and other food antimicrobials by automated turbidometry, *14*, 77–88.

Snowdon, A. L. (1990). *A Colour Atlas of Post Harvest Diseases and Disorders of Fruits and Vegetables*. (W. Scientific, Ed.). London.

Sommer, N. F. (1982). Postharvest Handling Practices and Postharvest Diseases of Fruit. *Plant Disease*, *66*(5), 357–364.

Sommer, N. F. (1989). Suppressing postharvest disease with handling practices and controlled environment. In S. La Rue, James and Johnson (Ed.), *Peaches, Plums and Nectarines. Growing and Handling for Fresh Market* (pp. 182–186). Oakland, California: University of California. Division of Agriculture and Natural Resources.

Spadaro, D., Droby, S. (2016). Development of biocontrol products for postharvest diseases of fruit: The importance of elucidating the mechanisms of action of yeast antagonists. *Trends in Food Science and Technology*, *47*, 39–49.

Spadaro, D., Gullino, M. L. (2005). Improving the efficacy of biocontrol agents against soilborne pathogens. *Crop Protection*, *24*(7), 601–613.

Sugar, D., Spotts, R. A., Oregon, S., Station, E., River, H. (1992). Sources of Inoculum of Phialophora malorum, casual agent of side rot of pear, *Phytopathology. 82*(7), 735–738.

Suslow, T. (2005). Postharvest handling for organic crops. *Division of Agriculture and Natural Resources*, 1–8.

Sutton, T. B., Aldwinckle, H. S., Agnello, A. M., Walgenbach, J. F. (2014). *Compendium of Apple and Pear Diseases and Pests* (Second Edition). APS press.

Takahashi, K. (1990). Application of calorimetric methods to cellular processes: with special references to quantitative evaluation of drug action on living cells. *Thermochimica Acta*, *163*, 71–80.

Taniwaki, M.H., Pitt, J.I., Hocking, A.D., F. G. H. (2006). Comparison of hyphal length, ergosterol, mycelium dry weight and colony diameter for quantifying growth of fungi from foods. In T. U. Hocking, A.D., Pitt, J.I., Samson, R.A. (Ed.), *Advances in Food Mycology*.

Springer.

Taniwaki, M. H., Hocking, A. D., Pitt, J. I., Fleet, G. H. (2001). Growth of fungi and mycotoxin production on cheese under modified atmospheres. *International Journal of Food Microbiology*, *68*(1–2), 125–133.

Tassou, C. C., Natskoulis, P. I., Magan, N., Panagou, E. Z. (2009). Effect of temperature and water activity on growth and ochratoxin A production boundaries of two Aspergillus carbonarius isolates on a simulated grape juice medium. *Journal of Applied Microbiology*, *107*(1), 257–268.

Tea, L. R., Romih, R. (2007). Growth media effects on morphology and 17 β -HSD activity in the fungus Curvularia lunata, *57*(4), 635–643.

Teh, C. H., Nazni, W. A., Nurulhusna, A. H., Norazah, A., Lee, H. L. (2017). Determination of antibacterial activity and minimum inhibitory concentration of larval extract of fly via resazurin-based turbidometric assay. *BMC Microbiology*, *17*(1), 36.

Thomidis, T., Exadaktylou, E. (2012). First Report of Aspergillus niger Causing Postharvest Fruit Rot of Cherry in the Prefectures of Imathia and Pella, Northern Greece. *Plant Disease*, *96*(458).

Thompson, A., K. (2010). *Controlled Atmosphere Storage of Fruits and Vegetables.* Second Edition. (Thompson ed.).

Timnick, M. B., Lilly, V. G., Barnett, H. L. (2015). Mycological Society of America The Effect of Nutrition on the Sporulation of Melanconium fuligineum in Culture, *43*(6), 625–634.

Trinci, A. P. J. (1972). Culture turbidity as a measure of mould growth. *Transactions of the British Mycological Society*, *58*(3), 467–473.

University of Illinois. (2000). *Gray-Mold Rot or Botrytis Blight of Vegetables*. Retrieved from

http://ipm.illinois.edu/diseases/series900/rpd942/

Usman, M. S., Ibrahim, N. A., Shameli, K., Zainuddin, N., Yunus, W. M. Z. W. (2012). Copper nanoparticles mediated by chitosan: Synthesis and characterization via chemical methods. *Molecules*, *17*(12), 14928–14936.

Valdramidis, V. P., Geeraerd, A. H., Van Impe, J. F. (2007). Stress-adaptive responses by heat under the microscope of predictive microbiology. *Journal of Applied Microbiology*, *103*(5), 1922–1930.

Valero, A., Marín, S., Ramos, A. J., Sanchis, V. (2007). Effect of preharvest fungicides and interacting fungi on Aspergillus carbonarius growth and ochratoxin A synthesis in dehydrating grapes. *Letters in Applied Microbiology*, *45*(2), 194–199.

Vijayakumar, P., Muriana, P. (2015). A Microplate Growth Inhibition Assay for Screening Bacteriocins against Listeria monocytogenes to Differentiate Their Mode-of-Action. *Biomolecules*, *5*(2), 1178–1194.

Viñas, I., Dadon, J., Sanchis, V. (1993). Citrinin-producing capacity of Penicillium expansum strains from apple packinghouses of Lerida (Spain). *International Journal of Food Microbiology*, *19*(2), 153–156.

Wang, X., Kim, K., Lee, C., Kim, J. (2008). Prediction of air filter efficiency and pressure drop in air filtration media using a stochastic simulation. *Fibers and Polymers*, *9*(1), 34–38.

Wargo, M. J., & Hogan, D. A. (2006). Fungal—bacterial interactions: a mixed bag of mingling microbes. *Current Opinion in Microbiology*, *9*(4), 359–364.

Wells, M., Uota, J. M. (1970). Germination and growth of five fungi in low-oxygen and high-carbon dioxide atmospheres. *Phytopathologia*, *60*, 50–53.

Wilson, C.L., Solar, J.M., El Ghaouth, A., Wiesniewski, M. E. (1997). Rapid Evaluation of Plant

Extracts and Essential Oils for Antifungal Activity Against Botrytis cinerea. *Plant Disease*, (81), 204–210.

Wilson, C. L., Wisniewski, M. E. (1989). Biological control of Fruits and Vegetables : an Emerging Technology . *Annual Reviews of Phytopathology*, *27*, 425–441.

Wilson, C. L., Wisniewski, M. E., Spadaro, D., Gullino, M. L., Sharma, R. R., Singh, D., … Inbar, J. (2005). Improving the efficacy of biocontrol agents against soilborne pathogens. *Biological Control. 15*, 425–441.

Wirtanen, G., Miettinen, H., Pahkala, S., Enbom, S., & Vanne, L. (2002). Clean air solutions in food processing. *VTT Publications*, (482), 3–95.

Wisniewski, M., Biles, C., Droby, S. (1991). The use of yeast Pichia guilliermondii as a biocontrol agent: characterization of attachment to Botrytis cinerea. In E. Wilson, C.L., Chalutz (Ed.), *Biological control of Postharvest Diseases of Fruits and Vegetables* (pp. 167–183). US Department of Agriculture.

WSU (2015). Washington State University Extension. http://postharvest.tfrec.wsu.edu/pages/N7I3A (Last access: 28/09/2017)

Xiao, C. (2006). Postharvest fruit rots in d'Anjou pears caused by Botrytis cinerea, Potebniamyces pyri, and Sphaeropsis pyriputrescens. Retrieved from http://www.plantmanagementnetwork.org/pub/php/diagnosticguide/2006/pears/

Zafra, G., Absalón, A. E., & Cortés-espinosa, D. V. (2015). Morphological changes and growth of filamentous fungi in the presence of high concentrations of PAHs. *Brazilian Journal of Microbiology. 941*, 937–941.

Zhang, Z., & Nan, Z. (2014). Erwinia persicina, a possible new necrosis and wilt threat to forage or grain legumes production. *European Journal of Plant Pathology*, *139*(2), 343–352.

Publications list in peer-reviewed journals of Davide Sardella:

☐ **D. Sardella**, V.P. Valdramidis, R. Gatt (2017). Physiological effects and mode of action of ZnO nanoparticles against postharvest fungal contaminants. *Food Research International*. (IF:3.08)
https://doi.org/10.1016/j.foodres.2017.08.019

☐ **D. Sardella**, V.P. Valdramidis, R. Gatt (2017). Assessing the efficacy of Zinc Oxide nanoparticles against Penicillium expansum by automated turbidimetric analysis. *Mycology*. (IF:2.37)
http://dx.doi.org/10.1080/21501203.2017.1369187.

☐ S. Decelis, **D. Sardella**, T. Triganza, J.P. Brincat, R. Gatt, V. Valdramidis (2017). Assessing the antifungal efficiency of filters coated with zinc oxide nanoparticles. *Royal Society Open Science. 4: 161032.* (IF:2.89)

☐ J.P. Brincat, **D. Sardella**, A. Muscat, S. Decelis, J. Grima, V. Valdramidis, R. Gatt (2016). A review of the state-of-the art in air filtration technologies as may be applied to cold storage warehouses. *Trend Food Science and Technology. 50: 175- 185* (IF: 5.19)

☐ **D. Sardella**, A. Muscat, J.P. Brincat, R. Gatt, S. Decelis, V. Valdramidis (2016). A comprehensive review of the pear fungal diseases. *International Journal of Fruit Science* (IF:0.50)

Submitted papers in peer-reviewed journals:

☐ **D. Sardella**, R. Gatt, S. Decelis, V. Valdramidis (2017). Modelling the growth of pear postharvest isolates at different temperature (submitted).

- **D. Sardella**, R. Gatt, V. Valdramidis (2017). Turbidimetric assessment of the growth of filamentous fungi and the antifungal activity of ZnO nanoparticles (submitted).

- **D. Sardella**, R. Gatt, V. Valdramidis (2017). Assessing the air filtration efficacy of compressed and uncompressed polyurethane foams (submitted).

- **D. Sardella**, P. Natskoulis, E. Gkana, E. Z. Panagou, V. Valdramidis (2017). Evaluation of the interactions between *Erwinia persicina's* biofilms and fungal isolates (submitted).

Conferences attended (abstracts):

- V. Valdramidis, R. Gatt, **D. Sardella (2017).** An introduction to quantitative microbiology (oral presentation). 5th IUMS (Yogyakarta, Indonesia, 19th - 20th January).

- **D. Sardella**, R. Gatt, S. Decelis, V. Valdramidis (2017). Phyisiological effects and mode of action of ZnO nanoparticles against postharvest fungal contaminants (poster). APS Annual Meeting 2017 (San Antonio, Texas, 3rd - 5th August).

- **D. Sardella**, R. Gatt, S. Decelis, V. Valdramidis (2017). Optimizing protocols to assess the efficacy of ZnO nanoparticles as antifungal agents (oral presentation and paper submitted to *Acta Horticulturae*). IV International Symposium on Postharvest Pathology (28th May - 3rd June, Kruger Park, South Africa).

- A. Muscat, **D. Sardella**, S. Marin, S. Decelis, V. Valdramidis. Characterization of fungal contaminants affecting preservation properties of *Pirus communis* var. *bambinella* (poster). Q-Safe International Conference (10th-12th April 2017, Syros, Greece).

- **D. Sardella**, R. Gatt, V. Valdramidis. Quantitative assessment of the efficacy of ZnO nanoparticles against *P. expansum* (oral presentation). Q-Safe International Conference. Q-Safe International Conference (10th-12th April 2017, Syros, Greece).

- **D. Sardella**, R. Gatt, S. Decelis, V. Valdramidis. Quantitative assessment of the efficacy of ZnO nanoparticles against selected fruit fungal contaminants (poster). American Phytopathologycal Society Annual Meeting 2016 (Tampa, Florida, 30th July - 3rd August 2016).

- **D. Sardella**, P. Natskoulis, E. Gkana, E. Panagou, V. Valdramidis. Evaluating the interactions within mixed biofilms of *Erwinia* spp. and fungal isolates (oral presentation). ICFM Workshop 2016 (Freising, Germany, 13th - 15th June).

- V. Valdramidis, T. Triganza, **D. Sardella**, R. Gatt, S. Decelis. Assessing the antifungal efficacy of filters coated with ZnO nanoparticles (oral presentation). ICFM Workshop 2016 (Freising, Germany, 13th - 15th June).

Awards and grants:

- Eddie Echandi Student Travel Award 2016 by American Phytopathological Society (APS).

- President's fund grant by Society for Applied Microbiology (SfAM) (2016).

- Short Term Scientific Mission (STSM Bacfoodnet COST Action) grant (2015).